Hybrid Chitosan-Alginate scaffolds for bone and cartilage tissue engineering

Zhensheng Li

A dissertation submitted in partial fulfillment of the
requirements for the degree of
Doctor of Philosophy

University of Washington

2007

Program Authorized to Offer Degree:

Department of Materials Science and Engineering

University of Washington
Graduate School

This is to certify that I have examined this copy of a doctoral dissertation by

Zhensheng Li

and have found that it is complete and satisfactory in all respects, and that any and all revisions required by the final examining committee have been made.

Chair of the Supervisory Committee:

Miqin Zhang

Reading Committee:

Miqin Zhang

Christopher Allen

Guozhong Cao

Date: July 20 2007

In presenting this dissertation in partial fulfillment of the requirements for the doctoral degree at the University of Washington, I agree that the Library shall make its copies freely available for inspection. I further agree that extensive copying of the dissertation is allowable only for scholarly purposes, consistent with "fair use" as prescribed in the U.S. Copyright Law. Requests for copying or reproduction of this dissertation may be referred to ProQuest Information and Learning, 300 North Zeeb Road, Ann Arbor, MI 48106-1346, 1-800-521-0600, to whom the author has granted "the right to reproduce and sell (a) copies of the manuscript in microform and/or (b) printed copies of the manuscript made from microform."

Signature 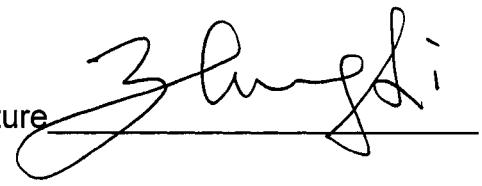

Date July 20, 2007

University of Washington

Abstract

Hybrid Chitosan Alginate Scaffolds for Bone and Cartilage Tissue Engineering

Zhensheng Li
Chair of the Supervisory Committee:
Associated Professor Miqin Zhang
Department of Materials Science and Engineering
College of Engineering

The regeneration of new bone or cartilage to restore the function of traumatized, damaged, or lost bone or cartilage is a major clinical and socioeconomic burden. In recent years, a new cutting-edge procedure, bone- and cartilage-tissue engineering, has emerged as a new strategy for healing musculoskeletal conditions. In this strategy, progenitors or mature cells are combined with biocompatible scaffolds to initiate partial or full bone and/or cartilage regeneration.

Scaffolding materials in tissue engineering should be bioactive and biodegradable. The synthetic polymers, such as PLA and PGA, are biodegradable, but not bioactive. Furthermore, their bulky degradation style and induction of foreign body reaction limit their clinical applications. Chitosan and alginate, two natural polymers, have proven to be biodegradable and bioactive for bone and cartilage regeneration. In this study, high-concentration (4.8% w/v) chitosan-alginate hybrid scaffolds were successfully synthesized through a thermally-induced phase separation technique. The produced hybrid scaffold was thoroughly characterized for mechanical and biological properties and compared

to pure chitosan scaffolds of the same concentration and similar porosity. The main pore sizes of the porous hybrid scaffolds was found to be 50–300 μm, which can be controlled through freezing and coalescence processes. The hybrid scaffolds demonstrated significantly-improved mechanical strength, water permeability and stability compared to pure chitosan scaffolds at increased porosity (92-95% vs. 87-89%).

The *in vitro* study showed that the hybrid scaffold induced better cell attachment and proliferation rate, and maintained the functionality of the cells better than chitosan scaffolds. The hybrid scaffolds were also shown to promote the bio-mineralization of MG-63 osteoblast and the production of collagen type II, and maintain the characteristic cell morphology of chondrocytes. *In vivo* study showed that the hybrid scaffolds were biocompatible and degradable, and ,promoted rapid vascularization, deposited connective tissue, and calcified matrix within the whole scaffold structure. The results support the potential applications of chitosan-alginate scaffolds as an alternative to other natural polymer-based scaffolds in tissue engineering. This study provides insights to the principles of interactions between biodegradable composite materials and biological systems, and the information for fabrication of scaffolds of different mechanical strengths for desired clinical applications.

Key words: tissue engineering, chitosan, alginate, lyophilization (freeze drying), bone, cartilage

Table of Contents

List of Figures

Figures Page

List of Tables

Acknowledgements

This work would not have been possible without funding provided by UWEB, a NSF national laboratory and TGIF. Contract number BSF-EEC-9529161, NSF-TIF,TGIF and NIH-BRP-N01-CO37122.

First of all, thanks to Professor Miqin Zhang for her friendship, enthusiasm, energy, and vision. She is always a great mentor and a wonderful friend to me. I began this process as a layman to engineering, but she trained me to think and write critically and creatively as an engineer. This work would not have been possible without her-, patience, guidance, and support.

I also would like to thank all my committee members. Thanks to Professor Cao, for his constructive advice on the theoretical analysis of this dissertation. Thanks to Professor Alex Jen for his spiritual support while I was going through the hardest time of my life. He is a true role model for both my future career and my life. Thanks to Dr. Chris Allenfor his guidance in the application of the scaffolds and his dedication and enthusiasm in revising this dissertation. Thanks to professor Jiang Shaoyi and professor Wei Li for the friendship and constructive discussions.

Again, thanks to Professor Zhang and her "dream team." Without their friendship, help, and cooperation, I could not have finished my work. They are my sisters and brothers; They have been like a family to me. Thanks to Narayan,

Matthew Leung, Ashleig Cooper, Dennis Edmonson, Steve Florczyk, Johnathan Gunn, Conroy Sun, Omid, Fareid, Chen Fang,

Thanks to the MSE staff members, Tom, Tuesday, Bob, and Kathy, for their support and cooperation. Thanks to the UWEB staff members and professors, Kip Hauch, Janet Guy, Colleen; the Botany SEM coordinators; and the Keck center coordinators, the 6th floor animal facilities and Vet Service People. Thanks to Professor Qi and Dr. Tian at the histopathological lab of the UW Health Science Center.

I also would like to thank my best friend, Kippy Dalton for correcting my spoken English and her effort in revising my dissertation.

Last but not least, I would like to thank my wife, Hui Peng, my two daughters, Cassie and Laura, my parents and parents-in-law. I cannot be myself with their support. They inspire me to keep reaching for my goals.

Chapter One

Introduction and Overview

1.1 Musculoskeletal Conditions and Challenges in Orthopedic Surgery

Bone and joint (musculoskeletal) diseases affect more than one billion individuals worldwide and this figure is increasing sharply with the aging of the global populations.[1] These diseases have an enormous impact on society, affecting people of all ages. In the United States, one out of 3 American adults reports arthritis or chronic joint pain, with 1 out of 7 Americans (36.4millions) reporting other musculoskeletal impairments. One out of 2 women and 1 out of 4 men over 50 years old will suffer an osteoporosis-related fracture in their resting life and the number of individuals over age 50 is expected to double by 2020. Each year, musculoskeletal conditions account for about 102.5 million visits to physicians' offices, 4.7 million hospital outpatient visits, 26.3 million emergency department visits, 2.4 million hospitalizations, and 7.6 million surgical procedures.[2,3]

Musculoskeletal conditions pose a huge socio-economic burden to the U.S., costing an estimated $300 billion every year ($254 billion in year 2000). On March 25, 2002, President George W. Bush [4] proclaimed the years 2002 through 2011 as the "National Bone and Joint Decade" to raise awareness about these conditions.

Orthopedic physicians and surgeons manage and treat most musculoskeletal conditions. The field of orthopedics, like many other specialties,

has expanded in response to the need to correct deformities, restore function, and alleviate pain. Orthopedic surgeons have succeeded in preventing major losses of bodily function. For thousands of years, there were five primary strategies for treating musculoskeletal conditions: "Relieving (symptoms)", "Removing (tumorous and infectious lesions)", "Repairing (fractures, soft tissue injuries and other disorders)", "Replacing (degenerative joints)" and "Rebuilding (or reconstruction of defects)." Today, virtually all orthopedic surgeries involve the last four 'Re' therapies and have produced remarkable results for many musculoskeletal diseases. The treatments for complex fractures (repairing), end-stage arthritic joint disease (replacement), limb deformities (resection), and almost all surgical conditions have recently demonstrated dramatic improvements. Patients with musculoskeletal diseases have more therapeutic options today than ever before.

However, there continues to be a dire need for improved technologies and therapies, particularly in the areas of repairing articular cartilage damage and severe bone defects. Current surgical treatments for large bone defects fall into two categories: bone transportation (the Ilizarov and other external fixing devices) and bone graft transplantation (auto-, allo- and xeno-grafts; different biomaterial implants). Osteotomy, followed by bone distraction (Ilizarov technique), takes advantage of the regenerative potential of bone[5], however the device is highly inconvenient for the patient and requires a long recovery period, often with complications. Graft transplants—those of vascularized bone or bone-

muscle or bone-muscle-skin—are widely accepted and used but have a high rate of complications such as infection and non-unions, insufficient autologous resources, and contour irregularities. Furthermore, graft transplants are often not an option for large reconstructions since they require large harvests of healthy tissue, which result in major donor site morbidity.[6] While allografting and xenografting are alternative strategies to autografting, they, too, have potential complications such as possible disease transmission, rejection of allograft tissue, major histo-incompatibility, graft versus host disease, and the potential need for expensive immunosuppressive medicine.[7] It is time for an entirely new method!

1.2 Regenerative Medicine

The challenges in orthopedic surgery demand a new kind of medicine—namely, regenerative medicine, a new category of surgery. Regenerative medicine has seen a recent emergence due to tissue engineering.

There are three key roles in tissue engineering: the cell—usually the progenitor cells; growth factors which stimulate cells to attach, proliferate, differentiate and functionalize; and scaffolds which support the cells' attachment and carry growth factors.

The scaffold plays a key role in tissue engineering, providing cells with a suitable growth environment, optimal oxygen levels, effective nutrient and waste transportation, and mechanical integrity. Scaffolds also provide 3D environments to bring cells close together so that they can organize to form tissues. When the scaffold is degraded, the cells produce extracellular matrix molecules (ECM) and

eventually form 3D structures mimicking the native tissue morphology and function. An ideal scaffold can also guide progenitor cell migration and stimulate their proliferation and differentiation.

1.3 Dissertation Overview

As cells and growth factors fall outside the realm of materials science, this dissertation is focusing on the scaffold. This dissertation will include, but not be limited to, the scaffold materials selection, porous structure synthesis, stability testing, mechanical testing, and *in vitro* and *in vivo* experiments.

Chapter one is the introduction and overview of the dissertation. Chapter two reviews the development, key roles and approaches, and requirements of tissue engineering. Chapter three reviews the categories and materials currently available for tissue engineering, including ceramics and synthetic polymers. Chapter four is dedicated to reviewing the physical, chemical, biological, and rheological properties of chitosan and alginate. This is the background knowledge for the materials selection in this project. Chapter five reports the synthesis and optimization of hybrid chitosan and alginate scaffolds, and the characterization of those scaffolds. This chapter also discussed the mechanism of freeze-drying and thermally induced phase separation.

Chapters six through eight discuss the applications of the hybrid chitosan-alginate scaffolds. Chapter six covers the experiments that use the scaffolds for cartilage tissue engineering. HTB-94 cell line cells were used as chondrocytes to test the biocompatibility of the scaffolds for cartilage regeneration. This work

showed that the hybrid scaffolds maintained the normal functional morphology of the chondrocytes in producing collagen type II. It is therefore appealing to consider using this hybrid scaffolds for in vivo cartilage tissue engineering. Chapter seven covers the application of bone tissue engineering and our in vivo study. Both in vitro and in vivo studies showed that the hybrid scaffolds were highly biocompatible and biodegradable, promoting biomineralization of MG-63 osteoblasts as early as three days after seeding. It also invoked rapid blood vessels formation and very limited foreign body reaction. Chapter eight focuses on the application of calcium alginate gel to improve cell seeding in these scaffolds. It is always a challenging goal in seeding highly density of cells on scaffolds to mimic the physiological condition in vivo conditions. On site gel formation of calcium alginate was studied in seeding cells on scaffolds. DNA quantification was used to compare the final cell distribution in different layers of the scaffolds. The results showed that on site calcium alginate gel formation is an effective method in improving initial cell seeding density.

Notes to Chapter One

1. UNPD. World population ageing:1950-2050. (2002).

2. AAOS. *Musculoskeletal Conditions in the U.S. (second edition)*. (1999).

3. USBJD. US Bone and Joint decade. http://www.usbjd.org.

4. Bush, G. W. National Bone and Joint Decade proclamation. Office of the press secretary (2002).

5. Ilizarov, G. A. & Ledyaev, V. I. The replacement of long tubular bone defects by lengthening distraction osteotomy of one of the fragments. 1969. Clin Orthop Relat Res, 7-10 (1992).

6. Cancedda, R., Dozin, B., Giannoni, P. & Quarto, R. Tissue engineering and cell therapy of cartilage and bone. Matrix Biol 22, 81-91 (2003).

7. El-Ghannam, A. Bone reconstruction: from bioceramics to tissue engineering. Expert Rev Med Devices 2, 87-101 (2005).

Chapter Two

Tissue Engineering and Scaffold Properties

2.1 Short history of tissue engineering

It was Wolter JR who first used the phase "Tissue Engineering" in 1984 by accident to describe the organization of an endothelium-like membrane on the surface of a long-implanted, synthetic ophthalmic prosthesis. He did not mean to use "Tissue Engineering" as we use it today[1]. In 1985, Dr. Y.C. Fung used the term "tissue engineering" in a proposal for NSF funding (NSF tissue engineering report 2001). Conceptually, he described tissue engineering as using engineering methodologies to study the level of biological organization between cells and organs. Today, the widely accepted definition for tissue engineering is "an interdisciplinary field that applies the principles of engineering and the life sciences toward the development of biological substitutes that restore, maintain, or improve tissue function," thanks to the highly-cited review by Langer and Vacanti in Science (1993) [2]. The term "tissue engineering" was, in fact, ascribed to Langer and Vacanti by some scholars.

Recently, a comprehensive definition of tissue engineering was made by the Pittsburgh Tissue Engineering Initiative (PTEI):

"Tissue engineering is the field of biomedicine that unites biology, engineering and medicine to restore or replace tissues and organs damaged by disease, injury or congenital anomaly. It has the potential to revolutionize health care treatment, improving the health and quality of life for millions of people worldwide, while, at the same time, saving hundreds of millions of dollars each

year in associated health care costs."

In 1994 the PubMed search engine showed that there were 10 published papers with the key words "tissue engineering"; by 1996, that number had doubled, and by 1998, that number had doubled again. In the 12-year interim, the field of research in tissue engineering has exploded; there are currently 6356 published papers. Promising tissue engineering research is underway in North America, Europe, Japan, and other parts of the globe.

2.2 Approaches and key roles in tissue engineering

In general, there are three main approaches to tissue engineering (Figure 2-1):

(i) Use isolated cells or cell substitutes as cellular replacement parts, e.g., simple skin tissue engineering;

(ii) Use acellular biomaterials capable of inducing tissue regeneration, e.g., using calcium phosphate in substituting natural bone; and

(iii) Use a combination of cells and materials and cellular factors (typical tissue engineering)

Tissue engineering was started as an interdisciplinary field. It continues to move forward together with stem cell research, gene therapy, new materials innovation, and new cellular factor discovery. It also has contributed to other key techniques in physics, chemistry and biology. Although there is a long list of involved subjects, three of them are most important:

i) Cells (the fundamental and key role in building tissue),

ii) Scaffolds (the three dimension porous structure in supporting the cells)

iii) Cellular factors (promoting the growth and differentiation and possible function expression).

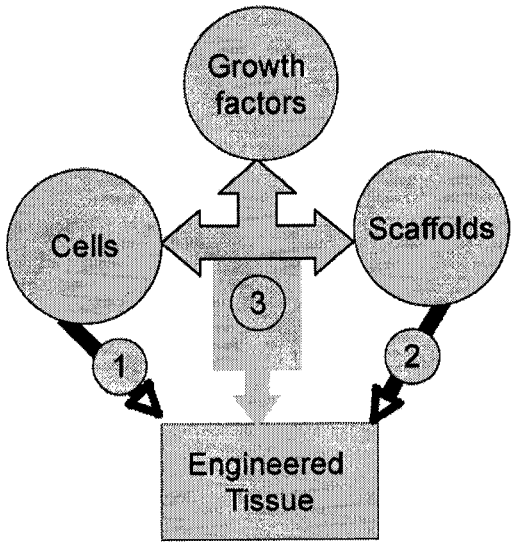

Figure 2- 1 Approaches and key roles for tissue engineering

2.3 Cells sources for tissue engineering

The stem cell and progenitor cell research development in recent years has opened new horizons for sources of cells issues for tissue engineering. In vitro tissue engineering requires the harvest of progenitor cells at various stages of differentiation for expansion and maturation on appropriate scaffolds in culture and subsequent implantation[3]. This form of tissue engineering is complicated by progenitor cell availability, difficulty in culturing some progenitor cell types, the need for cellular patterning and topographic control, and the need for providing a microcirculation for the development of larger, biologically meaningful tissues. Besides the cost is significantly high and the culture expansion is always at risk

of contamination. Moreover, there is evidence that autologous cells can invoke immunogenic with prolonged in-vitro culture. [4]

2.31 Progenitor cells

An ideal progenitor cell source should be easily expandable, non-immunogenic, and receptive to differentiation cues for the target tissue. The harvest of adequate numbers of progenitor cells for in vitro expansion can be problematic and depends on the cell source as well as the cell type. For example, the harvest of osteoblast is time consuming, relatively few cells are available after dissociation of bony tissue, and the cellular expansion rate is relatively low. Most differentiated progenitor cells have a limited capacity for self-renewal. Besides, regular culture techniques are not good for the long-term maintenance of certain cells. For example, the chondrocytes lose their normal morphology and function on Petri dishes or in flask culture. Hepatocytes rapidly lose their liver-specific characteristics when maintained in standard tissue culture[5] [6].

2.32 Stem cells

Stem cells are undifferentiated cells with a high proliferation capacity, the capability of self-renewal, and the potential for multilineage differentiation.

Totipotent stem cells are derived from the first two divisions of the fertilized oocyte and are able to form the embryo and the trophoblast of the placenta. A few days later, as the blastocyst forms, pluripotent stem cells can be harvested

from the inner cell mass and these are known as embryonic stem cells (ESCs). These cells can differentiate into any tissue arising from the three germ layers of the embryo but are not able to give rise to another embryo and its supporting tissues. Finally, multipotent stem cells can be harvested from mature tissues, and these are known as adult stem cells. Adult stem cells are being actively studied for tissue engineering because of the current ethical and sociopolitical debate

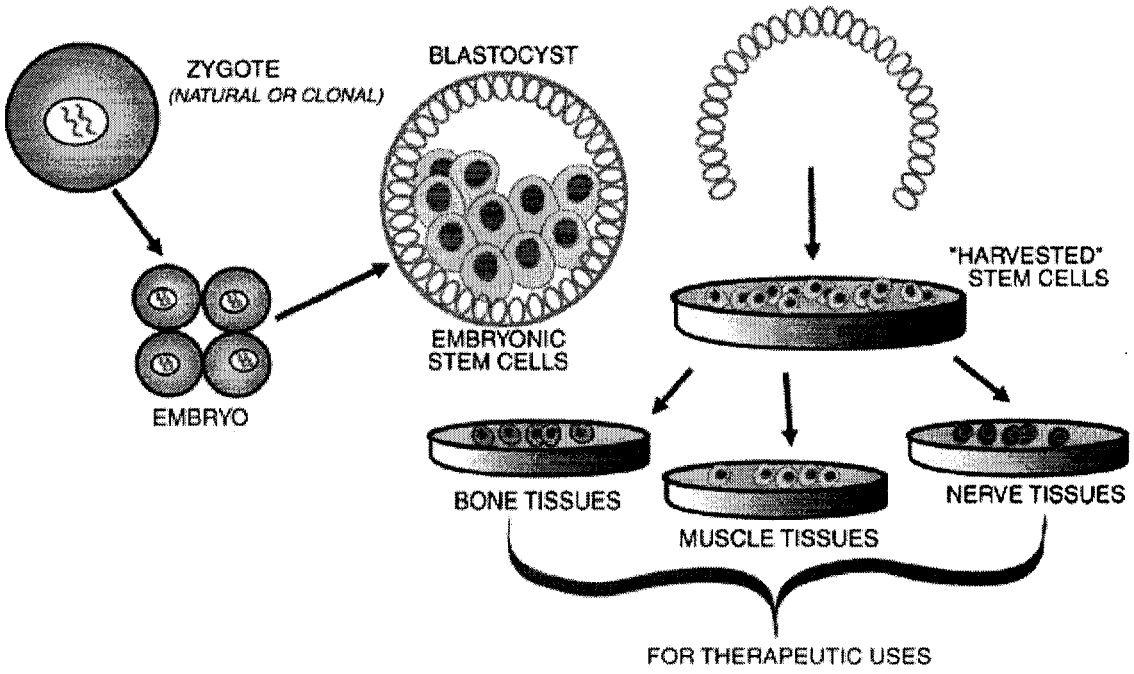

Figure 2- 2 Stem cells and their possible therapeutic application. (Courtesy ARHP, CA)

over the use of ESCs, and also because undifferentiated ESCs have been shown to give rise to teratomas and teratocarcinomas due to their unlimited proliferation capacity[6](Figure 2-1). Adult stem cells have been identified in bone marrow, trabecular bone, periosteum, muscle etc. As they were all derived from mesenchyme, they were also called mesenchymal stem cells (MSCs). MSCs are

low in immunogenic nature and they have significant differentiation plasticity[7-9] For instance, neural stem cells can differentiate into hematopoietic precursors and muscle cells, and dermal stem cells can give rise to neurons, glia, muscle, and fat cells. Bone marrow stromal cells can be induced to differentiate into osteoblasts, chondrocytes, myocytes, tendon cells, adipocytes, hepatocytes, or neural phenotypes.[7,9]Limitations with adult stem cell use include the lack of identifying markers and their scarcity in adults. It is estimated that 1 in 20 000 to 1 in 100 000 nucleated bone marrow cells is a stromal cell, representing 0.001%-0.01% of nucleated cells.[7,9] Whereas fat and muscle tissue are less cellular than bone marrow, the adult stem cell prevalence in these tissues may be as high as 1 per 4000 cells.[11] But adult stem cell numbers and their differentiation capacity decrease with advancing age. The density of MSCs in newborns is approximately 1 in 10, 000 as compared with 1 in 2, 000, 000 in an 80 year old.[10]

2.33 Cell lines

Most tissue engineering uses the primary cells harvested from human being or animals because they maintain the differentiated function and morphology. But the primary cells are difficult to survive and to maintain the differentiated functionality. They are also slow in proliferation or even display no proliferation. In addition, it is very expensive and elaborate to isolate the primary cells. For the convenience of in vitro experiments, cell lines were used. A cell line is a permanently established cell culture that will proliferate indefinitely given appropriate fresh medium and space. There are three ways to produce cell

lines, naturally occurred mutation or derivation from tumor cells and purposely infused to immortal cells. Usually the cell lines do not observe the Hayflick limit[12] and contact inhibition, but they still die. However as a group of cells, they are immortal. We compared the primary cells with cell lines in Form1. It is estimated that about 20% of human cell lines are different from the cells they are generally assumed to be.[13] The reason for this is that some cell lines exhibit vigorous growth and thus cross-contaminate cultures of other cell lines, in time overgrowing and displacing the original cells. The most common contaminant is the Hela cell line[14]. Cell lines can be used when general properties such as cell metabolism and morphology are investigated, but they should not be used for functionality of specific cells.[15,16] MG63 (ATCC CRL-1427) is a cell line harvested and derived from a 14 years old caucasian boy who suffered bone osteosarcoma, it maintains fibroblast morphology. This is a hypotriploid human cell line. The modal chromosome number was 66 occurring in 44% of cells. The rate of cells with higher ploidies was 2.0%. Eighteen to 19 marker chromosomes were common to all cells. Presently this is a good cell line that mimic the primary osteoblast.[17-19] Cell line SW1353 (ATCC HTB-94) was initiated by A. Leibovitz at the Scott and White Clinic, Temple, Texas in 1977 from a primary grade II chondrosarcoma of the right humerus obtained from a 72 years old female Caucasian. It functions like human chondrocytes and also maintains the chondrocytes morphology and functionality. Both cell lines are relatively stable in morphology and functionality. So far, no contamination or mutation has been

reported (ATCC data).

Table 2-1 Comparison of primary cells and cell lines

Cell type and source	Advantages	Disadvantages
Primary cells: Directly from human or animal tissue	1,retaining all differentiated function	1, very difficult to maintain vialbility and functionality 2, Slowly or not proliferate
Cell lines: Immortalized or tumor-derived	1, Relatively easy to maintain. 2, proliferate well, immortal.	1. Functional mutation 2, Safety issue

2.4 Cellular Factors and Challenges

Sustained delivery of osteogenic growth factors enhances bone growth in comparison with acute delivery of equivalents doses and certain bone growth factor combinations have enhancing effects on bone growth.[20-22] Cost-effective osseous tissue regeneration will depend on a better understanding of growth factor expression and doses in osteoneogenesis. Growth factors such as TGF-ß1, TGF-ß3, and BMP-2, BMP-4, and BMP-7 are all chondrogenic.[23-26] Other growth factors involved in chondrogenesis include IGF-I through VI, bFGF, connective tissue growth factor, and interleukin-1, interleukin-4, and interleukin-11. The activities of growth factors involved in chondrogenesis have yet to be fully defined, but they are known to be modulated by extracellular matrix proteins such as collagen, and by proteoglycans, which has implications for

chondrogenic scaffold development.[27-29]

FDA recently approved BMP-2 (Infuse, Medtronic Sofamore Danek, Memphis, TN) and BMP-7 (OP-1 Device, Stryker Biotech, Hopkinton, MA) products for limited orthopedic clinical applications. But commercially available BMP-2-containing and BMP-7-containing products deliver BMP doses of tens of milligrams per application, whereas naturally occurring BMPs comprise 0.1% of total bone weight, indicating that they exist in concentrations on the order of several micrograms per kilogram of bone. The cost-effective problem can also hinder the application of these cellular factors. Another significant challenge in osseous tissue engineering is the development of load-bearing, biodegradable scaffolds that are able to integrate into the surrounding bone and also serve as growth factor delivery system.[11]

2.5 Scaffolds for tissue engineering

Scaffolds provide cells with a suitable growth environment, optimal oxygen levels, and effective nutrient and waste transportation as well as mechanical integrity. Scaffolds also provided 3D environments to bring cells in close proximity so that they can organize to form tissues. While the scaffold is being degraded, the cells produced their own extracellular matrix (ECM) molecules and eventually formed 3D structures mimicking the native tissue in morphology.

Many factors affect the selection and properties of scaffold. These include but not limit to biocompatibility, porosity, pore size, surface properties, and pH, surface charge, and surface energy, biodegradability, mechanical properties, and

ideally, the ability to recruit progenitor cells. Several requirements have been identified as crucial for the production of tissue engineering scaffolds (Hutmacher, 2001).[30]

a) The scaffold should possess interconnecting pores of appropriate scale to favor tissue integration and vascularization.

b) They are made from material with controlled biodegradability or bio-resorbability so that tissue will eventually replace the scaffold.

c) They have appropriate surface chemistry to favor cellular attachment, differentiation and proliferation.

d) They possess adequate mechanical properties to match the intended site of implantation and handling.

e) They should not induce any adverse response.

f) They are easily fabricated into a variety of shapes and sizes.

2.51 Scaffold pore size and porosity

Pores are necessary for bone tissue formation because they allow migration and proliferation of progenitor cells, as well as vascularization. Besides, a porous surface improves mechanical interlocking between the implant biomaterial and the surrounding natural tissue, such as bone, providing greater mechanical stability at this critical interface.[31-33] Porosity is a physical property independent of the material and it is defined as the percentage of void space in a solid.

An ideal bone scaffold should have sufficient porosity to accommodate osteoblasts or osteoprogenitor cells to support cell proliferation and differentiation

and to enhance bone tissue formation. High porosity is important for scaffolds for any tissue engineering applications, including bone. High interconnectivities between pores are also desirable for uniform cell seeding and distribution, the diffusion of nutrients to and metabolites out from the cell/scaffold constructs.[34] Macroporosity (>50μm) has a strong impact on osteogenic outcomes, but microporosity (pore size <10 μm) and pore wall roughness play an important role as well. Hydroxyapatite ceramic rods with average pore size of 200 μm and smooth and dense pore walls failed to induce ectopic bone formation in dogs, in contrast to rods made from the same material with average pore size 400 μm but with rough and porous pore walls. Microporosity results in larger surface area that is believed to contribute to higher bone inducing protein adsorption as well as to ion exchange and bone-like apatite formation by dissolution and precipitation. Surface roughness enhances attachment, proliferation and differentiation of anchorage dependent bone forming cells.[33, 35]

Porous (pore size 150-500 μm) matrices with fully interconnected geometry and large surface-area-to-volume ratios facilitate cell in-growth and mass transfer of oxygen, nutrients, and metabolic byproducts. Small pores favored hypoxic conditions and induced osteochondral formation before osteogenesis, while large pores, that are well-vascularized, lead to direct osteogenesis (without preceding cartilage formation)[33]. Gradients in pore sizes are recommended for future studies focused on the formation of multiple tissues and tissue interfaces. There is a tradeoff between the degree of porosity and the scaffold's mechanical

stability, and this tradeoff must be balanced with the mechanical needs of the tissue to be replaced.

Scaffold pore size has been shown to influence cellular activity. The optimal scaffold pore size that allows maximal entry of cells as well as cell adhesion and matrix deposition has been shown to vary with different cell types[36, 37 38] . Scaffold pore size has been observed to influence adhesion, growth, and phenotype of a wide variety of cell types, notably endothelial cells, vascular smooth muscle cells, fibroblasts, osteoblasts, rat marrow cells, chondrocytes.[39] Scaffold heterogeneity has been shown to lead to variable cell adhesion and to affect the ability of the cell to produce a uniform distribution of extracellular matrix. A continuous in growth from the outer periphery was observed in the random pore size scaffolds, while scaffolds with same sized pores and solid walls promoted discontinuous ingrowth with bone islands throughout the whole scaffold. Scaffolds with same sized pores and porous walls resulted in both types of bone ingrowth[40]. It was hypothesized that discontinuous bone ingrowth may result in faster healing since bone will be forming not only from the margins but also throughout the whole space of the defect. These studies demonstrate the enhanced osteogenesis of porous versus solid implants, both at the macroscopic as well as the microscopic level.[33]

Hulbert et al[41] reported that the minimum pore size required to regenerate mineralized bone is generally considered to be 100 μm . In his study calcium aluminate cylindrical pellets with 46% porosity were implanted in dog femorals[41]

Large pores (100 - 150 and 150 - 200 μm) showed substantial bone ingrowth. Small pores (75 - 100 μm) resulted in ingrowth of non-mineralized osteoid tissue. Smaller pores (10 - 44 μm and 44 - 75 μm) were penetrated only by fibrous tissue. These results were correlated with normal Haversian systems that reach an approximate diameter of 100 - 200 μm.[41]

In conclusion, a pore size between 150-500μm with porosity >75% is a good choice for bone tissue engineering. This may vary depending on the cell size, cell morphology, scaffold degradation rate and the speed of ingrowth of blood vessels. It is also important to note that a larger pore size aids in the ingrowth of capillaries; but may also make it more difficult for cell organization into a 3D cluster and less of the cellular matrix will be formed.

2.52 Surface properties

The scaffold's surface is not only limited to the external surfaces, but also the interior surface of the pores which can be exposed to the cells and cellular factors. The nature of the surface can directly influence cellular response, ultimately affecting the rate and quality of new tissue formation. Initial events at the surface include the orientated adsorption of molecules from the surrounding fluid, creating a conditioned interface to which the cell responds. The gross morphology, as well as the microtopography and chemistry of the surface, determine which molecules can adsorb and how cells will attach and align themselves. The focal attachments made by the cells with their substrate

determine cell shape which, when transduced via the cytoskeleton to the nucleus, result in expression of specific phenotypes.[42, 43] Cell-adhesion molecule density affects the cellular migration rate. Too few molecules will result in cellular detachment from the surface, and too high a density of adhesion molecules will cause the cells to 'stick' and not migrate into the scaffold interstices.[4, 44-47]

2.53 Degradation and mechanical properties

Ideal scaffolds are degradable by cellular enzymes but must be stable long enough for the target cells to lay down their extracellular matrix[6, 48]. Premature degradation of a scaffold can negatively affect regenerated tissue volume, whereas scaffold persistence (e.g.,ceramics and silk) can inhibit tissue development. Moreover, it has been demonstrated that degradation of the same polymer can vary substantially between species, individuals, anatomic locations, and clinical situations, making it difficult to define optimal degradation rates for many scaffolds[11]. Because no single scaffold material is ideal, and because a single scaffold may not be ideal to support the various cell populations within a given tissue, the development of composite scaffolds is an active investigational area.[3, 34]

2.6 Challenges of tissue engineering

Tissue engineers have enjoyed fast development during the last decade due to the availability of resources and have contributed to exciting discoveries in stem cell research, innovations in material science and engineering technologies and

discoveries of all kinds of cellular factors and their possible carriers. Accompanying these advances, tissue engineering (especially cartilage and bone tissue engineering) has progressed notably in past decade. However, the challenges still remain; in particular, the complete restoration of the physiologic structural and mechanical properties of the native tissue. Engineering the complex architectures of these tissues may require the use of multiple cells types, composite scaffolds, novel fabrication techniques, or a combination of them all. Different cell types can influence each other in ways that cannot be reproduced through the application of one or two growth factors. Scaffolds must be fabricated such that they are capable of organizing different cell types and maintaining the cells' discrete phenotypic characteristics.

Notes to Chapter Two

1. Wolter, J. R. & Meyer, R. F. Sessile macrophages forming clear endothelium-like membrane on inside of successful keratoprosthesis. Trans Am Ophthalmol Soc 82, 187-202 (1984).

2. Langer, R. & Vacanti, J. P. Tissue engineering. Science 260, 920-6 (1993).

3. Sharma, B. & Elisseeff, J. H. Engineering structurally organized cartilage and bone tissues. Ann Biomed Eng 32, 148-59 (2004).

4. Meyer, U., Joos, U. & Wiesmann, H. P. Biological and biophysical principles in extracorporal bone tissue engineering. Part III. Int J Oral Maxillofac Surg 33, 635-41 (2004).

5. Hammond, J. S., Beckingham, I. J. & Shakesheff, K. M. Scaffolds for liver tissue engineering. Expert Rev Med Devices 3, 21-7 (2006).

6. Arosarena, O. Tissue engineering. Curr Opin Otolaryngol Head Neck Surg 13, 233-41 (2005).

7. Barry, F. P. & Murphy, J. M. Mesenchymal stem cells: clinical applications and biological characterization. Int J Biochem Cell Biol 36, 568-84 (2004).

8. Barry, F. P. Biology and clinical applications of mesenchymal stem cells. Birth Defects Res C Embryo Today 69, 250-6 (2003).

9. Devine, S. M., Peter, S., Martin, B. J., Barry, F. & McIntosh, K. R. Mesenchymal stem cells: stealth and suppression. Cancer J 7 Suppl 2, S76-82 (2001).

10. Salgado, A. J., Coutinho, O. P. & Reis, R. L. Bone tissue engineering: state of the art and future trends. Macromol Biosci 4, 743-65 (2004).

11. Muschler, G. F., Nakamoto, C. & Griffith, L. G. Engineering principles of clinical cell-based tissue engineering. J Bone Joint Surg Am 86-A, 1541-58 (2004).

12. Hayflick, L. The Limited In Vitro Lifetime Of Human Diploid Cell Strains. Exp Cell Res 37, 614-36 (1965).

13. MacLeod, R. A. et al. Widespread intraspecies cross-contamination of human tumor cell lines arising at source. Int J Cancer 83, 555-63 (1999).

14. Masters, J. R. HeLa cells 50 years on: the good, the bad and the ugly. Nat Rev Cancer 2, 315-9 (2002).

15. Nelson-Rees, W. A., Daniels, D. W. & Flandermeyer, R. R. Cross-contamination of cells in culture. Science 212, 446-52 (1981).

16. Nelson-Rees, W. A. Responsibility for truth in research. Philos Trans R Soc Lond B Biol Sci 356, 849-51 (2001).

17. Cenni, E. et al. Gene expression of bone-associated cytokines in MG63 osteoblast-like cells incubated with acrylic bone cement extracts in minimum essential medium. J Biomater Sci Polym Ed 13, 1283-94 (2002).

18. Hattar, S. et al. Behaviour of moderately differentiated osteoblast-like cells cultured in contact with bioactive glasses. Eur Cell Mater 4, 61-9 (2002).

19. Montanaro, L., Arciola, C. R., Campoccia, D. & Cervellati, M. In vitro effects on MG63 osteoblast-like cells following contact with two

roughness-differing fluorohydroxyapatite-coated titanium alloys. Biomaterials 23, 3651-9 (2002).

20. Scaduto, A. A. & Lieberman, J. R. Gene therapy for osteoinduction. Orthop Clin North Am 30, 625-33 (1999).

21. Lieberman, J. R. et al. The effect of regional gene therapy with bone morphogenetic protein-2-producing bone-marrow cells on the repair of segmental femoral defects in rats. J Bone Joint Surg Am 81, 905-17 (1999).

22. Woo, B. H. et al. Enhancement of bone growth by sustained delivery of recombinant human bone morphogenetic protein-2 in a polymeric matrix. Pharm Res 18, 1747-53 (2001).

23. Vehof, J. W., Takita, H., Kuboki, Y., Spauwen, P. H. & Jansen, J. A. Histological characterization of the early stages of bone morphogenetic protein-induced osteogenesis. J Biomed Mater Res 61, 440-9 (2002).

24. Vehof, J. W., Haus, M. T., de Ruijter, A. E., Spauwen, P. H. & Jansen, J. A. Bone formation in transforming growth factor beta-I-loaded titanium fiber mesh implants. Clin Oral Implants Res 13, 94-102 (2002).

25. Vehof, J. W. et al. Bone formation in transforming growth factor beta-1-coated porous poly(propylene fumarate) scaffolds. J Biomed Mater Res 60, 241-51 (2002).

26. Vehof, J. W., de Ruijter, A. E., Spauwen, P. H. & Jansen, J. A. Influence of rhBMP-2 on rat bone marrow stromal cells cultured on titanium fiber mesh. Tissue Eng 7, 373-83 (2001).

27. Guilak, F., Awad, H. A., Fermor, B., Leddy, H. A. & Gimble, J. M. Adipose-derived adult stem cells for cartilage tissue engineering. Biorheology 41, 389-99 (2004).

28. Goessler, U. R., Hormann, K. & Riedel, F. Tissue engineering with chondrocytes and function of the extracellular matrix (Review). Int J Mol Med 13, 505-13 (2004).

29. Goessler, U. R. et al. Expression of collagen and fiber-associated proteins in human septal cartilage during in vitro dedifferentiation. Int J Mol Med 14, 1015-22 (2004).

30. Sachlos, E. & Czernuszka, J. T. Making tissue engineering scaffolds work. Review: the application of solid freeform fabrication technology to the

production of tissue engineering scaffolds. Eur Cell Mater 5, 29-39; discussion 39-40 (2003).

31. Kuboki, Y. et al. BMP-induced osteogenesis on the surface of hydroxyapatite with geometrically feasible and nonfeasible structures: topology of osteogenesis. J Biomed Mater Res 39, 190-9 (1998).

32. Story, B. J., Wagner, W. R., Gaisser, D. M., Cook, S. D. & Rust-Dawicki, A. M. In vivo performance of a modified CSTi dental implant coating. Int J Oral Maxillofac Implants 13, 749-57 (1998).

33. Karageorgiou, V. & Kaplan, D. Porosity of 3D biomaterial scaffolds and osteogenesis. Biomaterials 26, 5474-91 (2005).

34. Liu, X. & Ma, P. X. Polymeric scaffolds for bone tissue engineering. Ann Biomed Eng 32, 477-86 (2004).

35. Yuan, H. et al. A preliminary study on osteoinduction of two kinds of calcium phosphate ceramics. Biomaterials 20, 1799-806 (1999).

36. Chvapil, M. Collagen sponge: theory and practice of medical applications. J Biomed Mater Res 11, 721-41 (1977).

37. Chvapil, M. et al. Laboratory and clinical testing of an intravaginal contraceptive collagen sponge. Contraception 15, 693-703 (1977).

38. Tsuruga, E., Takita, H., Itoh, H., Wakisaka, Y. & Kuboki, Y. Pore size of porous hydroxyapatite as the cell-substratum controls BMP-induced osteogenesis. J Biochem (Tokyo) 121, 317-24 (1997).

39. Zeltinger, J., Sherwood, J. K., Graham, D. A., Mueller, R. & Griffith, L. G. Effect of pore size and void fraction on cellular adhesion, proliferation, and matrix deposition. Tissue Eng 7, 557-72 (2001).

40. Simon, J. L. et al. Engineered cellular response to scaffold architecture in a rabbit trephine defect. J Biomed Mater Res A 66, 275-82 (2003).

41. Hulbert, S. F. et al. Potential of ceramic materials as permanently implantable skeletal prostheses. J Biomed Mater Res 4, 433-56 (1970).

42. Boyan, B. D., Hummert, T. W., Dean, D. D. & Schwartz, Z. Role of material surfaces in regulating bone and cartilage cell response. Biomaterials 17, 137-46 (1996).

43. Boyan, B. D., Lohmann, C. H., Romero, J. & Schwartz, Z. Bone and cartilage tissue engineering. Clin Plast Surg 26, 629-45, ix (1999).

44. Wiesmann, H. P., Joos, U. & Meyer, U. Biological and biophysical principles in extracorporal bone tissue engineering. Part II. Int J Oral Maxillofac Surg 33, 523-30 (2004).

45. Meyer, U., Joos, U. & Wiesmann, H. P. Biological and biophysical principles in extracorporal bone tissue engineering. Part I. Int J Oral Maxillofac Surg 33, 325-32 (2004).

46. Wiesmann, H. P., Nazer, N., Klatt, C., Szuwart, T. & Meyer, U. Bone tissue engineering by primary osteoblast-like cells in a monolayer system and 3-dimensional collagen gel. J Oral Maxillofac Surg 61, 1455-62 (2003).

47. MacArthur, B. D., Please, C. P., Taylor, M. & Oreffo, R. O. Mathematical modelling of skeletal repair. Biochem Biophys Res Commun 313, 825-33 (2004).

48. Andersson, H. & van den Berg, A. Microfabrication and microfluidics for tissue engineering: state of the art and future opportunities. Lab Chip 4, 98-103 (2004).

Chapter Three

Biomaterials for Bone and Cartilage Tissue Engineering

3.1 Introduction

Over the past 30 years, biomaterials have been developed and proposed as ideal scaffolds for bone and cartilage tissue engineering, yet very few have demonstrated clinical efficacy or have been clinically accepted. For bone and cartilage tissue engineering biomaterials, regardless of whether they are permanent or biodegradable, naturally occurring or synthetic, the scaffolds need to be biocompatible, osteoinductive, osteoconductive, osteointegrative[1], porous and mechanically compatible with native bone. These materials provide cell anchorage sites, mechanical stability and structural guidance. In vivo, the scaffolds provide the interface to respond to physiologic changes and aid in remodeling the extracellular matrix (ECM) to integrate with the surrounding native tissue.

3.11 Bone

There are two types of bones: cortical bones and cancellous bones. Both are relatively hypocellular and stress-oriented. Cortical bone makes up 80% of the skeleton, and is found in the outer shell of bone. It is composed of tightly-packed osteons or Haversian systems. Cortical bone has a slow turnover rate, a relatively high Young's modulus [2](Table 3-1), and a high resistance to bending and torsion.

Cancellous bones are less dense and more elastic than cortical bone, have smaller Young's modulus[2] (Table 3-1), and higher turnover rates. They are found in the epiphyseal and metaphyseal regions of long bones and throughout the interior of short bones. The bone tissue consists of three functional cells: osteoblasts, osteocytes and osteoclasts. Osteoblast is the non-mineralised component of bone matrix, e.g., osteoid. Osteocytes maintain bone and comprise 90% of all cells in the mature skeleton.

Osteoclasts act in opposition to osteoblasts, and their functions are to resorb bone tissue. Thus bone formation and resorption are coupled. Osteoblasts are usually differentiated from mesenchymal progenitor cells. They produce pro- å1 collagen (a major component of osteoid), osteocalcin and bone morphogenetic proteins (BMP). They initiate mineralization of osteoid material, possibly by modulating electrolyte fluxes between the extracellular fluid volume and osseous fluid.

Bone matrix is made up of organic components (40% dry weight in mature bone) and inorganic components (60% dry weight). The organic components include collagen I(up to 90% of the bone matrix), proteoglycans, osteocalcin (makes up 10-20% of the collagenous protein of bone) and various growth factors. Collagen provides bone's tensile strength, while proteoglycans contribute to the compressive strength of bone and osteocalcin attracts osteoclasts.

The inorganic component is mainly carbonatehydroxyapatite, approximated by the formula:

$$(Ca,X)_{10}(PO_4,HPO_4,CO_3)(OH,Y)_2$$

where X are cations (Mg,Na, K, Sr, Zn) [3, 4] that can substitute for the calcium ions, and Y are anions (chloride or fluoride ions) that can substitute for the hydroxyl group. Usually it is idealized as calcium hydroxyapatite.

$$Ca_{10}(PO_4)_6(OH)_2$$

The stoichiometric Ca to P molar ratio value for pure hydroxyapatite is 1.67. But the Ca to P molar ratio of animal bones ranges around 1.67, depending on the species, age, and type of bone.[5] Carbonatehydroxyapatite provides the compressive strength of bone. It is responsible for mineralization of the matrix. Mineralization is the transformation of hydroxyapatite from a soluble form to a solid form, starting at multiple nucleation sites and then spreading by accretion, or crystal growth. Primary mineralization occurs in gaps in collagen, while secondary mineralization occurs at the periphery.

3.12 Cartilage

Cartilage is a form of connective tissue composed of chondrocytes and a specialized extracellular matrix. This matrix consists of water, collagen, proteoglycans and other components such as adhesives and lipids. There are several different types of cartilage. Articular cartilage contains more collagen type II than other types of hyaline cartilage. It covers the bones of synovial joints and functions in load distribution and decreasing friction. The articular cartilage matrix

is avascular, aneural and alymphatic, relying on the process of diffusion to provide nutrients for the chondrocytes.

Chondrocytes are important in the control of matrix turnover through production of collagen, proteoglycans and enzymes for cartilage metabolism. Articular collagen consists 90-95% type II collagen (accounting 10-20% of wet matrix weight) and a small amounts of types V, VI, IX, X and XI collagen. Collagen forms a cartilaginous framework which provides tensile strength.[6] Articular cartilage is a highly hydrated material. Water distribution varies, making up 65% of wet weight at the deep zone and 80% at the surface. Weight bearing capacity is made possible through regional changes in water content which allow deformation of the cartilage surface in response to stress. Water provides nutrition and lubrication of cartilage.

Other types of cartilage include fibrocartilage, elastic cartilage, and physeal cartilage. Fibrocartilage contains abundant thick bundles of mostly type I collagen which can be seen with the light microscope. This type of cartilage is found at ligament and tendon insertions into bone, in menisci, intervertebral discs etc. Fibrocartilage provides good resistance to shear and compression forces. Elastic cartilage is characterized by the presence of elastic fibers within the matrix that increase elasticity in tissues such as the external ear and trachea. Physeal cartilage provides longitudinal growth to immature long bones.

3.2. Three generations of biomaterials

Hench[7] *et al.* divided biomaterials into three generations according to their properties. During the 1960's and 1970's, the first generation of biomaterials was developed for use inside the human body. The goal of all early biomaterials was to "achieve a suitable combination of physical properties to match those of the replaced tissue with a minimal toxic response in the host."[8, 9] By 1980, there were more than 50 implanted devices (prostheses) in clinical use made from 40 different materials and some 2-3 million prosthetic parts were implanted in patients in the United States annually. A common feature of most of the materials was their biological "inertness."[8-11] The principle of these biomaterials development was to reduce the immune response to the foreign body to a minimum.

The second generation of biomaterials are "bioactive" components that elicit a controlled action and reaction in the physiological environment.[10, 12, 13] These bioactive materials include varieties of orthopedic and dental implants, such as various compositions of bioactive glasses, ceramics, glass-ceramics, and composites. In the mid-1980's synthetic hydroxyapatite (HA) ceramics began to be routinely used as porous implants, powders, and coatings on metallic prostheses to provide bioactive fixation.[12, 14, 15]These second generation biomaterials were resorbable biomaterials that exhibited clinically relevant controlled chemical breakdown and resorption. In this manner, the interface

Table 3 1 Mechanical properties of human bone and cartilage[2, 6]

Type of bone	Direction and type of load	Ultimate strength(MPa)	Modulus of elasticity(GPa)
Cortical bone (mid femoral)	Longitudinal tension	133	17
	Longitudinal compression	193	17
	Longitudinal shear	68	3
	Transverse tension	51	11.5
	Transverse compression	33	11.5
Cancellous bone	Axial	5.3-6.8	0.441-0.445
Cartilage	Longitudinal Tension	3.7-10.5	0.7-15.3(MPa)

problem is resolved when the foreign material is replaced by regenerating tissues, and ultimately results in no significant difference between the implant site and the host tissue.[7, 12]

Living tissues can respond to changing physiological loads or biochemical stimuli, but synthetic materials cannot which limits the lifetime of artificial body parts made by these biomaterials. It also signals that we have reached a limit to our current medical paradigm that emphasizes replacement of tissues. The third generation of biomaterials is clinically demanding that they must be cell and gene-activating materials.[7, 16] Third-generation biomaterials are being designed to stimulate specific cellular responses at the molecular level. The separate concepts of bioactive materials and resorbable materials must converge:

bioactive materials are being made resorbable and resorbable polymers are being made bioactive. Molecular modifications of resorbable polymer systems elicit specific interactions with cell integrins and thereby direct cell proliferation, differentiation, and extracellular matrix production and organization.[7] Third-generation biomaterials involve molecular tailoring of resorbable polymers for specific cellular responses by immobilizing specific proteins, peptides, and other biomolecules onto a material which mimic the extracellular matrix (ECM) environment and provide a multifunctional cell adhesive surface.[17-20]

3.3 Selection criteria of materials for tissue engineering

Lanza, Langer and Vacanti[21] stated that the key role of an ideal material is to elicit a desirable cell response. It should support tissue growth (such as promoting cell-cell communication, cell availability to nutrients, growth factors etc.) guide tissue response (such as enhancing some cell responses while inhibiting others), and enhance cell attachment and cell activation. The biomaterial also needs to prevent unwanted biological response (e.g. block antibodies against allogenic or xenografts). In addition it should possess: i) manufacturing feasibility (sufficient quantity); ii) capability of forming material into a final product design, iii) mechanical properties for short-term function that do not interfere with long-term function; iv) low or negligible toxicity of degradation.

3.4 Bioceramics

Calcium phosphate was first used clinically by Albee in 1922 and 30 years later

by Ray.[3, 22] With the development of tissue engineering and nanotechnology, more research has been focused on calcium phosphate ceramics.

The commercially available calcium phosphate ceramics can be divided by composition into at least four categories as shown in Table 2 and 3: (1) hydroxyapatite; (2) β-tricalcium phosphate, $Ca_3(PO_4)_2$; (3) biphasic calcium phosphate, a mixture of hydroxyapatite and beta-tricalcium phosphate; and (4) unsintered CaP or a calcium deficient apatite $(Ca,Na)_{10}(PO_4\ HPO_4)_6(OH)_2$.

3.41 CaP bioceramics in tissue engineering.

CaP biomaterials have a high affinity for proteins, making them ideal carriers for bioactive peptides, bone growth factors, or MSCs.[23-25] It is generally accepted that CaP biomaterials are osteoconductive but not osteoinductive, but there are reports of its possible osteoinductive properties.[26, 27] This osteoinductive property was found to be associated with the specific geometry of CaP biomaterial. Reddi attributed this phenomenon to the binding of an optimum amount of endogenous bone morphogenetic protein (BMP) in circulation to the CaP biomaterial allowing the biomaterial to become osteoinductive[24]. It was concluded that the geometry of the BMP carrier is one of the important factors controlling the efficacy of the cell phenotype induction.[27] These investigators determined that the optimal pore size of porous blocks of hydroxyapatite as BMP carriers to induce direct bone formation was 100 to 400 μm. Ohgushi and Toquet et al respectively reported that MSCs from bone marrow can be cultured in porous CaP biomaterials (ceramic hydroxyapatite, coralline hydroxyapatite,

biphasic CaP) in vitro and implanted as a tissue engineered material for bone regeneration.[23, 25, 28]However, dissolution and degradation of the bioceramics remains a problem for independent bone regeneration. In vitro dissolution of CaP materials depends on the composition (hydroxyapatite versus b-tricalcium phosphate), and sources of the materials of similar composition (hydroxyapatite from natural or synthetic origin). The extent of dissolution will depend on particle size, porosity (microporosity and macroporosity), specific surface area, and crystallinity (reflecting crystal size and perfection).[3, 22, 29, 30] For synthetic CaP, the extent of dissolution in acidic buffers is the highest for amorphous calcium phosphate, followed by tetracalcium phosphate, alpha-tricalcium phosphate, β-tricalcium phosphate, and is the lowest for hydroxyapatite.[30] With biphasic calcium phosphates, the dissolution property depends on the hydroxyapatite to beta-tricalcium phosphate ratio: the higher the ratio, the lower the extent of dissolution.[22] In vivo data confirm the in vitro observations on comparative degradation of CaP biomaterials. The factors that influence dissolution properties in vitro (composition, surface area, surface topography, microporosity and macroporosity) also were operative factors in vivo. Therefore, it is possible to use an appropriate CaP material with appropriate biodegradation for particular clinical applications. With biphasic calcium phosphates, control of biodegradation (and bioactivity) by adjusting the hydroxyapatite to beta-tricalcium phosphate ratio has been suggested.[22]

CaP ceramics are bioactive, osteoconductive and conditionally osteoinductive

with very strong compressive mechanical strength but poor tensile mechanical properties. CaP is very good to use as a coating materials for biotolerant metals but is poor in independently as load bearing scaffolds. And the poor degradation rate in vivo also limits its using in large amount in vivo.

3.5 Polymeric materials

The scaffolds for bone tissue engineering should be fabricated from biocompatible polymers that do not have the potential to elicit an immunological or foreign body reaction. The chosen polymer can degrade at a controlled rate in concert with tissue regeneration. The degradation products should not be toxic and must be easily excreted by metabolic pathways. Many types of polymeric materials have been used for bone tissue engineering.[31, 32, 7] They can be simply categorized as naturally derived materials (such as collagen, fibrin, chitosan, alginates) and synthetic polymers (such as poly(lactic acid) (PLA), poly(glycolic acid) (PGA), and their copolymers PLGA). Naturally derived materials have the

Table 3-2 Synthetic calcium phosphate ceramics and the commercially products

Synthetic CaP ceramics	Molecular structure	Commercial Products
Calcium hydroxyapatite	$Ca_{10}(PO_4)_6(OH)_2$	Calcitite®, Osteograf®
beta-tricalcium phosphate	$Ca_3(PO_4)_2$	Synthograf®, Augmen®
Biphasic Calcium Phosphate		Triosit®, MBCP®, Osteosynt®
Calcium deficient apatite	$Ca,Na)_{10}(PO_4\ HPO_4)_6(OH)_2$	Osteogen®

Table 3-3 Natural Calcium phosphate products and the commercial product

Natural CaP ceramics	Source	Commercial Products
Cadaver bones	Human	Tissue bank products
Bovine bone derived	cow	BioOss®, Endobone®, BoneAp®
Coral derived	Coralline hydroxyapatite	Interpore®, Pro-Osteon®

potential advantage of biological recognition that may positively support cell adhesion and function, but they may exhibit immunogenicity and contain pathogenic impurities. There is also less control over their mechanical properties and biodegradability. An advantage of synthetic polymers is that they are reproducible at large-scale production with consistent properties of strength, degradation rate and microstructure. Therefore, synthetic biodegradable polymers have already been widely used as vehicles for cell transplantation and scaffolds for tissue engineering. The drawbacks of synthetic biodegradable

polymers are that the degradation products always initiate some immunity problems and accelerate the degradation. Some synthetic polymers degrade in a bulky style and the scaffolds can be cracked in short pieces that limit their use in tissue engineering.

3.51 Synthetic Polymers

The following section presents an overview of the synthetic biodegradable polymers that are currently being used or investigated for use in wound closure (sutures, staples); orthopedic fixation devices (pins, rods, screws, tacks, ligaments); dental applications (guided tissue regeneration); cardiovascular applications (stents, grafts); and intestinal applications (anastomosis rings). Most of the commercially available biodegradable devices are polyesters composed of homopolymers or copolymers of glycolide and lactide. There are also devices made from copolymers of trimethylene carbonate and caprolactone, and a suture product made from polydioxanone.

Polyglycolide (PGA)

Polyglycolide is the simplest linear aliphatic polyester. PGA was used to develop the first totally synthetic absorbable suture, marketed as Dexon in the 1960s by Davis and Geck, Inc. (Danbury, CT). Glycolide monomer is synthesized from the dimerization of glycolic acid. Ring-opening polymerization yields high-molecular-weight materials, with approximately 1—3% residual monomer present (Figure3-1A). PGA is highly crystalline (45—55%), with a high melting point (220—225°C) and a glass-transition temperature of 35—40°C. Because of the

high degree of crystallization, PGA is not soluble in most organic solvents; highly fluorinated organics such as hexafluoroisopropanol being exceptions. Fibers from PGA exhibit high strength and modulus and are too stiff to be used as sutures except in the form of braided material. Sutures of PGA lose about 50% of their strength after 2 weeks and 100% at 4 weeks, and are completely absorbed in 4—6 months. In an effort to reduce the stiffness of the resulting fibers, glycolide acid has been copolymerized with other monomers.

Polylactide (PLA)

Lactide is the cyclic dimer of lactic acid that exists as two optical isomers, d and l. L-lactide is the naturally occurring isomer, and d,l-lactide is the synthetic blend of d-lactide and l-lactide. The homopolymer of l-lactide (LPLA) is a semicrystalline polymer. These types of materials exhibit high tensile strength and minimal elongation, and consequently have a high modulus that makes them more suitable for load-bearing applications such as in orthopedic fixation and sutures. Poly(dl-lactide) (DLPLA) is an amorphous polymer exhibiting a random distribution of both isomeric forms of lactic acid, and is unable to arrange into an organized crystalline structure. This material has lower tensile strength, increased elongation, and a higher degradation rate, making it more attractive as a drug delivery system. Poly(l-lactide) is about 37% crystalline, with a melting point of 175—178°C and a glass-transition temperature of 60—65°C. The degradation time of LPLA is much slower than that of DLPLA, requiring more than two years to be completely absorbed.

Copolymers of l-lactide and dl-lactide have been prepared to disrupt the crystallinity of l-lactide and accelerate the degradation process, thus providing control over the degradation of the system.[33]

Using the polyglycolide and poly(l-lactide) properties as a starting point, it is possible to copolymerize the two monomers to extend the range of homopolymer properties (Figure3-1B). Copolymers of glycolide with both l-lactide and dl-lactide have been developed for device and drug delivery applications. It is important to note that there is not a linear relationship between the copolymer composition and the mechanical and degradation properties of the materials. For example, a copolymer of 50% glycolide and 50% dl-lactide degrades faster than either homopolymer (see Figure3-1C). Copolymers of l-lactide with 25—70% glycolide are amorphous due to the disruption of the regularity of the polymer chain by the other monomer. A copolymer of 90% glycolide and 10% l-lactide was developed by Ethicon as an absorbable suture material under the trade name of Vicryl. It absorbs within 3—4 months but has a slightly longer strength-retention time.

PGA, PLA, and their copolymer PLGA, are the most popular and widely used synthetic polymeric materials in bone tissue engineering.[32, 34, 35]These polymers, having a long history of use as degradable surgical sutures and have gained FDA approval for certain human use and are reasonably biocompatible. The ester bonds in these polymers are hydrolytically labile, and these polymers degrade by non-enzymatic hydrolysis.

The degradation products of PGA, PLA and PLGA are nontoxic, natural metabolites and are eventually eliminated from the body in the form of carbon dioxide, carbonate and water. The degradation rates of these polymers can be tailored to satisfy requirements ranging from several weeks to several years by altering the chemical composition (e.g. the LA/GA ratio in the PLGA copolymers), crystallinity, molecular weight[36-38], and molecular weight distribution. Although these polymers have already been widely used in bone tissue engineering research, there are ongoing research efforts aimed at improving the functionality of these polymers to further expand their applications.

3.52 Limitations of synthetic biomaterials

The degradation of synthetic polymers under both in vitro and in vivo conditions, releases acidic by-products which raise concerns that the scaffold microenvironment may not be ideal for tissue growth. Lactic acid is releases from PLLA during degradation[39], reducing the pH, which further accelerates the degradation rate due to autocatalysis[40, 41]resulting in a highly acidic environment adjacent to the polymer. Such an environment may adversely affect cellular function.[42] Cells attached to scaffolds are faced with several weeks of in vitro culturing before the tissue is suitable for implantation. During this period, even small pH changes (6.8-7.5) in the scaffold microenvironment can significantly affect bone marrow stromal cell expression of osteoblastic phenotypic markers.[42] Furthermore, particles released during polymer degradation can affect bone-remodeling processes[43] along with eliciting an inflammatory response and

inducing bone resorption *in vivo*.[44, 45]

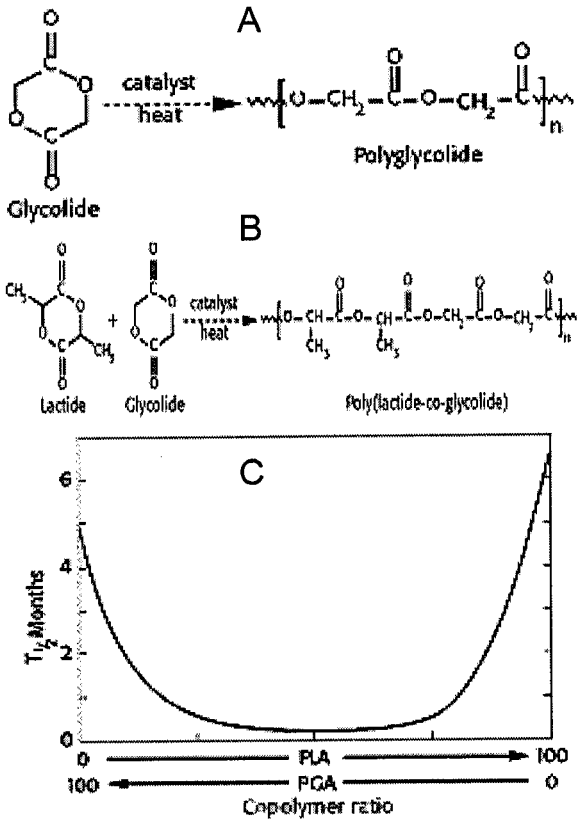

Figure 3-1 PGA, PLGA reaction and half-life of PLA and PGA homopolymers and copolymers implanted in rat tissue. (Courtesy of Journal of Biomedical Materials Research, 11:711, 1977.)

3.6 Composite polymer ceramic scaffolds

Each single polymer and ceramic material has its own characteristic advantages and disadvantages. Composite materials often show an excellent balance between strength and toughness and usually improved characteristics compared to their individual components. As a matter of fact, natural bone matrix is an organic/inorganic composite material of collagen and apatite. From this point of view, composite materials are a better choice for bone tissue

engineering scaffolds.[46-50] It is well established that hydroxyapatite (HA) mimics the natural bone mineral and has been found to possess good mechanical and osteoconductive properties.[47, 49-51] Our group developed highly porous biodegradable chitosan/apatite composite scaffolds through a thermally induced phase separation technique. Porosity achieved was as high as 95%. The mechanical properties of the composite scaffolds were significantly improved over those of the pure polymer scaffolds. The compressive modulus reached the same range as trabecular bone.[47, 49] The results consistently suggest that the strategy of using composite scaffolds of biodegradable polymers and bone mineral-like inorganic compounds is a viable approach in bone tissue engineering.

Notes to Chapter Three

1. LeGeros, R. Z. & Craig, R. G. Strategies to affect bone remodeling: osteointegration. J Bone Miner Res 8 Suppl 2, S583-96 (1993).

2. Cullinane DM, E. T. Biomechanics of bone. In: Bilezikian JP, Raisz LG, Rodan GA, editors. Principles of bone biology. 17-32 (2002).

3. LeGeros, R. Z. Properties of osteoconductive biomaterials: calcium phosphates. Clin Orthop Relat Res, 81-98 (2002).

4. LeGeros, R. Z. Calcium phosphate materials in restorative dentistry: a review. Adv Dent Res 2, 164-80 (1988).

5. LeGeros, R. Z. Calcium phosphates in oral biology and medicine. Monogr Oral Sci 15, 1-201 (1991).

6. Parsons, J. R. Cartilage. In: Black, J., and Hastings, G., eds. Handbook of Biomaterials Properties. 40-46 (1998).

7. Hench, L. L. & Polak, J. M. Third-generation biomedical materials. Science 295, 1014-7 (2002).

8. Hench, L. L. Biomaterials: a forecast for the future. Biomaterials 19, 1419-23 (1998).

9. Hench, L. L. Biomaterials. Science 208, 826-31 (1980).

10. Hench, L. L. Bioactive ceramics. Ann N Y Acad Sci 523, 54-71 (1988).

11. Hench, L. L. Ceramics, glasses, and composites in medicine. Med Instrum 7, 136-44 (1973).

12. Hench, L. L., Xynos, I. D. & Polak, J. M. Bioactive glasses for in situ tissue regeneration. J Biomater Sci Polym Ed 15, 543-62 (2004).

13. Thompson, I. D. & Hench, L. L. Mechanical properties of bioactive glasses, glass-ceramics and composites. Proc Inst Mech Eng [H] 212, 127-36 (1998).

14. Hench, L. L. & Wilson, J. Surface-active biomaterials. Science 226, 630-6 (1984).

15. Saravanapavan, P. et al. Binary CaO-SiO(2) gel-glasses for biomedical applications. Biomed Mater Eng 14, 467-86 (2004).

16. Polak, J. & Hench, L. Gene therapy progress and prospects: in tissue engineering. Gene Ther 12, 1725-33 (2005).

17. Kim, B. S., Putnam, A. J., Kulik, T. J. & Mooney, D. J. Optimizing seeding and culture methods to engineer smooth muscle tissue on biodegradable polymer matrices. Biotechnol Bioeng 57, 46-54 (1998).

18. Kim, B. S. & Mooney, D. J. Development of biocompatible synthetic extracellular matrices for tissue engineering. Trends Biotechnol 16, 224-30 (1998).

19. Ratner, B. D. The engineering of biomaterials exhibiting recognition and specificity. J Mol Recognit 9, 617-25 (1996).

20. Ratner, B. D. Surface modification of polymers: chemical, biological and surface analytical challenges. Biosens Bioelectron 10, 797-804 (1995).

21. Robert Lanza, R. L., Joseph Vacanti. Principles of tissue engineering (academic press, 2000).

22. LeGeros, R. Z., Lin, S., Rohanizadeh, R., Mijares, D. & LeGeros, J. P. Biphasic calcium phosphate bioceramics: preparation, properties and applications. J Mater Sci Mater Med 14, 201-9 (2003).

23. Ohgushi, H. & Caplan, A. I. Stem cell technology and bioceramics: from cell to gene engineering. J Biomed Mater Res 48, 913-27 (1999).

24. Reddi, A. H. Morphogenesis and tissue engineering of bone and cartilage: inductive signals, stem cells, and biomimetic biomaterials. Tissue Eng 6, 351-9 (2000).

25. Toquet, J. et al. Osteogenic potential in vitro of human bone marrow cells cultured on macroporous biphasic calcium phosphate ceramic. J Biomed Mater Res 44, 98-108 (1999).

26. Ripamonti, U., Ma, S. & Reddi, A. H. The critical role of geometry of porous hydroxyapatite delivery system in induction of bone by osteogenin, a bone morphogenetic protein. Matrix 12, 202-12 (1992).

27. Kuboki, Y. et al. BMP-induced osteogenesis on the surface of hydroxyapatite with geometrically feasible and nonfeasible structures: topology of osteogenesis. J Biomed Mater Res 39, 190-9 (1998).

28. Ohgushi, H., Miyake, J. & Tateishi, T. Mesenchymal stem cells and bioceramics: strategies to regenerate the skeleton. Novartis Found Symp 249, 118-27; discussion 127-32, 170-4, 239-41 (2003).

29. Koerten, H. K. & van der Meulen, J. Degradation of calcium phosphate ceramics. J Biomed Mater Res 44, 78-86 (1999).

30. LeGeros, R. Z. Biodegradation and bioresorption of calcium phosphate ceramics. Clin Mater 14, 65-88 (1993).

31. Liu, X. & Ma, P. X. Polymeric scaffolds for bone tissue engineering. Ann Biomed Eng 32, 477-86 (2004).

32. Athanasiou, K. A., Niederauer, G. G. & Agrawal, C. M. Sterilization, toxicity, biocompatibility and clinical applications of polylactic acid/polyglycolic acid copolymers. Biomaterials 17, 93-102 (1996).

33. Yang, S., Leong, K. F., Du, Z. & Chua, C. K. The design of scaffolds for use in tissue engineering. Part I. Traditional factors. Tissue Eng 7, 679-89 (2001).

34. Stock, U. A. & Mayer, J. E., Jr. Tissue engineering of cardiac valves on the basis of PGA/PLA Co-polymers. J Long Term Eff Med Implants 11, 249-60 (2001).

35. Athanasiou, K. A., Agrawal, C. M., Barber, F. A. & Burkhart, S. S. Orthopaedic applications for PLA-PGA biodegradable polymers. Arthroscopy 14, 726-37 (1998).

36. Cenni, E. et al. Gene expression of bone-associated cytokines in MG63 osteoblast-like cells incubated with acrylic bone cement extracts in minimum essential medium. J Biomater Sci Polym Ed 13, 1283-94 (2002).

37. Hattar, S. et al. Behaviour of moderately differentiated osteoblast-like cells cultured in contact with bioactive glasses. Eur Cell Mater 4, 61-9 (2002).

38. Montanaro, L., Arciola, C. R., Campoccia, D. & Cervellati, M. In vitro effects on MG63 osteoblast-like cells following contact with two roughness-differing fluorohydroxyapatite-coated titanium alloys. Biomaterials 23, 3651-9 (2002).

39. Reed, A. M., Gilding, D. K. & Wilson, J. Biodegradable elastomeric biomaterials--polyethylene oxide/polyethylene terephthalate copolymers. Trans Am Soc Artif Intern Organs 23, 109-15 (1977).

40. Vert, M., Mauduit, J. & Li, S. Biodegradation of PLA/GA polymers: increasing complexity. Biomaterials 15, 1209-13 (1994).

41. Vert, M., Li, S. M. & Garreau, H. Attempts to map the structure and degradation characteristics of aliphatic polyesters derived from lactic and glycolic acids. J Biomater Sci Polym Ed 6, 639-49 (1994).

42. Kohn, D. H., Sarmadi, M., Helman, J. I. & Krebsbach, P. H. Effects of pH on human bone marrow stromal cells in vitro: implications for tissue engineering of bone. J Biomed Mater Res 60, 292-9 (2002).

43. Wake, M. C., Gerecht, P. D., Lu, L. & Mikos, A. G. Effects of biodegradable polymer particles on rat marrow-derived stromal osteoblasts in vitro. Biomaterials 19, 1255-68 (1998).

44. Bergsma, J. E. et al. In vivo degradation and biocompatibility study of in vitro pre-degraded as-polymerized polyactide particles. Biomaterials 16, 267-74 (1995).

45. Suganuma, J. et al. In vivo evaluation of collagen-coated Dacron fiber in bone. Clin Mater 15, 43-50 (1994).

46. Zhang, R. & Ma, P. X. Poly(alpha-hydroxyl acids)/hydroxyapatite porous composites for bone-tissue engineering. I. Preparation and morphology. J Biomed Mater Res 44, 446-55 (1999).

47. Zhang, Y. & Zhang, M. Synthesis and characterization of macroporous chitosan/calcium phosphate composite scaffolds for tissue engineering. J Biomed Mater Res 55, 304-12 (2001).

48. Lu, H. H., El-Amin, S. F., Scott, K. D. & Laurencin, C. T. Three-dimensional, bioactive, biodegradable, polymer-bioactive glass composite scaffolds with improved mechanical properties support collagen synthesis and mineralization of human osteoblast-like cells in vitro. J Biomed Mater Res 64A, 465-74 (2003).

49. Zhang, Y., Ni, M., Zhang, M. & Ratner, B. Calcium phosphate-chitosan composite scaffolds for bone tissue engineering. Tissue Eng 9, 337-45 (2003).

50. Khan, Y. M., Katti, D. S. & Laurencin, C. T. Novel polymer-synthesized ceramic composite-based system for bone repair: an in vitro evaluation. J Biomed Mater Res A 69, 728-37 (2004).

51. Zhao, F. et al. Preparation and histological evaluation of biomimetic three-dimensional hydroxyapatite/chitosan-gelatin network composite scaffolds. Biomaterials 23, 3227-34 (2002).

Chapter Four

Chitosan and Alginate

4.1 Chitosan

Natural polymers include cellulose, chitin, chitosan, alginate, collagen, gelatin, silk, fibrin etc. Collagen, gelatin and fibrin are popularly used, but these materials are mainly harvested and/or purified from animals or cadavers which can pose a threat of immunogenicity, disease transmission, ethical problems, etc. The retrieval of a sufficient quantity and purity is also very expensive. Due to the physical, chemical, biological, rheological and degradation properties of chitosan and alginate they are a popular biomaterials and are herein investigated.

4.11 Source and structure of chitosan

Chitosan, a partially de-acetylated derivative of chitin, is extracted from arthropod exoskeletons, such as crabs, shrimp and some bacteria. Structurally, chitosan is a linear polysaccharide consisting of β(1→4) linked D-glucosamine residues with a variable number of randomly located N-acetyl-glucosamine groups. It thus shares some characteristics with various GAGs and hyaluronic acid present in articular cartilage due to the nearly identical structure (shown in Figure4-1). Depending on the source and preparation procedure, chitosan's average molecular weight may range from 50 to 1000 KDa. Commercially available preparations have degrees of deacetylation ranging from 50 to 90%.

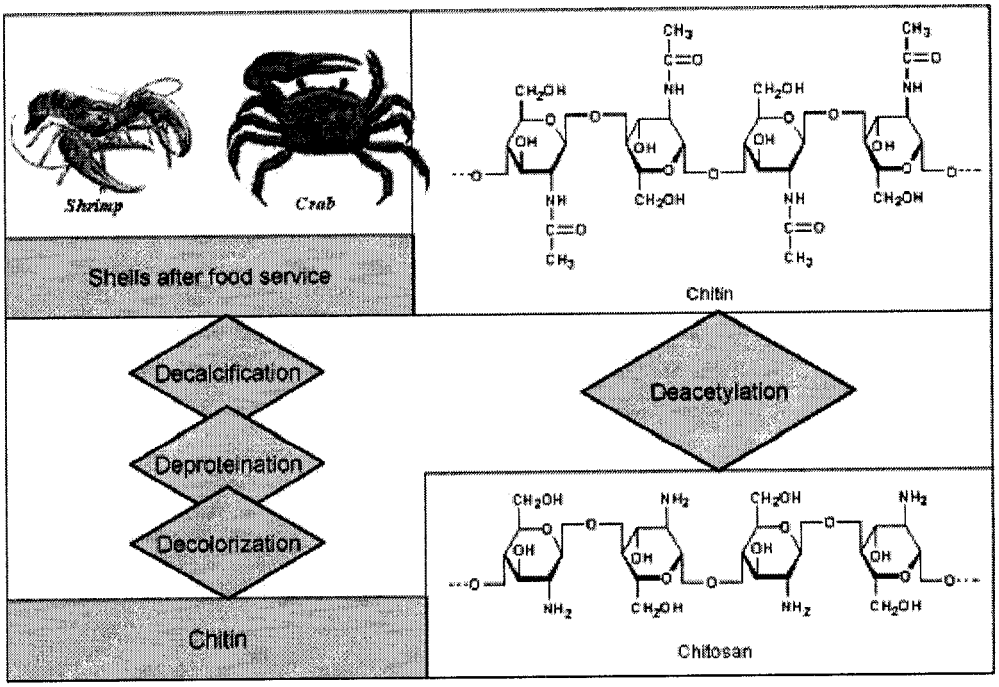

Figureure 4-1 The sources, extracting process and molecular structure of chtin and chitosan

4.12 Physical and chemical properties

Chitosan is a semi-crystalline polymer with the crystallinity a function of the degree of deacetylation. Crystallinity is maximum for both chitin (i.e. 0% deacetylated) and fully deacetylated (i.e. 100%) chitosan. Minimum crystallinity is achieved at intermediate degrees of deacetylation. Chitosan has a unique chemistry: it is a polycation in both neutral and acidic solutions (p*K*a equal to 6.0). It is normally insoluble in aqueous solutions above pH 7, but in dilute acids, the free amino groups are protonated and the molecule becomes fully soluble below pH 5. Therefore it is a neutral biopolymer at physiological situation (pH7-7.4), which is favorable for a broad variety of industrial and biomedical applications. The cationic behavior of chitosan is exploited in the recovery of

proteins from food processing wastes and in the chelation of heavy metals from waste water.[1, 2] Chitosan may also be chemically modified with the activation of the amine groups. Chitosan can be surface modified by carboxylates through N,N-(3-dimethylamino-propyl)-N'-ethyl carbodiimide (EDC) and N-hydroxysuccinimide (NHS) (Figure4-2). Polysaccharides or amino acids have been added to chitosan purposely for tissue engineering by several groups. Mao used this method to attach the hyaluronic acid to chitosan and gelatin scaffold surface.[3] Lee used this method to attach the growth factor TGF-1 to chitosan microspheres.[4] Chitosan has also been modified by arginine to make an anticoagulation biomaterials.[5] Chitosan and gelatin were tethered to electrospun nanofibrous poly(acrylonitrile-co-maleic acid) (PANCMA) matrix surfaces have been used to fabricate dual-layer biomimetic supports for enzyme immobilization. [6] With EDC and NHS as coupling agents, chitosan can also react with almost any polysaccharide that has active carboxyl groups.

4.13 Biological properties

Much of chitosan's potential as a biomaterial stems from its cationic nature due to the amine groups and high charge density in aqueous solution. The charge density allows chitosan to form insoluble ionic complexes or complex coacervates with a wide variety of water-soluble anionic polymers. Complex formation has been documented with anionic polysaccharides such as GAGs and alginates (Figure. 4-3), as well as synthetic polyanions such as poly(acrylic acid).[7-11]

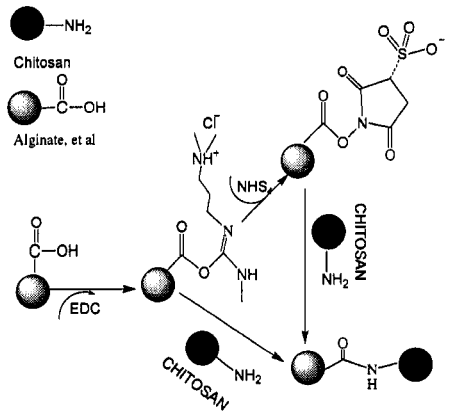

Figureure 4-2. EDC, NHS coupled carboxylates reaction for chitosan and alginate

Due to the dependence of chitosan charge density on pH, transfer of these ionic complexes to physiological pH can result in dissociation of a portion of the immobilized polyanion. This property can be used as a technique for local delivery of biologically active polyanion such as DNA and GAGs. The cationic nature of chitosan is primarily responsible for electrostatic interactions with anionic GAG, proteoglycans and other negatively charged molecules. Associations with various polysaccharides are of great interest because a large number of cytokines/growth factors are linked to GAG (mostly with heparin and heparan sulphate). To this end, a scaffold incorporating a chitosan–GAG complex may retain and concentrate growth factors secreted by colonizing cells.[12] Moreover, the presence of the N-acetylglucosamine moiety on chitosan also suggests related bioactivities. In fact, chitosan oligosaccharides have a stimulatory effect on macrophages, and both chitosan and chitin are chemical attractants for neutrophils both in vitro and in vivo.

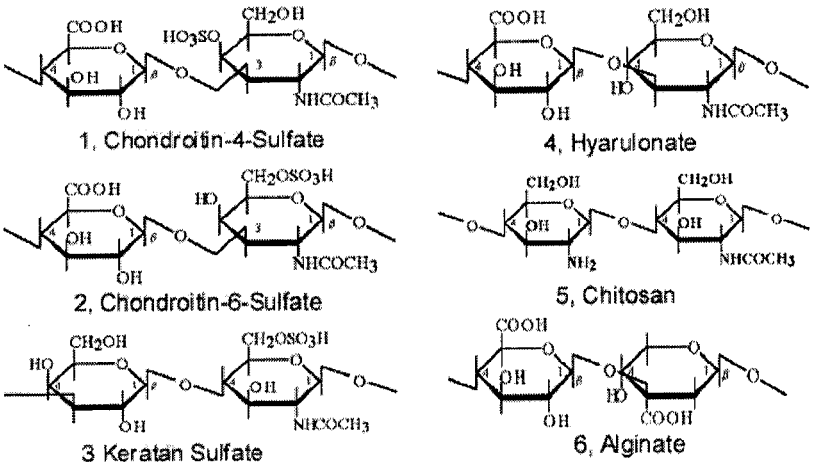

Figure 4-3 The molecular structures of Chitosan, Alginate and GAGs.

4.14 Degradation and In vivo Response

In vivo, chitosan is degraded by enzymatic hydrolysis, primarily by lysozyme, which appears to target acetylated residues. However, there is some evidence that some proteolytic enzymes show low levels of activity with chitosan. The degradation products are chitosan oligosaccharides of variable length and the degradation kinetics appears to be inversely related to the degree of crystallinity which is due to the degree of deacetylation. Highly deacetylated forms (e.g. >85%) exhibit the lowest degradation rates and may last several months in vivo, whereas samples with lower levels of deacetylation degrade more rapidly. This issue has been addressed by derivatizing the molecule with side chains of various types.[13-17] Such treatments alter molecular chain packing and increase the amorphous fraction, thus allowing more rapid degradation. They also inherently affect both the mechanical and solubility properties.

In general, these materials have been found to evoke a minimal foreign

body reaction. In most cases, no major fibrous encapsulation has been observed. Formation of normal granulation tissue, often with accelerated angiogenesis, appears to be the typical course of healing. Within the first week, a significant accumulation of neutrophils in the vicinity of the implants is often seen, but this dissipates rapidly and a chronic inflammatory response does not develop. The stimulatory effects of chitosan and chitosan fragments on immune cells mentioned above may play a role in inducing local cell proliferation and ultimately integration of the implanted material with the host tissue.

4.15 Rheological properties

J. Desbrieres et al[1,2,8,18] reported the rheological properties with different concentrations of chitosan solution and different temperatures (preparation temperature).

1. Influence of Concentration. The influence of the concentration on the rheological curves is presented in Figure4-4. For low concentrations the solutions exhibit a Newtonian behavior, but increasing the polymer concentration leads to the appearance of a non-Newtonian behavior. Chitosan is able to form hydrophobic intermolecular domains at concentrations larger than 1 g/L. These domains are stable and only affected by heating or by the addition of salt, urea, or ethanol.[1] The nature of the stabilization of aggregates causing a heterogeneous structure in the polymer solution is still unclear.[2,18] It is suggested that neither hydrogen bonds nor hydrophobic interactions are responsible for the aggregation of chitosan. The aggregates are concentration dependent, so it is

more difficult to get higher concentrations of chitosan solution.

2. Influence of temperature. Testing the gel at a high concentration of 52.85 g/L, taking into account the complex viscosities at 0.02 Hz, an activation energy equal to 25.4 kJ/mol was measured in the 278-323 K temperature range when experiments were carried out for discrete temperature values. This value is smaller than the maximal value found previously (38 kJ/mol.)[1] As already proven with other polysaccharides, it may be the consequence of an increase of the stiffness of the macromolecular chain related and the increase of intermolecular interactions when the polymer concentration increases, these interactions limiting the mobility of the chains or the increase of intra-chain hydrogen bonds.

But when a continuous temperature increase was performed on the gel from 278 to 353 K at a frequency of 0.1 Hz, the derivated curve $\ln\eta^* = f(1/T)$ showed the viscosity deceased. Figure 4-4 showed that two extremums domains are observed and dynamic rheological experiments show that the change in the slope at high temperature corresponds to the gel-sol transition during the temperature increase at 341K, e.g. 68°C.

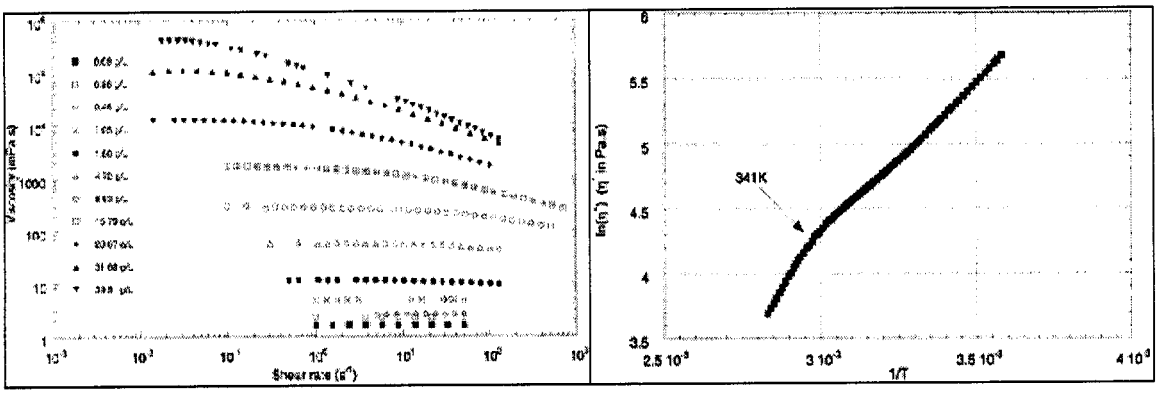

Figure 4-4 The concentration, shear rate and viscosity relationship (left) and the equation of $\ln\eta^* = f(1/T)$ for the relationship of viscosity and temperature (right). (Both are cropped from J. Desbrieres[1] with permission.)

4.2 Alginate

4.21 Alginate source and characteristics

Alginates are usually extracted from seaweed, such as brown algae, or from some bacterial species. They consist of unbranched, binary copolymers of 1-4 linked β-D-mannuronic acid (M) and α-L-guluronic acid (G), of widely varying composition and sequential structure (MMM-blocks, GGG blocks and MGM-blocks)(Figure4-5). The structure is influenced by the seaweed source as well as the growing conditions of the weeds. The block structure ultimately dictates the gelling properties of the alginate produced. Durvillea and ascophyllum species tend to be high in mannuronic acid (MM blocks) whereas alginate sources such as laminaria hyperborea stems tend to have a higher guluronic acid content (GG blocks).

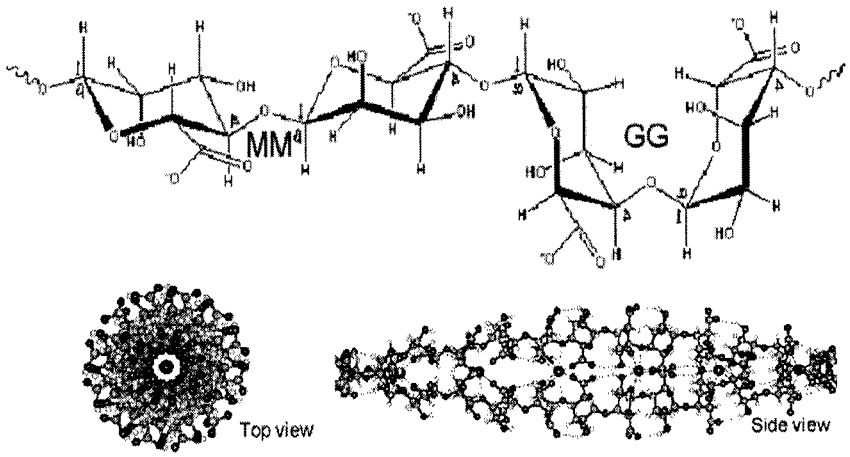

Figure 4-5 Molecular structure and the secondary structure of alginate (Courtesy Martin Chaplin)

4.22 Biological properties

Alginate is classified as an anionic mucoadhesive polymer due to its carboxyl end groups. It has been reported that polyanion polymers are more effective bioadhesives than polycation polymers or nonionic polymers.[19] Peppas et al found that mucoadhesion is achieved by chain penetration across a polymer–mucosa interface.[20,21] These studies showed that alginate has a higher mucoadhesive strength than polymers such as polystyrene, chitosan, carboxymethylcellulose and poly(lactic acid). De Vos et al reported that it was the physical imperfections of the individual capsules of medicine rather than the chemical composition of alginate that caused immunogenicity.[22] Alginate implants rich in α-guluronic acid are also reported to have less immunological responses at the implant sites than polyvinyl alcohol or agarose gels.[23] Studies employing alginates as surgical gauzes or films have also demonstrated that not only is alginate completely absorbed (biodegradable) in animal tissues, but the

tissue reaction is found to be very minimal.[24] Studies by Wee et al[24,25]also documented that little or no specific inflammatory response was associated with the upper nasopharynx when high α-guluronic acid alginate microbeads were used in mice. Studies[23,26]showed that mitogenic impurities which are found in commercial alginate but not in purified alginate are solely responsible for the side effects observed. Side effects included cytokine release and inflammatory reactions. Other groups have also shown that alginate rich in mannuronic acid seem to activate cytokine production more than guluronic-rich alginate.

4.23 Stability and degradation

Gelation of alginate occurs when the carboxyl groups of the polymers are cross-linked with multi-valent cation (e.g. Ca^{2+}, Ba^{2+}, La^{3+}, Fe^{3+}). With the cations in the center, the alginate formed an egg-box-like secondary structure (Figure.4-6). The strength of the gel varies depending on the nature of the cross-linking cation, the length of the polymeric chains, the M:G ratio and the percentage of the block structures. Therefore, hydrogels of varying mechanical strength, elasticity and swelling characteristics can be produced.[27] When cross-linked with Ba^{2+} or Ca^{2+}, high-M alginates result in elastic gel, whereas microcapsules based on high-G alginate exhibit high mechanical strength. High G-containing alginate tend to form more rigid gels at a very specific concentration of cation whereas higher M- alginate tend to form softer gels and over a wider range of conditions. As alginate is a linear polymer, the viscosity is determined by the molecular weight, rigidity and extension of the chain. Mixing of high-M and high-G alginates

is an easy way for designing gels of desired strength and formability, particularly if such material is taken from algae of the same genus. Suitable algal sources for such alginate mixtures are *Lessonia nigrescens* and *Lessonia trabeculata*.

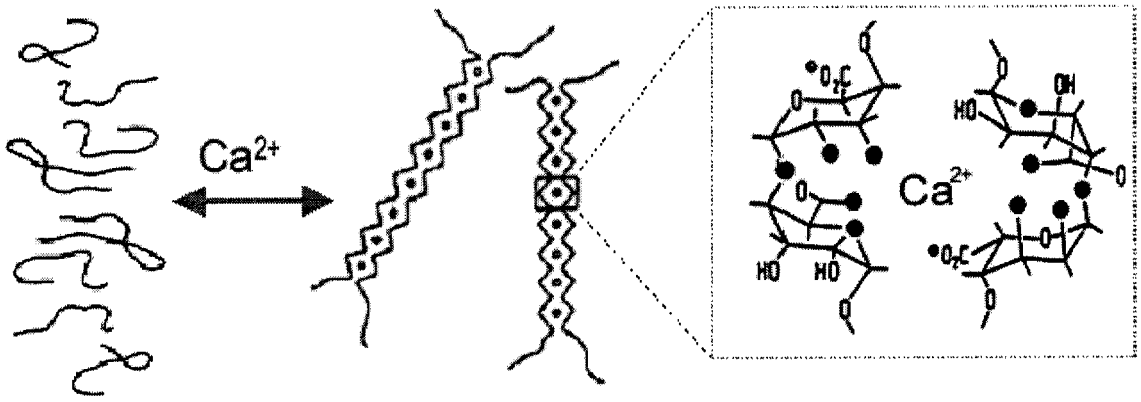

Figure 4-6 The egg box theory of calcium alginate gel formation (modified from Allen Hoffman)

Degradation of a Ca^{2+} crosslinked alginate gel can occur by removal of the Ca^{2+} ions. This can be accomplished with the use of a chelating agent such as EDTA, lactate, citrate and phosphate. As Ca^{2+} ions are removed, the crosslinking in the gel decreases and the gels are destabilized.[24, 28] Alginate gels will also degrade and precipitate in a 0.1 M phosphate buffer solution and will completely dissolve in 0.1 M sodium citrate at pH 7.8[29]. Degradation of the gel can be prevented by storing the gel in a medium that contains free Ca^{2+} ions and by keeping the Na^{+}: Ca^{2+}ratio less than 25:1 for high-GG alginates and 3:1 for low GG-alginates.[30-32]

Like all polymers, alginates can be degraded by proton catalyzed hydrolysis which is dependent on time, pH, and temperature. A crosslinked alginate matrix delivery system, when exposed to low pH, can therefore undergo a reduction in

alginate molecular weight. This results in faster degradation and release of a molecule when the gel is reequilibrated in a neutral pH solution.[24, 33]

Alginate forms strong complexes with polycations including chitosan, polypeptides (such as polylysine) and synthetic polymers (such as polyethyleneimine). These complexes do not dissolve in the presence of Ca^{2+} chelators and can be used to stabilize the gel or make strong scaffolds.[7,10,11,24]

4.24 Alginate extraction and purification

Crude commercial alginates are not recommended as starting materials as they contain many inorganic and organic impurities including non-natural constituents. These impurities can cause some unexpected immunoreaction when such alginate is used in vivo.[24] These alginates are usually polluted with components of bacterial, fungal, animal and anthropogenic origin. Treatment of the raw algal material by formaldehyde causes further complications because of partially unknown interactions between alginate and impurities. Commercial products can contain spores or components of gram-positive bacteria commonly occurring in marine environments (e.g. *Bacillus anthracis, Bacillus cereus* and *Bacillus thuringiensis*).[34,35] Contamination by gram-positive debris has not received attention by workers in the field, but is extremely important for the production of biocompatible alginates. Furthermore, due to the harvesting and extraction process, the viscosity (closely linked to the molecular weight) of commercial alginates is also rather low, enhancing the risk of graft failure since the cytotoxicity of polymers increases with decreasing molecular mass. These

disadvantages do not exist when fresh stipe of brown algae (free of overgrowth by epiphytes) are harvested directly from the sea, peeled and, most importantly, subjected to antimicrobial treatment. The products of subsequent extraction and purification can be improved further if the surface of the stipe are physically cleaned. This treatment removes immunogenic surface proteins of non-plant origin that are frequently found in alginates after extraction and purification. Alginate is extracted by using a mixture of appropriate Ca2+-chelating agents and purified by repeated alcohol (or acetone) precipitation. Under these conditions, clinical-grade alginates of extremely high-viscosity (>30 mPa s; 0.1% w/v solution) can be routinely produced on a large scale.[27]

4.25 Rheological properties

Very few studies have been conducted on the rheological properties of alginate salts alone, especially for high concentrations of alginate (>3%w/v). It is usually studied together with other polymers, such as starch[36], polyacrylate[37], chitosan[8], or some chemical reagents such as riboflavin.[38] Experiments found that alginate gel is easily autoclaved when the concentration is between 0.5-3.0%(w/V) which partially degrades the gel strength and stability.[39] Alginate gel strength decreases with the increase of temperature; Increased concentration will also increase the viscosity. Daubert[40] et al reported a study aiming to characterize the rheological properties of alginate/starch mixed gels. The mixed gels were subjected to compression tests for rheological characterization at large strain deformation. Oscillatory shear results showed that hot (80°C) mixtures of

alginate/starch formed weak gels which became stronger upon cooling (to 5°C). For a given concentration of alginate, gel strength (G') increased by 2-5 times with added starch (2-10% w/w). Fracture stress and strain of the mixed gels under large deformation were not always consistent with gel strength. For different types and concentrations, starch acts as filler in an alginate matrix or may form a co-network resulting in different fracture behavior and textural properties.

4.3 chitosan-alginate composite

Chitosan or alginate alone has low mechanical strength and high rates of degradation. This consequently resulted in their use in composites and in chemical modification by cross-linking to improve material properties and reduce degradation rates.[41] Mixing of alginate and chitosan will form a polyion complex which has rheological properties similar to pure chitosan. Masuda et al confirmed that the carboxyl anion of alginate and amino cation of chitosan can form complexes. The complex develops most markedly at a mixing ratio of 1:1 to 1:2 in molar ratio depends on the specific chitosan and alginate being used. Practically, the mixing ratio of the two polymers is usually prepared in weight ratio.[8] The structure and yield of chitosan-alginate complex are strongly dependent on the mixing ratio of the component polymers. The complex ratio of 1:1 to 1:2 develops a heterogeneous structure which produces relatively rough surface on the bulky scaffolds. [1, 8, 18]

Low concentration chitosan and alginate (<3%w/v) are frequently used for

beads or film synthesis for drug release especially growth factors release as the neutral gel forming conditions facilitate these protein based growth factor to be incorporated.[9, 42-47] So far, to the best of our knowledge, we are the only group using high concentrations of chitosan and alginate (>3% w/v) complex in making scaffolds for tissue engineering. High concentration hybrid chitosan alginate scaffolds will be discussed more in later chapters.

Notes to Chapter Four

1. Desbrieres, J. Viscosity of semiflexible chitosan solutions: influence of concentration, temperature, and role of intermolecular interactions. Biomacromolecules 3, 342-9 (2002).

2. Delben, F., Lapasin, R. & Pricl, S. Flow properties of N-(carboxymethyl) chitosan aqueous systems in the sol and gel domains. Int J Biol Macromol 12, 9-13 (1990).

3. Mao, J. S., Liu, H. F., Yin, Y. J. & Yao, K. D. The properties of chitosan-gelatin membranes and scaffolds modified with hyaluronic acid by different methods. Biomaterials 24, 1621-9 (2003).

4. Lee, J. E. et al. Effects of the controlled-released TGF-beta1 from chitosan microspheres on chondrocytes cultured in a collagen-chitosan-glycosaminoglycan scaffold. Biomaterials 25, 4163-73 (2004).

5. Liu, W. G., Zhang, J. R., Cao, Z. Q., Xu, F. Y. & Yao, K. D. A chitosan-arginine conjugate as a novel anticoagulation biomaterial. J Mater Sci Mater Med 15, 1199-203 (2004).

6. Ye, P., Xu, Z. K., Wu, J., Innocent, C. & Seta, P. Nanofibrous poly(acrylonitrile-co-maleic acid) membranes functionalized with gelatin and chitosan for lipase immobilization. Biomaterials (2006).

7. Li, Z., Ramay, H. R., Hauch, K. D., Xiao, D. & Zhang, M. Chitosan-alginate hybrid scaffolds for bone tissue engineering. Biomaterials 26, 3919-28 (2005).

8. Matsumoto, T., Kawai, M. & Masuda, T. Rheological properties and fractal structure of concentrated polyion complexes of chitosan and alginate. Biorheology 30, 435-41 (1993).

9. Wang, L., Khor, E. & Lim, L. Y. Chitosan-alginate-CaCl(2) system for membrane coat application. J Pharm Sci 90, 1134-42 (2001).

10. Li, X. The use of chitosan to increase the stability of calcium alginate beads with entrapped yeast cells. Biotechnol Appl Biochem 23 (Pt 3), 269-72 (1996).

11. Li, Z. & Zhang, M. Chitosan-alginate as scaffolding material for cartilage tissue engineering. J Biomed Mater Res A 75, 485-93 (2005).

12. Madihally, S. V. & Matthew, H. W. Porous chitosan scaffolds for tissue engineering. Biomaterials 20, 1133-42 (1999).

13. Zhang, H. & Neau, S. H. In vitro degradation of chitosan by a commercial enzyme preparation: effect of molecular weight and degree of deacetylation. Biomaterials 22, 1653-8 (2001).

14. Ren, D., Yi, H., Wang, W. & Ma, X. The enzymatic degradation and swelling properties of chitosan matrices with different degrees of N-acetylation. Carbohydr Res 340, 2403-10 (2005).

15. Kim, K. W., Thomas, R. L., Lee, C. & Park, H. J. Antimicrobial activity of native chitosan, degraded chitosan, and O-carboxymethylated chitosan. J Food Prot 66, 1495-8 (2003).

16. Kiang, T., Wen, J., Lim, H. W. & Leong, K. W. The effect of the degree of chitosan deacetylation on the efficiency of gene transfection. Biomaterials 25, 5293-301 (2004).

17. Aye, K. N., Karuppuswamy, R., Ahamed, T. & Stevens, W. F. Peripheral enzymatic deacetylation of chitin and reprecipitated chitin particles. Bioresour Technol 97, 577-82 (2006).

18. Kj et al. Effect of surfactant concentration, pH, and shear rate on the rheological properties of aqueous systems of a hydrophobically modified chitosan and its unmodified analogue. Polymer Bulletin 38, 71 (1997).

19. Vasir, J. K., Tambwekar, K. & Garg, S. Bioadhesive microspheres as a controlled drug delivery system. Int J Pharm 255, 13-32 (2003).

20. Colombo, P. et al. Drug diffusion front movement is important in drug release control from swellable matrix tablets. J Pharm Sci 84, 991-7 (1995).

21. Khare, A. R. & Peppas, N. A. Release behavior of bioactive agents from pH-sensitive hydrogels. J Biomater Sci Polym Ed 4, 275-89 (1993).

22. De Vos, P., De Haan, B., Pater, J. & Van Schilfgaarde, R. Association between capsule diameter, adequacy of encapsulation, and survival of microencapsulated rat islet allografts. Transplantation 62, 893-9 (1996).

23. Spargo, B. J., Rudolph, A. S. & Rollwagen, F. M. Recruitment of tissue resident cells to hydrogel composites: in vivo response to implant materials. Biomaterials 15, 853-8 (1994).

24. Wee, S. & Gombotz, W. R. Protein release from alginate matrices. Adv Drug Deliv Rev 31, 267-285 (1998).

25. J. Schuh, W. F., W. Gombotz and S.F. Wee. Intranasal localization and antibody response to polycation-coated ova-encapsulated alginate microbeads. Vet. Pathol 33 (1996).

26. Otterlei, M. et al. Induction of cytokine production from human monocytes stimulated with alginate. J Immunother 10, 286-91 (1991).

27. Zimmermann, H. et al. Towards a medically approved technology for alginate-based microcapsules allowing long-term immunoisolated transplantation. J Mater Sci Mater Med 16, 491-501 (2005).

28. Smidsrod, O. & Skjak-Braek, G. Alginate as immobilization matrix for cells. Trends Biotechnol 8, 71-8 (1990).

29. Kwok, K. K., Groves, M. J. & Burgess, D. J. Production of 5-15 microns diameter alginate-polylysine microcapsules by an air-atomization technique. Pharm Res 8, 341-4 (1991).

30. Grandolfo, M. et al. Culture and differentiation of chondrocytes entrapped in alginate gels. Calcif Tissue Int 52, 42-8 (1993).

31. Paoletti, S., Gamini, A. & Zanetti, F. Conformational aspects of ionic polysaccharides: laser light scattering of aqueous solutions of hyaluronic acid and alginate. Biochem Soc Trans 19, 494-5 (1991).

32. Cesaro, A., Delben, F. & Paoletti, S. Thermodynamics of the proton dissociation of natural polyuronic acids. Int J Biol Macromol 12, 170-6 (1990)

33. Puolakkainen, P. A. et al. Novel delivery system for inducing quiescence in intestinal stem cells in rats by transforming growth factor beta 1. Gastroenterology 107, 1319-26 (1994).

34. Leinfelder, U. et al. A highly sensitive cell assay for validation of purification regimes of alginates. Biomaterials 24, 4161-72 (2003).

35. Zimmermann, H. et al. Fabrication of homogeneously cross-linked, functional alginate microcapsules validated by NMR-, CLSM- and AFM-imaging. Biomaterials 24, 2083-96 (2003).

36. Tschimirov, J. I. et al. [Rheological properties of a calcium alginate-potato starch hydrolysate-water system]. Nahrung 23, 501-8 (1979).

37. Fuongfuchat, A., Jamieson, A. M., Blackwell, J. & Gerken, T. A. Rheological studies of the interaction of mucins with alginate and polyacrylate. Carbohydr Res 284, 85-99 (1996).

38. Baldursdottir, S. G. et al. Riboflavin-photosensitized changes in aqueous solutions of alginate. Rheological studies. Biomacromolecules 4, 429-36 (2003).

39. Duggirala, S. & Deluca, P. P. Rheological characterization of cellulosic and alginate polymers. PDA J Pharm Sci Technol 50, 290-6 (1996).

40. Daubert., V. D. T. a. C. Rheological and textural properties of alginate-starch mixed gels: effects of starch type and concentration. 2001 AACC Annual Meeting (2001).

41. Karageorgiou, V. & Kaplan, D. Porosity of 3D biomaterial scaffolds and osteogenesis. Biomaterials 26, 5474-91 (2005).

42. Lai, H. L., Abu'Khalil, A. & Craig, D. Q. The preparation and characterisation of drug-loaded alginate and chitosan sponges. Int J Pharm 251, 175-81 (2003).

43. T Takahashi, K. T., Y Machida, T Nagai. Characteristics of Polyion-complex of chitosan with sodium alginate and sodium polyacrylate. Int. J. Phar 61, 35-41 (1990).

44. Bodmeier, R., Chen, H. G. & Paeratakul, O. A novel approach to the oral delivery of micro- or nanoparticles. Pharm Res 6, 413-7 (1989).

45. Yan, X., Khor, E. & Lim, L. Y. PEC films prepared from Chitosan-Alginate coacervates. Chem Pharm Bull (Tokyo) 48, 941-6 (2000).

46. Zheng, C. H., Liang, W. Q., Li, F., Zhang, Y. P. & Fang, W. J. Optimization and characterization of chitosan-coated alginate microcapsules containing albumin. Pharmazie 60, 434-8 (2005).

47. Coppi, G., Iannuccelli, V., Leo, E., Bernabei, M. T. & Cameroni, R. Chitosan-alginate microparticles as a protein carrier. Drug Dev Ind Pharm 27, 393-400 (2001).

Chapter Five

Hybrid chitosan-alginate scaffold synthesis and characterization

5.1 Introduction

Biodegradable porous polymer scaffolds are widely used in tissue engineering to provide a structural template for cell seeding and extracellular matrix formation. Several processing technologies have been reported to fabricate porous polymeric scaffolds for bone or cartilage regeneration, including solvent casting and salt leaching[1], gas foaming[2], rapid prototyping[3], and thermally induced phase separation.[4-7]Each of these techniques presents its own advantages, but none is devoid of drawbacks. For example, solvent casting and salt leaching can produce highly porous scaffolds with porosity up to 93% and median pore diameters up to 500 μm[1], but it can only be used to produce thin wafers or membranes no more than 3-mm thick.[8] Additionally the organic solvents used in this method must be fully removed to avoid any possible damage to the cells that will be seeded on the scaffold. The gas foaming method can easily produce a thick skin and the pores are not well interconnected.[2, 8] The excessive heat used during compression molding prohibits the incorporation of any temperature sensitive material into the polymer matrix. Thermally induced phase separation is the first step of lyophilization, which is a widely applied method in scaffold synthesis, biological products protection, and bioactivity preservation. It separates the polymer from

water and pores will appear after the water is removed by vaporization and desorption. We employed this method in synthesize hybrid chitosan-alginate scaffold and more details will be discussed later based on our experimental results.

5.2 Materials and facilities

Chitosan (Mw 400,000, 85-90% deacetylated), sodium alginate powders (from brown algae, Mw 50-100,000), glacier acetic acid, and calcium chloride were purchased from Sigma-Aldrich. Facilities included freeze dryer, freezer (-10, -20°C), blender (Oster), 24-well culture plates (Corning Ltd.), pH meter and electronic thermometer.

5.21 Scaffold synthesis

Protocol I

We first separately dissolved 4.8 grams of sodium alginate 120 ml 1N NaOH and 4.8 gram of chitosan in 80 ml 1N acetic acid. The two gels were mixed under constant stirring in a blender for one hour to obtain a homogeneous 4.8% w/v (2.4% chitosan and 2.4% alginates) chitosan-alginate solution. The pH of the chitosan-alginate solution was adjusted to pH7.4 by adding glacial acetic acid. The solution was loaded into 24-well cell culture plates and maintained in a freezer at –20°C for 24 hours. The samples were then lyophilized in a freeze dryer until dried. The dried scaffolds were again crosslinked with 1% w/v $CaCl_2$

solution for 5-10 minutes. The scaffolds were soaked in DI water overnight to remove unbound $CaCl_2$. The samples were dried again in the freeze dryer. [9, 10]

Protocol II

Recently, a renewed protocol was used in making these scaffolds. As shown in Figure 1, this setup facilitated the polymer dissolving and temperature control. The beaker was supported by a warming pot equipped with a sensitive temperature control system. Inside the beaker, a strong electric stirrer ensured that the polymers were well blended. Chitosan pellets (7.2 gram) and sodium alginate powder (7.2 gram) were added directly into 300ml DI water in the beaker. The blender was used to mix well the chitosan pellets and sodium alginate powder. Sodium alginate can slowly dissolve in DI water, but the chitosan cannot dissolve. Despite this, the chitosan pellets were well dispersed in water. After the temperature of the water rose to 80°C, 3 ml glacial acetic acid was added into 300ml DI water to dissolve the chitosan until there were no visble chitosan pellets. Finally, a small electric blender (Oster) was used to blend the mixture to get a uniform sol before loading into the 24 well cell culture plates.

5.22 Optimizing scaffold synthesis conditions

To optimize conditions for the synthesis of scaffolds, we designed a series of experiments to test the effects of altering various parameters including polymer concentration, freezing temperature, final PH, polymer ratio and coarsening time. We also listed an excluding criteria as below:

a). The process is easy to perform and control.

b). The hybrid solution can be easily loaded into the 24-well plates.

c). The scaffolds produced can maintain good exterior morphology, display no shrinkage or large defects.

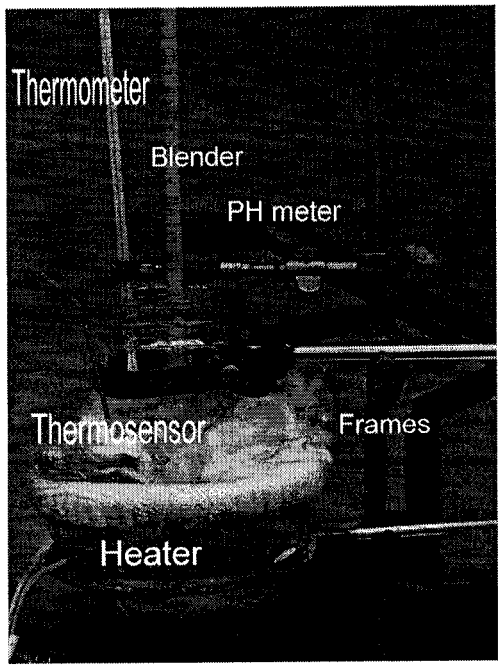

Figure 5-1. The experimental setup of protocol II.

d). The scaffolds can maintain good morphology in DI water and PBS after crosslinking without significant swelling or dissolving.

Any conditions that violate the above mentioned criteria were excluded, and we did not experiment within those conditions to make scaffolds. For example, a polymer concentration (either chitosan or alginate, or composites) larger than six percent is very viscous which creates difficulty in making the sol and loading them to the plates. Additionally, we studied only ph values of 3, 5, 7 9 and 11, as a ph of less than 1 or bigger than 13 is not physiologically compatible.

We studied the effects of only one parameter at a time; we did not experiment

on any two or three parameter-combined conditions.

i). Different polymer concentration (other parameters: -20°C, pH7, coarsening time 24 hours at -20°C.)

2%, 3%, 4%, 4.8%, 5.6%

ii). Different frozen temperature (other parameters: 4.8%, pH 7, coarsening time: 24 hours at -20°C)

-10°C, -20 °C, -70°C, -180°C.

iii). Different pH value (4.8%, -20°C, coarsening time 24 hours at -20°C)

pH 3, 5, 7, 9, 11.

iv). Coarsening time (4.8%, -20°C, pH7).

1). 0 hour, 2hours, 4hours at room temperature.

2). 2 hours, 12hours, 24 hours, 48hours at -20°C.

5.3 Characterization

5.31 SEM morphology

The pores' morphology, wall texture, size and distributions were analyzed by SEM. We also compared chitosan/alginate scaffolds with the pure chitosan scaffolds. All scaffolds were sectioned into cylinders of 3mm thickness. Some samles were sectioned vertically in order to view the vertical structure of the samples. All samples were coated with Au/Pd. The Environmental SEM JOEL 840A and 7000 models were used for these samples. Digital pictures were taken and used to measure pore size and morphology.

The achieve an accurate measurement of pore size, we used the software provided by the SEM JOEL 7000 model. Two hundred pores were counted at random and categorized into 5 groups according their longest diameters: less than 100μm, 100-200μm, 201-300μm, 301-400μm, and larger than 400μm.

5.32. Porosity, pore sizes and interconnectivity

i) Mercury infiltration

Mercury intrusion porosimetry is a method used to measure both porosity and pore size. The scaffolds are placed in a penetrometer and infused with mercury under increasing pressure. As the pressure (P) increases, the radius of pores (r) that can be filled decreases according to the Washburn equation[11].

$$P = 2\delta \cos\theta/\gamma$$

where δ is the surface tension of mercury and θ is the contact angle. The open porosity(π) (porosity accessible to mercury intrusion) is given as[12]

$$\pi = V_{intrusion}/V_{scaffold}$$

where $V_{intrusion}$ is the total intrusion volume of mercury and $V_{scaffold}$ is the volume of the scaffold.

ii) Liquid displacement method

The open porosity can be calculated by the liquid displacement method as well[12, 13]. The scaffold is submerged in a known volume (V1) of liquid that is not a solvent for the scaffold and a series of brief evacuation-repressurization cycles is conducted to force the liquid into the pores of the scaffold. After these cycles the volume of the liquid and liquid –impregnated scaffold is V2. When the liquid-

impregnated scaffold is removed, the remaining liquid volume is V3 and open porosity is given as[14, 15]:

$$\pi=(V1-V3)/(V2-V3)\ X100\%$$

iii) Water absorption

Hybrid chitosan-alginate scaffolds were compared with pure alginate scaffolds. They were from the same size module and same morphology. We compared their water or PBS absorption capability to see the pore interconnectivity. If the pores are interconnected, the PBS or water will easily fill in. If the pore is closed, then the PBS solution or water cannot fill in. We used 7 samples from each group and weighed them before we immerse them into PBS (Dry weight, Wd). After the samples were immersed in the PBS for five minutes, we picked the sample out and wiped the surface with Kiwi tissue, then quickly measured the wet weight (Wet weight, Ww). We calculated the water absorption capacity by the equation:

$$\text{Absorption capacity} = (Ww-Wd)/Wd$$

5.33 Mechanical testing

i) Compression test

The compressive mechanical strength and modulus of the scaffolds were tested using an Instron 4505 mechanical tester with 10 KN load cells following the guidelines in ASTM D5024-95a.[10,16]The specimens were in cylindrical morphology of 13 mm diameter and 12mm thickness. The crosshead speed of

the Instron tester was set at 0.4 mm per minute and the load was applied until the specimens were compressed to approximately 30% of their original thickness.

ii) Tensile test

Tensile mechanical properties were evaluated by stress–strain response using a micro-tensile testing machine designed for high accuracy with small sample testing. The load cell has a loading range of ±30 grams with an incremental accuracy of 0.001 grams. The data were acquired through a computer interface connected to a load transducer (Model SS-2) and an electronic signal conditioner (PTC Electronics, Wyckoff, NJ) on the test machine. The load was applied by a stepper motor system (Motion Group, Clovis, California) controlled by a Lab-VIEW routine written by the authors. Nanofibrous mats were cut in rectangular shape with a cross section of 60 mm^2. The tensile modulus was calculated from the stress verses strain curve.

5.34 Stability and degradation

i) Shape Retention

Shape retention capability of the chitosan-alginate composite scaffolds was tested by immersing them into solution of varying pH. We used 1N HCl (pH= 0) as acidic solution, 1N NaOH (pH=14) as basic solution and simulated body fluid SBF (pH=7.4) as physiological solution. All samples were sectioned into a cylindrical disk with average diameter around 13mm and thickness of 3mm. We

measured scaffold diameter changes at different time points as a monitor of the size retention capability.

5.35 FTIR

Infrared Spectroscopy was used to characterize scaffolds in powder form before and after coacervation. A dried sample of 2 mg was carefully mixed with 300 mg dry KBr and pressed into a pellet using a macro KBr die kit. The solid pellet was placed in a magnetic holder. The system was purged before testing. Polarized Fourier Transformed Infrared (FTIR) spectra of 2000 scans at $8cm^{-1}$ were obtained using a Nicolet 5DX spectrometer with a DTGS detector and a solid transmission sample compartment.

5.4 Results and Discussion

5.41 Optimization of scaffolds synthesis

We made a diverse selection of scaffolds under different conditions. Some of these scaffolds were obviously of bad morphology or in very poor mechanical condition. We excluded these specimens by the criteria listed previously. As shown in Tables 5-1, 5-2 and 5-3, we finally optimized the range of conditions including concentration of chitosan and alginate 3 to 4.8%(W/V), pH 5 to 9, freezing temperature of -10°C to -20°C, and coarsening time 24 hours at -20°C. We did not list a table for the coarsening time changes, as no significant difference among the various coarsening times though pore morphologies are found by SEM inspection. (Figure 5-3)

Table 5-1 Diversity of scaffolds by different final polymer concentration

Concentration	2%	3%	4%	4.80%	5.60%
Exterior Morphology	Poor	Good	better	better	good
Uniform of the pores	Not	Yes	Yes	Yes	Not
Macro-defects	huge pores	big pores	No	No	skin, bubble defects
Shape retention	Swelling	No swelling	No swelling	No swelling	slight swelling
Mechanical strength	poor	good	better	better	best
Water intrusion	good	better	better	good	bad

Table 5-2 Diversity of scaffolds by different frozen temperature

Frozen temperature °C	0	-20	-70	-180
Exterior Morphology	good	very good	bad	very bad
Uniform of the pores by naked eye	yes	Yes	No	No
Macro-defects	No	No	shattered	Debris
Shape retention	Swelling	No swell	NA	NA
Mechanical strength by hand	good	good	NA	NA
water intrusion	Good	Good	NA	NA

Table 5-3 Diversity scaffolds by different final PH of the solution

pH	pH=3	pH=5	ph=7	pH=9	pH=11
Exterior Morphology	poor	best	better	good	poor
Pores uniformity	No	Yes	Yes	Yes	No
Macro-defects	shrinkage pores	No	No	No	shrinkage
Shape retention	swelling	No swelling	No swelling	No swelling	Slight swelling
Mechanics	poor	best	better	much better	poor
Water intrusion	good	better	better	good	bad

To optimize the conditions for scaffold production, we need to know the mechanism of the freeze-drying process. Freeze-drying or lyophilization is the process of removing water from a composite or product by sublimation and desorption. This process is performed in lyophilization equipment that consists of a drying chamber, a condenser (to trap water vaporized from the product), a cooling system (to supply refrigerant to the shelves and condenser) and a vacuum system (to reduce the pressure in the chamber and condenser to facilitate the drying process).

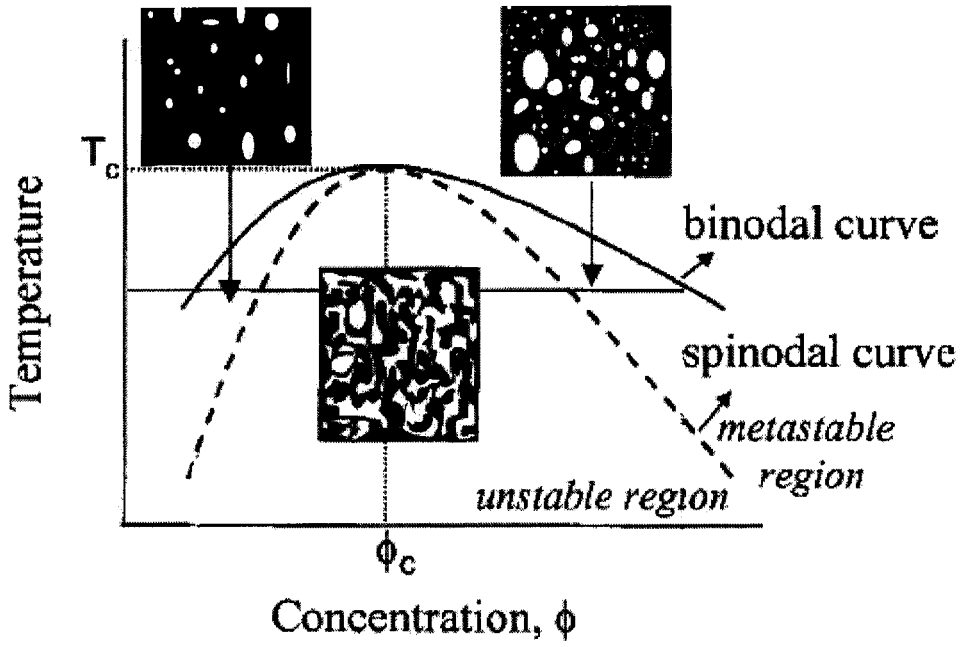

Figure 5- 2. The temperature-concentration polymer phase diagram

The lyophilization cycles consist of three steps: Freezing, primary drying, and secondary drying. Freezing is the first step of lyophilization, a thermally induced phase separation (TIPS) happening in the process. Figure 5-2 is a general temperature-concentration polymer phase diagram. Above the curves, the polymers are in a homogeneous one phase status, and below the curves (bimodal curve) there is a two-phase region. The spinodal curve is defined as the line at which the second-derivative Gibbs free energy of the mixture is equal to zero, and it divides the two-phase region into an unstable and a metastable region. If the system is quenched into the metastable region, phase separation occurs in a nucleation and growth mechanism, leading to a bead like or isolated cellular structure. On the other hand, if the system temperature is quenched into the unstable region, the phase separation takes place in a spinodal

decomposition mechanism, resulting in a microporous interconnected structure as reported.[17-20] For the chitosan and alginate composites, as reported by Metsumoto[21], a uniform sol is formed when the temperature is above 80°C and the sol is transformed to a uniform gel when the temperature drops to approximate 70°C, the polymer rich phase containing chitosan and alginate, the polymer poor phase containing water and some water-soluble salts, such as sodium acetic, acetic acid etc. With decreased temperature, the gel strength increases.[21-24] Spinodal decomposition or nucleation happens in the early stage of the gel formation or phase separation, but in the later stages, the coalescence of phase separated droplets continuously proceeds to minimize the interfacial free energy associated with the interfacial area. This process is called coarsening.[18-20] During the coarsening process, the small pores will merge to be bigger ones and increase the interconnectivity of the pores. Therefore it increases the size and uniformity of the pores. The longer the coarsening time, the larger the pores produced and the greater their interconnectivity. To attain macroporous interconnecting scaffolds, it is highly desirable to use the coarsening effect. For the chitosan and alginate composites, we controlled the coarsening process both at room temperature and at -20°C. Room temperature coarsening can also help to remove any possible gas bubbles. As for the -20°C coarsening, we compared different time periods of 0, 2, 12, 24 and 48 hours. For all the coarsening samples, we processed with two hours of room temperature coarsening. The scaffolds without coarsening were very deformed. The SEM

showed a sheet-like structure with large fractures, and no regular pores were formed. The 2 hours-coarsening scaffold produced relatively uniform pores but there were still some sheets-like structures seen. The 12 hours coarsening scaffolds showed fewer sheet-like structures on both side-view and top-view of pictures. For the SEM images of 12, 24, and 48 hours coarsening, no significant differences were seen (Figure 5-3).

In the freezing process, the rate of cooling will also influence the structure of the final scaffold morphology[25]. If the water freezes quickly, the ice crystals will be small. This may cause a finer pore structure in the scaffolds with higher resistance to flow of water vapor and also contribute to longer primary drying time. If freezing is slower, ice crystals will grow from the cooling surface and may be larger. The resultant scaffolds may have coarser pore structure and perhaps a shorter primary drying time. The method of cooling will also affect the structure and appearance of the matrix and final product. If the solution is frozen in holders on the cooled shelf, ice will grow from the bottom of the holder toward the top, while immersion in a cooling fluid will cause crystal growth from the bottom and sides of the holder. This will cause the final scaffolds to assure either a sheet-like structure or a directional tube-like structure.[26] However, a long term, effective coarsening process can adjust the morphology of the pores.

In the primary drying phase, the chamber pressure is reduced, the surface temperatures on the scaffolds and on the condenser are different and a heat flow exists, which will cause the frozen scaffolds to sublime the frozen water and the

vapor to be trapped in the condenser. That which cannot be trapped will be pumped out. The condenser must have sufficient surface area and cooling capacity to hold all of the sublimed water from the batch at a temperature lower than the scaffold temperature. It is important to control the drying rate and the temperature difference during this phase. If the pressure is too low, the dried product can be displaced out of the container by escaping water vapor. If the scaffold in the chamber exceeds the ice vapor pressure of the product, water may not be able to sublimate causing the pressure to melt the water which would destroy the pore structures.. If the temperature difference is too high, the large heat flow will melt the frozen water inside the scaffolds which would also destroy the pore structure and crush the scaffold. This result would change the physical characteristics of the dried material, making it visually unappealing.

At the end of primary drying, all polymer poor phase waters were dried, and the heat flow by the temperature difference will increase the scaffold surface temperature. The final temperature can reach the temperature outside the jar, or the room temperature. The increased temperature desorbs bound water in the polymer rich phase (pore walls) such as the water of crystallization. This process is referred to as secondary drying or desorption.

With our optimization experiments, we found the best scaffolds were made when the concentration was between 3.5% and 4.8% with chitosan and alginate at 1:1 ratio, PH between 5-7, freeze temperature at -20°C and coarsening time of 24 hours at -20°C. We can easily conclude that there were many variables to control

the morphology, porosity, pore size and mechanical strength of the composite chitosan and alginate scaffolds. For the consistency of our characterization experiments and in vitro biological tests, we used only 4.8% (2.4%chitosan and 2.4%alginate) scaffolds made at PH 5-7 and frozen at -20°C with 24 hours coarsening time at -20°C.

All the scaffolds were made with same concentration (4.8%), same pH value, and same freezing temperature; only the coarsening time varied. Figure A shows the scaffolds without coarsening time. Figure B shows the scaffold with 2 hours room temperature with 2 hours -20°C. Figure C shows the scaffold with 2 hours room temperature with 12 hours -20°C. Figures A,B, C are the top view image. Figures A',B' and C' are the vertical views of A,B and C respectively.

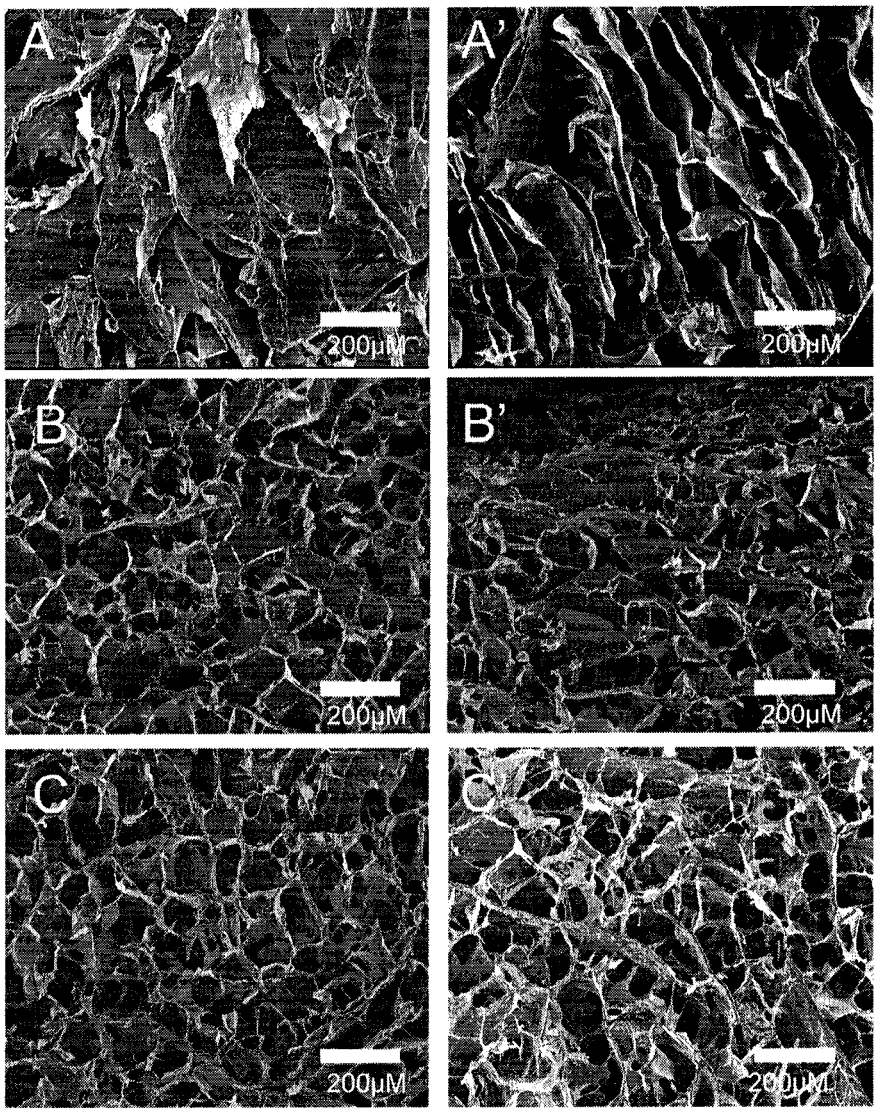

Figure 5-3 The SEM pictures of the scaffolds with different coarsening time

5.42 Pore structure and pore size distribution

The pore structures of the hybrid scaffolds are not uniform; they are typically bird's nest-like morphology with many shattered fragments. Numerous small pores interconnect the big pores. The pore wall is rough. Comparatively, the pore structure of pure chitosan looks less like a bird's nest, there are fewer fragments and fewer small interconnecting pores. The pore walls are smooth. Figure 5-4

compares the pore structure and pore walls of the hybrid chitosan-alginate scaffolds and the pure chitosan scaffolds.

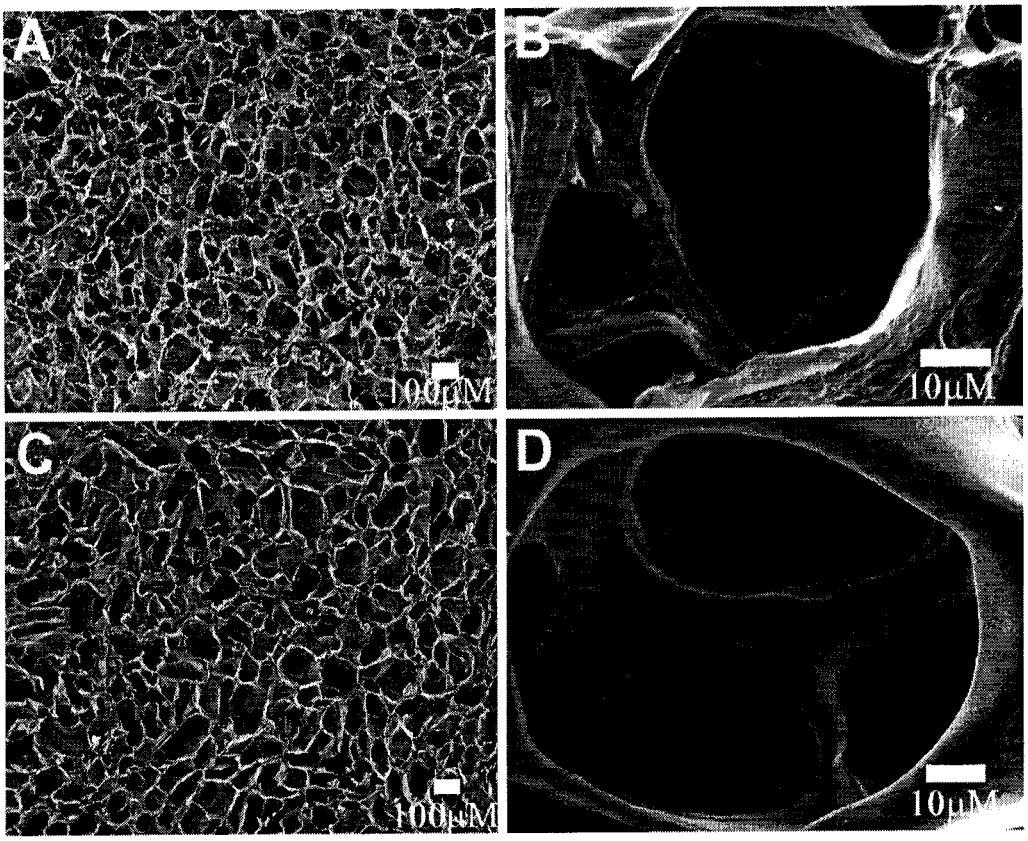

Figure 5- 4 SEM microphotographs of the cross sections of porous scaffolds. A and B: chitosan-alginate scaffold, and C and D: pure chitosan scaffold.

We measured the pore size with software provided by the JOEL 7000 SEM. Two hundred random pores were measured by their longest diameter. The results were categorized into 5 groups. We also compared the pore size with the pure chitosan scaffolds. We did not measure the small pores on the large pore wall as we regarded them as part of the pore wall. The average pore size of hybrid

scaffolds is larger than the pore size of pure chitosan scaffolds (242 ±45μm vs 226±52μm).

The porosities of hybrid chitosan-alginate and pure chitosan scaffolds in this study by liquid displacement method were determined to be 91.94 ± 0.90% and 84.86 ± 2.18% respectively. The mercury intrusion porosimentry tests showed the porosity of the hybrid scaffolds is 92-95%, while the porosity of pure chitosan scaffolds is around 87-89%.

5.43 Mechanical properties

Scaffolds for bone tissue engineering must have mechanical strength capable of supporting bone tissue growth at the site of implantation and maintaining sufficient integrity during both *in vitro* and *in vivo* cell growth [27-29]. One of the major challenges in the fabrication of porous polymer scaffolds is the tradeoff interest between adequate material porosity and mechanical strength. A highly porous structure is necessary for cell ingrowth and proliferation, but the mechanical strength decreases with the increasing porosity[29]. The results of compression testing for both chitosan (4.8%) and chitosan-alginate scaffolds (4.8%) are shown in Figure5-5. The elastic modulus was calculated as the slope of the initial linear portion of the stress-strain curve. The compressive yield stress for pure chitosan and chitosan-alginate scaffolds, as shown in Figure 5-5 are 0.125 ± 0.015 MPa and 0.46 ± 0.022 MPa, respectively. The Young's module of the pure chitosan is 2.56 ± 0.41 MPa while the chitosan and alginate scaffold has Young's modulus of 8.16 ± 1.57 MPa. To the best of our knowledge, such high

compressive strength and Young's modulus have not been reported on natural polymer-based tissue engineering scaffolds that have porosity above 90%.

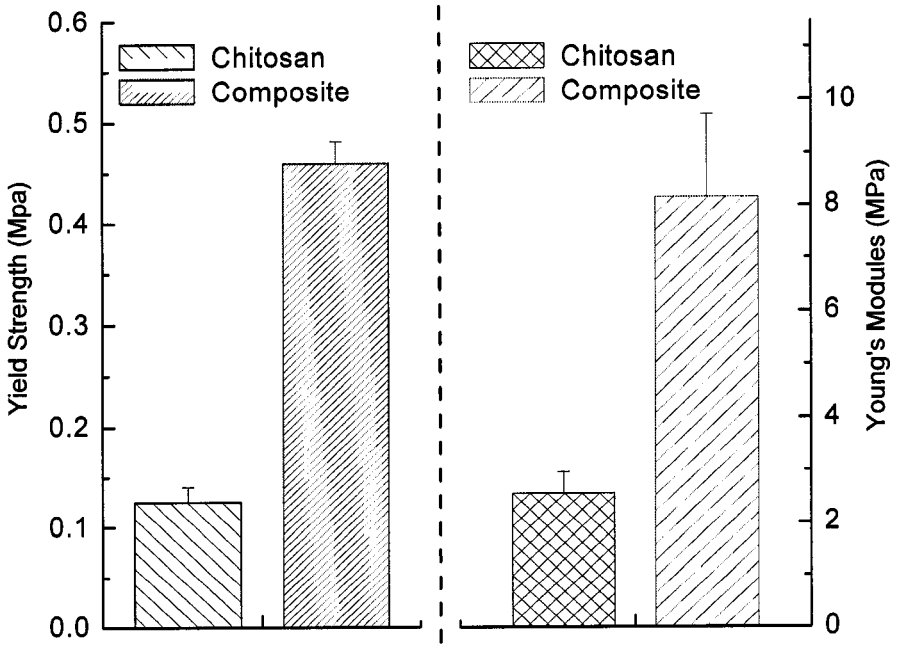

Figure 5- 5. Compressive strength and modulus of chitosan and chitosan-alginate scaffolds.

We also tested the tensile mechanical strength for 4% chitosan-alginate, pure chitosan and pure alginate scaffolds. We chose to test on the 4% scaffolds rather than the 4.8% scaffolds because recently we were successful in making 4% pure alginate scaffolds with good external morphology and texture. Figure 5-6 shows that the pure alginate scaffold (4% w/v) is the strongest scaffold in

tensile strength (0.79MPa, strain 0.0091) among the three scaffolds. The pure chitosan (4% w/v) is the weakest scaffold in tensile strength (0.41, Strain 0.00825). The hybrid chitosan-alginate (4% w/v) scaffold falls between the other two scaffolds (0.48, strain 0.0069).

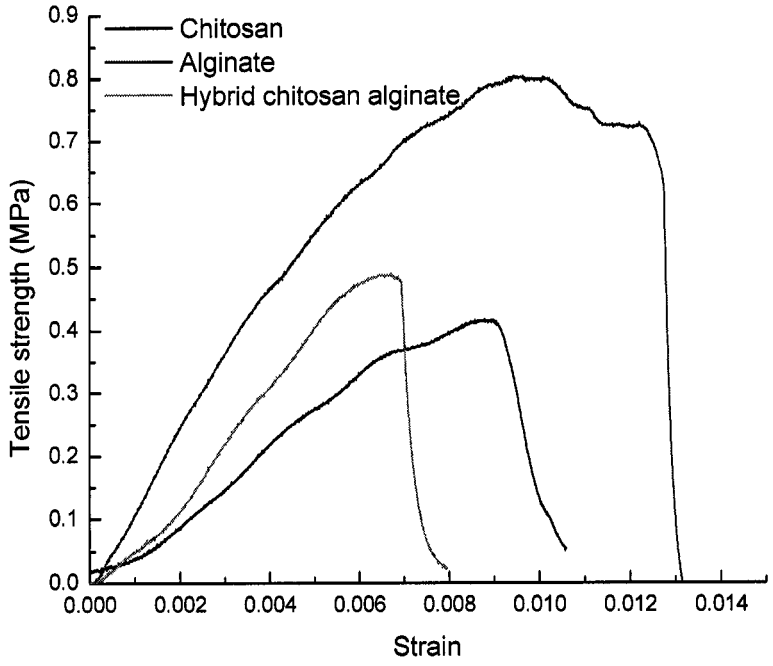

Figure 5- 6 Tensile tests for the chitosan-alginate scaffolds and pure chitosan, pure alginate scaffolds.

5.44 Stability and degradation

Water intrusion or water permeability is a very important property that will affect possible nutrient diffusion and transportation in the scaffolds. We tested the water permeability by the water intrusion method. The results showed that the hybrid chitosan and alginate can be thoroughly wet almost immediately after the scaffolds are immersed. The absorption rate was 11.79 (±0.62,n=6) folds of

dry weight. Comparatively, the pure chitosan scaffolds were slow in the water intrusion (Figure 5-7). Five minutes after immersion, the absorption rate was only 5.4(±0.29, n=4) folds of the dry weight; 15 minutes later, it had reached 8.18(±0.18, n=4) folds. Thirty minutes later, it reached a stable rate of 9.29(±0.39, n=4) folds and there were still some parts of the pure chitosan scaffold remained water impermeable. This was likely caused by the hydrophobic chitin that remained in chitosan.

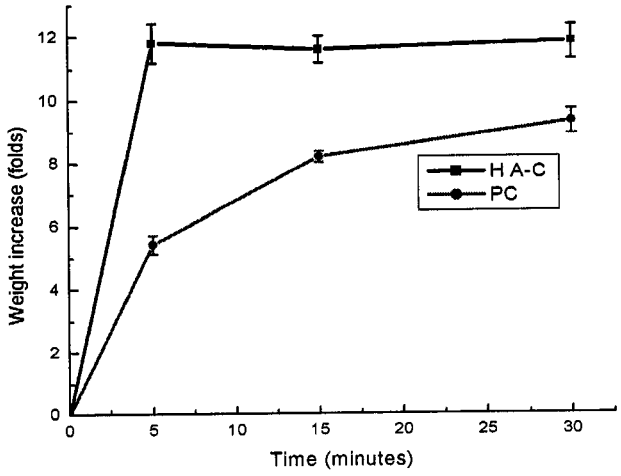

Figure 5- 7. Water permeability of hybrid chitosan-alginate scaffolds and pure chitosan scaffolds

Swelling behavior and structural stability of scaffolds are critical for their practical use in tissue engineering. Most natural polymers, including chitosan, swell readily in biological fluids. *In vitro* culture studies[30] indicated that initial swelling is desirable and the resultant increase in pore size facilitates cell attachment and growth in a three-dimensional fashion. However, continuous swelling would lead to loss of mechanical integrity and production of compressive stress to surrounding tissue. Swelling behavior of a scaffold depends heavily on pH value

at the implantation site. The swelling behavior of scaffolds prepared in this study was investigated by exposure to media of a different pH. The scaffolds were cylindrical in shape with a diameter of 13 mm and a thickness of 3 mm. The inset in Figures 5-8 shows optical images of (A) chitosan-alginate and (B) chitosan scaffolds in a simulated body fluid (pH = 7.4) after two weeks of sample immersion. The chitosan-alginate scaffold appeared to retain its overall size and cylindrical shape, while swelling was noted on the chitosan scaffold.

Swelling behavior was quantified by measuring the diameters of samples as function of sample immersion time in solutions of 1N HCl (pH = 0), 1N NaOH (pH = 14), and simulated body fluid (SBF) (pH = 7.4). The swelling behavior of the chitosan scaffolds differed distinctly in three solutions of different pH (Figure 5-8). The chitosan scaffold in 1N HCl started to swell rapidly and the sample was dissolved in two hours. The chitosan scaffold in SBF solution (pH= 7.4) also swelled over time with its diameter increased by ~ 20% within two hours but underwent a minor swelling thereafter at a significantly reduced rate. The chitosan scaffold in 1N NaOH basic solution (pH = 14) swelled initially (< 5%) but retained its overall size thereafter for weeks. The chitosan scaffold is stable only in solutions of physiological or high pH. In contrast to the chitosan scaffold, the swelling behavior of the chitosan-alginate scaffold was about the same in all three solutions: except an initial swelling (within a half hour), it retained its overall size through the period of study (6 weeks). The initial swelling process is due to the regaining of desorption water during the secondary freeze-drying. This

suggests that the chitosan-alginate scaffold is stable regardless of the solution's pH value. This flexibility makes the scaffold applicable to a wider range of clinical situations. Swelling and degradation of pure chitosan involve the protonation of amino/imine groups on material surface and the mechnical relaxation of coiled chitosan chains.[31-33] The stability of chitosan-alginate scaffold can be attributed to (1) the interaction of amine groups on chitosan with carboxyl groups on alginate which prevents the protonation of amino groups on chitosan, and (2) the carboxyl groups on alginate that buffers the solution and slows down chitosan degradation.

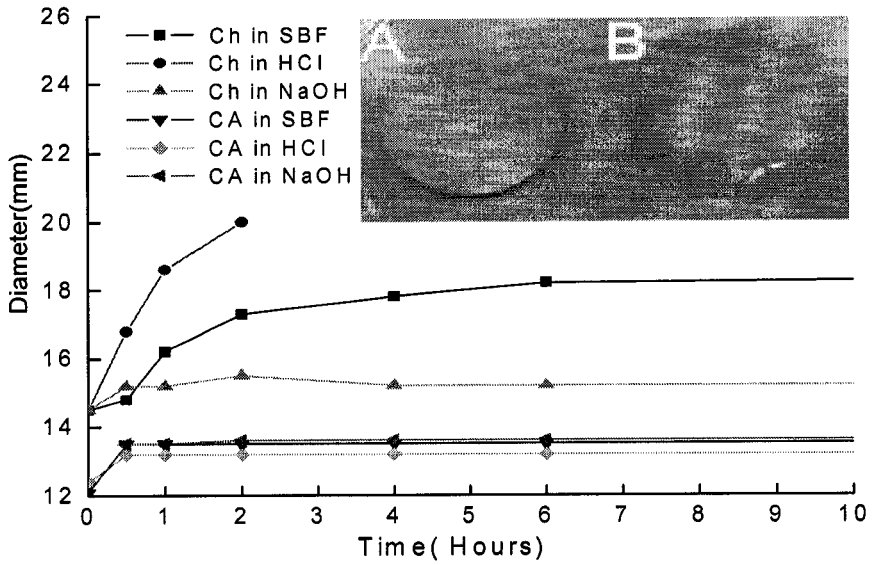

Figure 5- 8. Shape retention Change in sample diameter as a function of sample immersion time in 1N HCl, 1N NaOH, and SBF solutions. Ch and CA in the legend denote pure chitosan and chitosan-alginate scaffolds, respectively. Inset: Images of A chitosan-alginate and B pure chitosan scaffolds after two weeks of sample immersion in simulated body fluid.

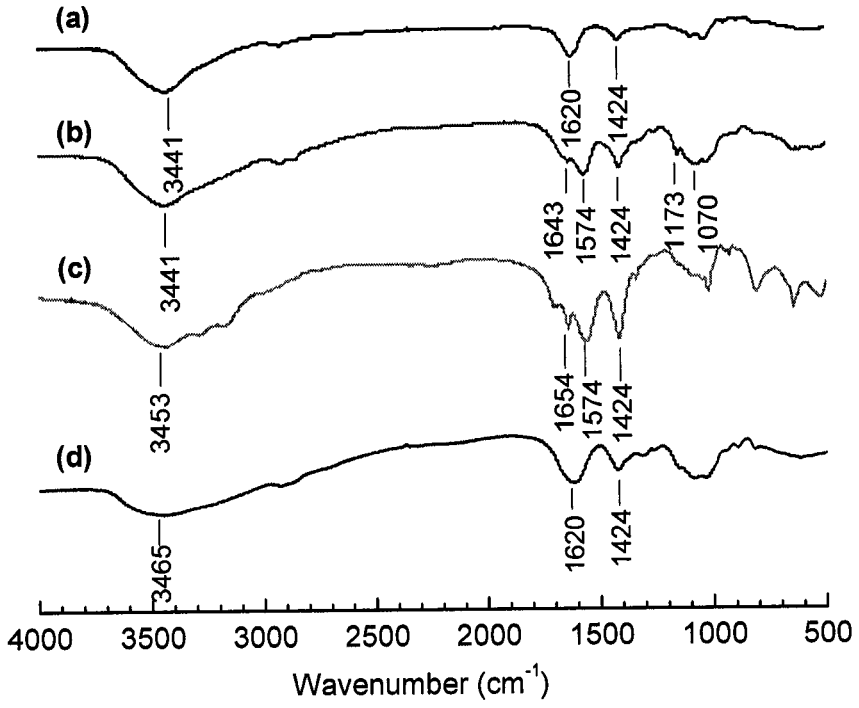

Figure 5- 9. FTIR of spectra of scaffolds

5.45 FTIR analysis

FTIR analysis showed strong ionic interactions between chitosan and alginate to form a chitosan-alginate complex (Figure. 5-9). The characteristic peak of alginate (Figure 5-9**a**) is seen at 1620 cm^{-1} corresponding to carbonyl (C=O) bond. The chitosan spectrum (Figure 5-9**b**) shows characteristic bands of amide-I (1643 cm^{-1}), amide II (1574 cm^{-1}), and amino group (1173 cm^{-1}). Chitosan used in these experiments was 85% deacetylated. The double amide

peaks for chitosan correspond to the partial N-deacetylation of chitin.[34] The peaks at 1424 cm^{-1} and 1070 cm^{-1} in both alginate and chitosan scaffolds correspond to carboxyl -COOH and C-O stretching bands, respectively. In the chitosan-alginate spectrum (Figure 5-9**c**), amide II peaks were significantly intensified, amide I peak shifted from 1643 cm^{-1} to 1654 cm^{-1}, and the peak of amino group (1173 cm^{-1}) was absent. These changes suggest the formation of chitosan-alginate complex as a result of the ionic interaction between the negatively charged carbonyl group (-COOH) of alginate and the positively charged amino group ($-NH_2$) of chitosan.[35-37] An apparent change in spectrum is seen after chitosan-alginate was cross-linked with $CaCl_2$ (Figure 5-9**d**). The amide-I (C=O, 1643 cm^{-1}) and amide-II (C-N, 1574 cm^{-1}) bands were replaced by a new band (1620 cm^{-1}), as a result of the interaction of two residual carboxylic groups on alginate linking adjacent coacervates into a network matrix.

Notes to Chapter Five

1. Mikos, A. G., Lyman, M. D., Freed, L. E. & Langer, R. Wetting of poly(L-lactic acid) and poly(DL-lactic-co-glycolic acid) foams for tissue culture. Biomaterials 15, 55-8 (1994).

2. Gravel, M., Vago, R. & Tabrizian, M. Use of natural coralline biomaterials as reinforcing and gas-forming agent for developing novel hybrid biomatrices: microarchitectural and mechanical studies. Tissue Eng 12, 589-600 (2006).

3. Yang, S., Leong, K. F., Du, Z. & Chua, C. K. The design of scaffolds for use in tissue engineering. Part II. Rapid prototyping techniques. Tissue Eng 8, 1-11 (2002).

4. Li, Z. & Zhang, M. Chitosan-alginate as scaffolding material for cartilage tissue engineering. J Biomed Mater Res A 75, 485-93 (2005).

5. Guan, J., Fujimoto, K. L., Sacks, M. S. & Wagner, W. R. Preparation and characterization of highly porous, biodegradable polyurethane scaffolds for soft tissue applications. Biomaterials 26, 3961-71 (2005).

6. Zhao, L. & Chang, J. Preparation and characterization of macroporous chitosan/wollastonite composite scaffolds for tissue engineering. J Mater Sci Mater Med 15, 625-9 (2004).

7. Cao, Y., Davidson, M. R., O'Connor, A. J., Stevens, G. W. & Cooper-White, J. J. Architecture control of three-dimensional polymeric scaffolds for soft tissue engineering. I. Establishment and validation of numerical models. J Biomed Mater Res A 71, 81-9 (2004).

8. Yang, S., Leong, K. F., Du, Z. & Chua, C. K. The design of scaffolds for use in tissue engineering. Part I. Traditional factors. Tissue Eng 7, 679-89 (2001).

9. Li, Z., Ramay, H. R., Hauch, K. D., Xiao, D. & Zhang, M. Chitosan-alginate hybrid scaffolds for bone tissue engineering. Biomaterials 26, 3919-28 (2005).

10. Zhang, Y. & Zhang, M. Calcium phosphate/chitosan composite scaffolds for controlled in vitro antibiotic drug release. J Biomed Mater Res 62, 378-86 (2002).

11. Maspero, F. A., Ruffieux, K., Muller, B. & Wintermantel, E. Resorbable defect analog PLGA scaffolds using CO2 as solvent: structural characterization. J Biomed Mater Res 62, 89-98 (2002).

12. Karageorgiou, V. & Kaplan, D. Porosity of 3D biomaterial scaffolds and osteogenesis. Biomaterials 26, 5474-91 (2005).

13. Zhao, F. et al. Preparation and histological evaluation of biomimetic three-dimensional hydroxyapatite/chitosan-gelatin network composite scaffolds. Biomaterials 23, 3227-34 (2002).

14. Zhang, R. & Ma, P. X. Porous poly(L-lactic acid)/apatite composites created by biomimetic process. J Biomed Mater Res 45, 285-93 (1999).

15. Zhang, R. & Ma, P. X. Poly(alpha-hydroxyl acids)/hydroxyapatite porous composites for bone-tissue engineering. I. Preparation and morphology. J Biomed Mater Res 44, 446-55 (1999).

16. Zhang, Y. & Zhang, M. Synthesis and characterization of macroporous chitosan/calcium phosphate composite scaffolds for tissue engineering. J Biomed Mater Res 55, 304-12 (2001).

17. ED, S. Late stage of decomposition in binary mixtures. Phys Rev A 20, 595 (1979).

18. Yuan, Z. & Favis, B. D. Macroporous poly(L-lactide) of controlled pore size derived from the annealing of co-continuous polystyrene/poly(L-lactide) blends. Biomaterials 25, 2161-70 (2004).

19. Yoo, P. J., Suh, K. Y., Kang, H. & Lee, H. H. Polymer elasticity-driven wrinkling and coarsening in high temperature buckling of metal-capped polymer thin films. Phys Rev Lett 93, 034301 (2004).

20. Xie, X. M. et al. Interface-Induced Coarsening Process in Polymer Blends. J Colloid Interface Sci 234, 24-27 (2001).

21. Matsumoto, T., Kawai, M. & Masuda, T. Rheological properties and fractal structure of concentrated polyion complexes of chitosan and alginate. Biorheology 30, 435-41 (1993).

22. Desbrieres, J. Viscosity of semiflexible chitosan solutions: influence of concentration, temperature, and role of intermolecular interactions. Biomacromolecules 3, 342-9 (2002).

23. Delben, F., Lapasin, R. & Pricl, S. Flow properties of N-(carboxymethyl) chitosan aqueous systems in the sol and gel domains. Int J Biol Macromol 12, 9-13 (1990).

24. Murata, Y., Jinno, D., Kofuji, K. & Kawashima, S. Properties of calcium-induced gel beads prepared with alginate and hydrolysates. Chem Pharm Bull (Tokyo) 52, 605-7 (2004).

25. O'Brien, F. J., Harley, B. A., Yannas, I. V. & Gibson, L. J. The effect of pore size on cell adhesion in collagen-GAG scaffolds. Biomaterials 26, 433-41 (2005).

26. Madihally, S. V. & Matthew, H. W. Porous chitosan scaffolds for tissue engineering. Biomaterials 20, 1133-42 (1999).

27. Porter, B. D. et al. Mechanical properties of a biodegradable bone regeneration scaffold. J Biomech Eng 122, 286-8 (2000).

28. Chu, T. M., Orton, D. G., Hollister, S. J., Feinberg, S. E. & Halloran, J. W. Mechanical and in vivo performance of hydroxyapatite implants with controlled architectures. Biomaterials 23, 1283-93 (2002).

29. Thomson, R. C., Yaszemski, M. J., Powers, J. M. & Mikos, A. G. Fabrication of biodegradable polymer scaffolds to engineer trabecular bone. J Biomater Sci Polym Ed 7, 23-38 (1995).

30. Shanmugasundaram, N. et al. Collagen-chitosan polymeric scaffolds for the in vitro culture of human epidermoid carcinoma cells. Biomaterials 22, 1943-51 (2001).

31. Khalid, M. N., Agnely, F., Yagoubi, N., Grossiord, J. L. & Couarraze, G. Water state characterization, swelling behavior, thermal and mechanical properties of chitosan based networks. Eur J Pharm Sci 15, 425-32 (2002).

32. Vachoud, L., Zydowicz, N. & Domard, A. Physicochemical behaviour of chitin gels. Carbohydr Res 326, 295-304 (2000).

33. Aiba, S. Studies on chitosan: 3. Evidence for the presence of random and block copolymer structures in partially N-acetylated chitosans. Int J Biol Macromol 13, 40-4 (1991).

34. M Sugimoto, M. M., Hitoshi Sashiwa, H Saimoto, Y Shigemasa. Preparation and characterization of water soluble chitin and chitosan derivatives. Carbohydrate Polymers 36, 49-59 (1998).

35. Wang, L., Khor, E. & Lim, L. Y. Chitosan-alginate-CaCl(2) system for membrane coat application. J Pharm Sci 90, 1134-42 (2001).

36. C.J. Brine, P. A. S., J.P. Zikakis. Advances in Chitin and Chitosan (ed. C Mireles, M. M., J Bouzas, JA Torres) (Elsevier, London, 1992).

37. T Takahashi, K. T., Y Machida, T Nagai. Characteristics of Polyion-complex of chitosan with sodium alginate and sodium polyacrylate. Int. J. Phar 61, 35-41 (1990).

Chapter Six

Hybrid chitosan-alginate scaffolds for cartilage tissue engineering

6.1 Introduction

Millions of people suffer from degeneration of articular cartilage in primary osteoarthritis or following trauma. Since the damaged articular cartilage has a very limited capability for self-healing, functional restoration of diseased and damaged human articular cartilage is highly desirable. Tissue engineering is recognized as a promising strategy for regeneration of long-lasting cartilage and has been studied intensively in both research and clinical practice. For cartilage treatment in tissue engineering, a scaffold serves to support chondrocyte cell attachment and proliferation for new tissue regeneration as the scaffold gradually degrades.[1-3] An ideal scaffold in this context should be tissue compatible at the site of implantation and biodegradable, have a highly porous structure of a three-dimensionally interconnected network and sufficient mechanical strength, and closely mimic the naturally occurring environment in the articular cartilage matrix.[4] Collagen type II and GAG, two components of the cartilage-specific extracellular matrix (ECM), have been shown to play a critical role in regulating expression of chondrocytic phenotype and supporting chondrogenesis both in vitro and in vivo.[5-7]

A number of biologically derived or synthetic polymers have been studied as potential scaffolds for cartilage tissue repair,[8, 9] including collagen-based sponges and gels,[10,11,12] fibrin,[13] hyaluronic acid,[14] polyglycolide,[15] poly(lactide-

coglycolide),[16] and peptide hydrogel.[17] These materials can support chondrocytes for formation of collagen and proteoglycan, but the results have been inconsistent with the morphology of generated cartilage tissue ranging from hyaline-like to fibrous in quality.[18-20] This may be due to the fact that the chemical compositions and structures of these scaffolds do not match well with the extracellular matrix of articular cartilage.

Recently, there has been an increased interest in the use of naturally occurring polymers as scaffolds for cartilage regeneration. Chitosan, a partially deacetylated derivative of chitin composed of *N*-acetylglucosamine, is biologically renewable, biodegradable, biocompatible, non-antigenic, non-toxic, and bio-functional. It shares some characteristics with various GAGs and hyaluronic acid present in articular cartilage.[4] Chitosan has been used as a scaffold for cartilage repair.[4, 19, 21] Studies have shown that chondrocyte cells retain a round shape on a chitosan-coated surface and produce their characteristic ECM components such as collagen type II and proteoglycan. Alginate is a family of polyanionic copolymers derived from brown sea algae and comprises 1,4-linked β-D-mannuronic (M) and α-L-guluronic (G) residues in varying proportions. Alginate is soluble in aqueous solutions and forms stable gels at room temperature in the presence of certain divalent cations (i.e., Ba^{2+}, Ca^{2+}). Alginate beads have been developed to recover or expand primary chondrocytes. They promote cell proliferation and retain cell functionality and phenotype.[22, 23,24]Here, chitosan-alginate was studied for potential use as a scaffolding material for cartilage repair

and regeneration. The demonstrated major advantage of this hybrid material is its superior mechanical properties that neither chitosan nor alginate alone can attain.[25] Unlike chitosan or alginate, the chitosan-alginate scaffold can be prepared from solutions of neutral pH, offering an additional advantage of allowing proteins or drugs to be uniformly incorporated in its matrix structure with no or minimal denaturization.[25] Cell attachment, proliferation and phenotype of chondrocytes on porous chitosan and chitosan-alginate scaffolds were studied and compared. The microstructures of scaffolds and the morphology of cells were characterized by scanning electron microscopy (SEM). Cell functionality was examined by identification of collagen biosynthesis through SDS-PAGE electrophoresis and Western Blot.

6.2 Materials and methods

6.21 Materials

Chitosan (MW 400,000; 85% deacetylated), sodium alginate, sodium dodecyl sulfate (SDS), Dulbecco's phosphate buffered saline, antibiotics, penicillin, and streptomycin were obtained from Sigma-Aldrich (St. Louis, MO). Fetal bovine serum (FBS) was obtained from Hyclone, UT. Chondrocytes from cell line HTB-94 (American Type Culture Collection, ATCC) were used as received. Dulbecco's Modified Eagle Medium (DMEM) 1X, containing high glucose, L-glutamine, 110 mg/L, sodium pyruvate, and pyridoxine hydrochloride, was obtained from Invitrogen Life Technologies (Grand Island, NY). Alamar Blue solution was obtained from Alamar BioSciences (Sacramento, CA). 4-15% SDS-

PAGE 12-well gel, Coomassie Blue staining solution, and blot transfer buffer solution were obtained from Bio-Rad (Hercules, CA). CytoBuster™ Protein Extraction Reagent was purchased from EMD, Biosciences, CA. Urea was obtained from J. T. Baker (Phillipsburg, NJ). The primary antibody, secondary antibody (goat anti-mouse antibody conjugated with HRP), and ECL detection solutions were obtained from Chemicon International (Temecula, CA). All other reagents were of analytical grade.

6.22 Preparation of chitosan-alginate and chitosan scaffolds

(See 5.2 of Chapter Five)

6.23 Cell culture

The scaffolds were sterilized with ethylene oxide gas and presoaked in a 12-well cell culture plate containing DMEM culture medium for a couple of days before cell seeding. Approximately 1 million chondrocyte cells in 1 ml Dulbecco's Modified Eagle Medium (DMEM) were seeded on each scaffold disc. The DMEM medium contained 10% fetal bovine serum (FBS), 50 IU ml^{-1} penicillin, and 50 μg ml^{-1} streptomycin. The scaffolds were transferred to another cell culture plate after 3 hours of cell seeding. The culture medium in the plate was changed in 24 hours for the first time and every three days thereafter. A hemocytometer was used to determine the concentration of cells in cell suspension. The morphology of cells cultured on scaffolds was examined by scanning electron microscopy (SEM, JEOL, JSM-840A). For SEM observation, scaffolds were fixed with

Karnovsky's fixative overnight at room temperature and dehydrated in 50%, 75%, 95%, 100% ethanol, respectively for 2 hours. The samples were then dried by a critical point drying apparatus, coated with Au/Pd, and examined with SEM.

6.24 Cell proliferation and viability

Cell proliferation was assessed using the Alamar Blue assay. Scaffolds were seeded with cells in DMEM cell culture medium. After 24 hours of cell seeding, the scaffolds were washed with PBS and placed into12-well culture plates. 2 ml of 10% v/v Alamar Blue in DMEM medium was added to each well containing scaffolds and the plates were incubated for 4 hours at 37°C. Absorbance of the solution in each plate, which is proportional to the number of cells attached to the sample, was measured with a micro plate reader (Molecular Device, Versamax^{TM} tunable microplate reader) at wavelengths of 570 and 600 nm. A calibration curve generated from a known number of chondrocytes reacting with the Alamar Blue was used to calculate the number of cells. Samples were assayed at 3, 7, 14 and 21 days, respectively after cell culture.

Cell viability was assessed using a Live vs. Dead assay kit (Molecular Probes). Chitosan-alginate and chitosan scaffolds cultured with cells for 21 days were placed in phosphate-buffered saline containing vital dye calcein-AM and nuclear stain ethidium homodimer-1 (both from Live/Dead assay Kit). Calcein-AM is a non-fluorescent, cell-permeant fluorescein derivative, which is converted by cellular enzymes into cell-impermeant and highly fluorescent calcein. Calcein accumulates inside live cells with intact membranes and causes the cells to

fluoresce green. Ethidium-homodimer-1 enters dead cells with damaged membranes and undergoes a 40-fold enhancement of fluorescence upon binding to their DNA causing the nuclei of dead cells to fluoresce red. This staining showed both live and dead cells attached on the scaffold. Images of cultured chondrocyte cells on scaffolds were acquired using an inverted fluorescent microscope equipped with a CCD camera.

6.25 Histology

Scaffolds seeded with chondrocyte cells were washed twice with PBS and fixed with 4% paraformaldehyde for histological assay. The scaffolds were embedded in paraffin and cut into 5 μm thick sections using a microtome. The sections were stained with Masson's trichrome, specifically, treated with Biebrich scarlet-acid fuchsin, phosphomolybdic-phosphotugnstic acid, and aniline blue solutions for 5, 10, and 3 minutes, respectively. The stained sections were then mounted on glass slides, and examined with a Nikon 200 microscope.

6.26 Electrophoresis and Western Blot

The extracted cellar proteins from cells cultured on scaffolds were analyzed by sodium dodecyl sulfate polyacrylamide gel electrophoresis (SDS-PAGE). The scaffolds were harvested in triplet after 14 days and 21 days of cell culture, respectively. After harvest, the scaffolds were washed twice with PBS and placed in 50 ml tubes. 0.1% proteinase in CytoBuster™ protein extraction reagent was used to extract proteins from the cells grown on scaffolds. The extraction solution

was transferred to a 10 ml test tube and centrifuged at 14,000 rpm for 10 min. After centrifugation, the supernatant was removed, and the pallet was washed with cold 90% ethanol and air-dried. The pellet was treated by 10M urea and boiled in 100°C water bath for 5 min for protein denaturization. An equal amount of the protein was extracted from each sample as quantified by UV spectroscopy and added into a well of the electrophoresis gel apparatus for protein analysis. Proteins were subjected to electrophoresis on a 4–15% polyacrylamide gel, and the protein bands were acquired with Coomassie Blue staining.

Western blot assay was performed to further confirm the production of collagen type II following the SDS-PAGE electrophoresis. The proteins in the polyacrylamide gel were first equilibrated in transfer buffer for 15 min and then electrophoretically transferred to nitrocellulose membranes. The transfer unit was run at 100 volts for 1 hour in transfer buffer. The successfully transferred membrane was blocked with 5% Blot-Quickblocker in TBST (Tris-Buffered Saline + 1% triton) buffer for 20 min at room temperature. Primary mouse anti-human type II collagen monoclonal antibody was diluted 1000 folds by the blocker solution, and the diluted antibody was incubated with the nitrocellulose membrane for 90 min at room temperature. After incubation, the membrane was washed five times with TBST buffer on a rotator for 10 min each, and incubated with the secondary antibody diluted at 1:2000 in TBST solution containing 0.5% Blot-Quickblocker for 90 min at room temperature. The membrane was then washed five times with 100 ml 1XTBST buffer for 10 min each and transferred

into a solution with ChemiLucent diluted at 1:1000 in peroxide solution of equal volume of peroxide buffer and luminol/enhancer. Finally the membrane was placed together with Kodak negative film in a cassette in a dark room to expose light for protein blots.

6.3 Results

6.31 Microstructures of Scaffolds

Figure 1 shows the SEM images of the microstructures of (A) chitosan-alginate and (B) chitosan scaffolds. Both scaffolds have a highly porous structure with a fairly even pore distribution and a pore size ranging from 100 to 300 μm, a favorable size range for cell growth.[26] The surface and pore walls of the pure chitosan scaffold are relatively smooth, while the surface of the chitosan-alginate scaffold is relatively rough and embedded with small grooves.

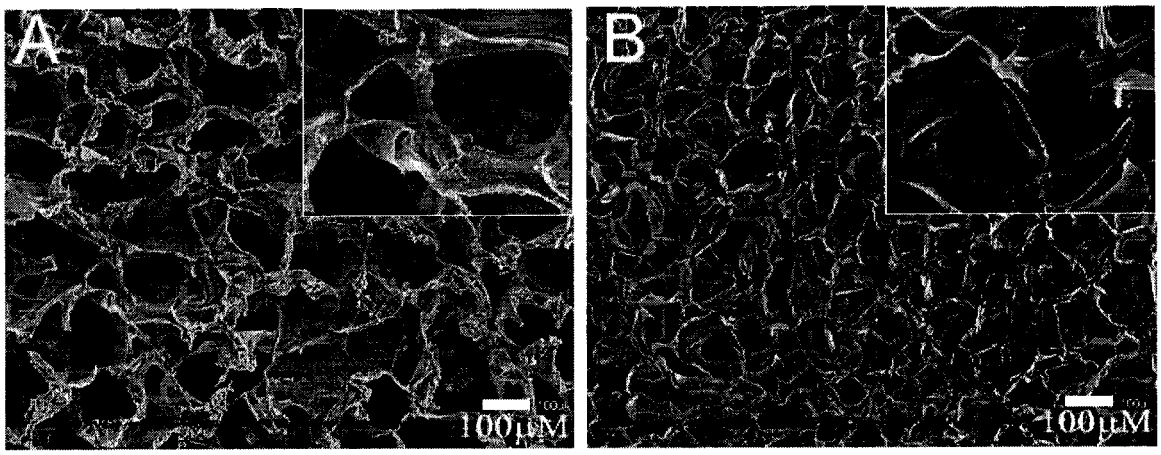

Figure 6- 1 SEM images of (A) chitosan-alginate and (B) pure chitosan scaffolds. The insets detail the pore interconnectivity of the microstructures

The further magnified images shown in Figure 1 as insets illustrate a high degree of pore interconnectivity for both chitosan-alginate and chitosan scaffolds.

6.32 Cell proliferation

Chondrocyte-like HTB-94 cell line was selected as our model cell line because it can express the characteristic features of chondrocytes with eternal growth capability. Cell proliferation on both chitosan and chitosan-alginate scaffolds as a function of time was assessed using the Alamar Blue assay, and the results are shown in Figure 2.

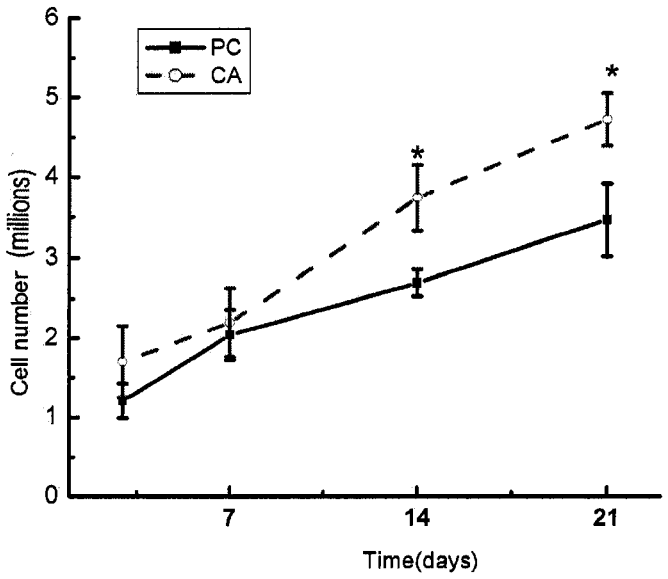

Fig 6- 2. Cell proliferation as measured by the Alamar Blue assay. PC stands for pure chitosan scaffold, CA for chitosan-alginate scaffold. The star mark shows the time points where a significant difference exits.

The cells on both scaffolds were doubled within the first week of cell culture and continued to increase over time. Three samples in triplet were tested and the results were analyzed by a non-parametric test. No significant difference in cell number was observed between the chitosan and chitosan-alginate scaffolds at day 3 and day 7 after cell culture. However, the cell number on the chitosan-alginate scaffold became notably higher than that on the chitosan scaffold at day 14 and day 21.

6.33 Cell viability

The fluorescence microscopic images of both live (green) and dead (red) cells on chitosan-alginate and chitosan scaffolds incubated with chondrocyte cells for 21 days are shown in Figures 3A and 3B, respectively.

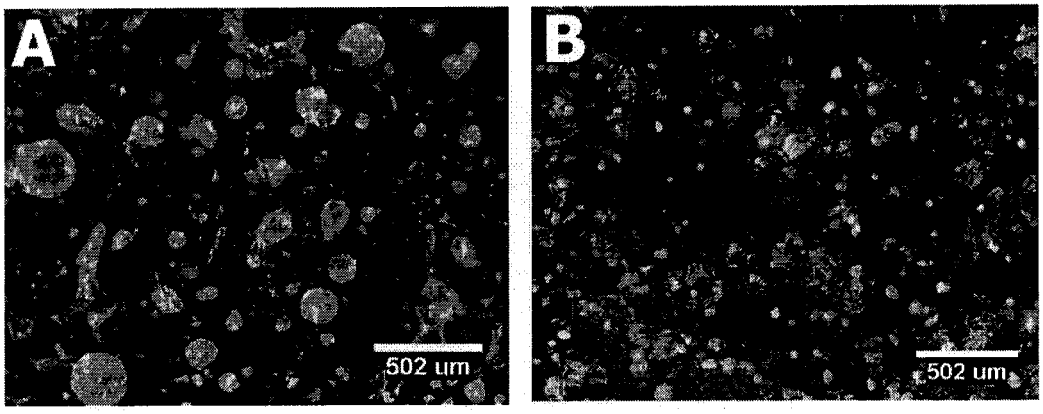

Figure 6- 3. Fluorescence microscopic images of chondrocytes on (A) chitosan-alginate and (B) pure chitosan scaffolds after 21 days of cell culture. Live and dead cells fluoresce green and red, respectively.

On both scaffolds, the majority of cells were alive; a small number of dead cells were distributed sporadically among the live cells. On the chitosan-alginate scaffold, the majority of cells formed clusters, while the remaining isolated cells

exhibited round-shape morphology. Cells on the chitosan scaffold formed fewer clusters than on the chitosan-alginate scaffold, and mostly exhibited a spread morphology, which is typical for fibroblast-like cells.

6.34 Cell morphology

Figure. 6-4 shows SEM images of chondrocyte cells grown on chitosan-alginate (A, C) and chitosan (B, D) scaffolds after 14 and 21 days of cell culture. Figures 4E and 4F show the the images taken at day 21 at a higher magnification in order to detail the cell morphology. At day 14, chondrocyte cells on both scaffolds proliferated well and exhibited a spherical morphology. At day 21, however, the cells on the chitosan scaffold became more flattened and started to assume a fibroblast-like morphology, while the cells on the chitosan-alginate scaffold retained their initial spherical morphology.

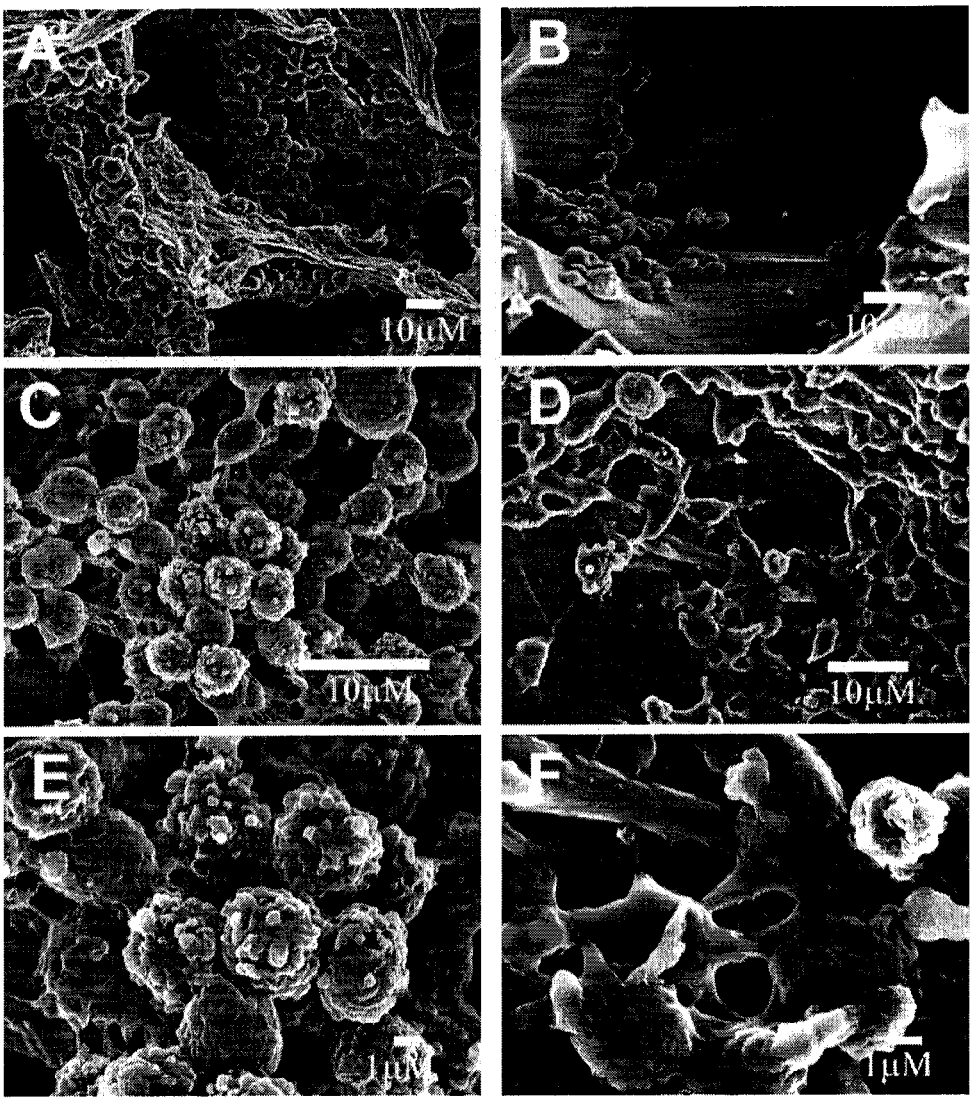

Figure 6- 4. SEM images of chondrocyte cells grown on (A) chitosan-alginate and (B) chitosan scaffolds after 14 days cell culture, and on (C) chitosan-alginate and (D) chitosan scaffolds after 21 days of cell culture. E and F are the images of higher magnification of C and D, respectively

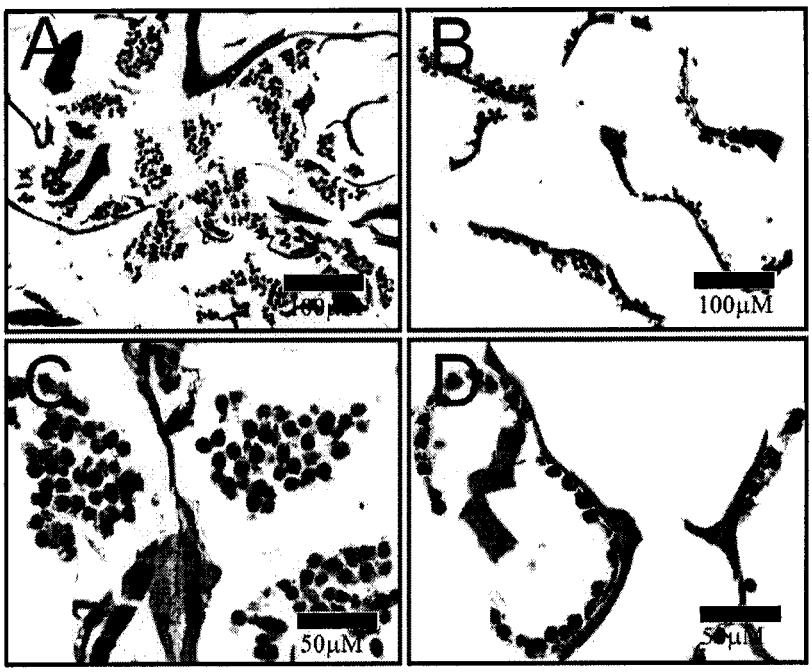

Figure 6- 5. Optical micrographs of chondrocytes seeded on (A, C) chitosan-alginate and (B, D) chitosan scaffolds stained with Masson's trichrome at day 14. (C) and (D) with 200× are images of higher magnification of (A) and (B) with 100×.

Masson's trichrome was used to stain the harvested scaffolds in order to study the interaction of cells with materials and to visualize the formation of collagen. Figure 6-5 shows the optical images of chondrocyte cells stained with Masson's trichrome and grown on chitosan-alginate scaffolds (A and C) and chitosan scaffolds (B and D) after 14 days of cell culture, with cell nuclei appearing in red and collagen in blue. The cells on the chitosan-alginate scaffold had smaller nuclei and larger cytoplasm, in contrast to the cells on the chitosan scaffold which had larger nuclei and smaller cytoplasm. Furthermore, the cells on the chitosan-alginate scaffold tended to form aggregates with spherical cell

morphology, while those grown on the chitosan scaffold exhibited a dominant monolayer growth.

6.35 Cell functionality

Cell functionality was assessed by electrophoresis of cellular proteins in terms of the production of collagen type II. The proteins extracted from the cells grown on the scaffolds were analyzed, and the results are shown in Figure 6A. Lane 1 and lane 2 correspond to the protein extracted from cells on chitosan-

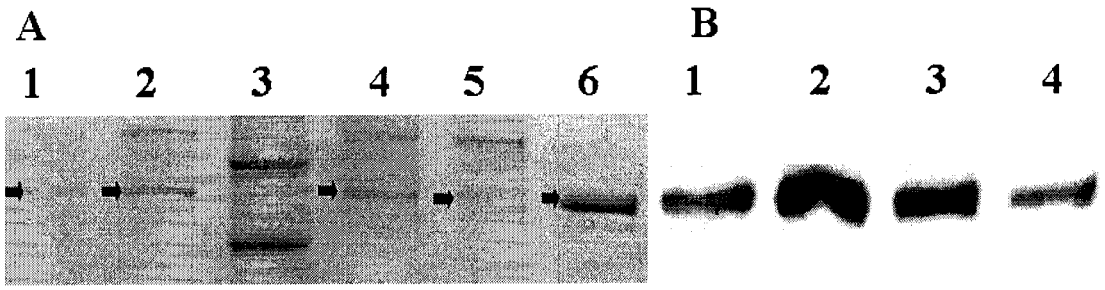

alginate

Figure 6- 6. (A) SDS-PAGE of proteins extracted from chitosan-alginate and chitosan scaffolds for assessment of collagen biosynthesis. Lane 6: standard purified collagen II. Lane 3: standard proteins with different molecular weights. Lanes 1 and 2: proteins from chitosan-alginate scaffolds harvested at day 14 and day 21, respectively. Lanes 4 and 5: proteins from chitosan scaffolds harvested at day 14 and day 21, respectively. (B) Western Blot assay result. Lanes 1 and 2: proteins extracted from cells on chitosan-alginate scaffolds at day 14 and day 21, respectively. Lanes 3 and 4: protein extracted from chitosan scaffolds at day 14 and day 21, respectively.

scaffolds at day 14 and day 21, respectively, after cell culture. Lane 3 is the standard protein molecular weight indicator. Lane 4 and lane 5 are the proteins extracted from cells on pure chitosan scaffolds at day 14 and day 21, respectively, after cell culture. Lane 6 represents the standard human collagen type II. The electrophoresis results show that collagen type II bands were seen at

day 14 and day 21 for both types of scaffolds on the corresponding lanes with molecular weight slightly below 150 kD. However, the intensity of collagen type II band for the chitosan-alginate scaffold increased over time from day 14 (lane 1) to day 21 (lane 2), as opposite to slightly decrease in collagen type II intensity observed for the chitosan scaffold for the same time period (lane 4 and lane 5, respectively). The biosynthesis of cartilage-specific collagen type II by chondrocytes on both chitosan and chitosan-alginate scaffolds was further confirmed by the Western Blot analysis. Mouse anti-human type II collagen monoclonal antibody was used to detect the cartilage-specific collagen type II. Figure 6B shows the bands of cellular proteins extracted from cells on chitosan-alginate (lane 1 and 2) and chitosan (lane 3 and 4) scaffolds. Collagen type II bands were seen in all lanes. However, for the chitosan-alginate scaffold collagen type II content increased from day 14 (lane 1) to day 21 (lane 2) while for the chitosan scaffold collagen type II content decreased over the same time period, which is consistent with the results from SDS-PAGE assay.

6.4 Discussion

Cell attachments, proliferation, and differentiation on a material are the indications of the cellular compatibility of the material and the suitability of the material for tissue engineering applications. Our experimental results show that HTB-94 chondrocyte cells attached well on both chitosan and chitosan-alginate scaffolds without involvement of special cell adhesion techniques such as dynamic seeding and incorporation of adhesion peptides. The cell adhesion

property of chitosan is believed to be related to its polycationic nature, as it has been shown that cell adhesion is inhibited with increasing degree of deacetylation and thus decrease in positive charge.[27] Chitosan-alginate hybrid material appeared to inherit such cellular adhesive property. The cells increased consistently on both chitosan and chitosan-alginate scaffolds over cell culture time, and proliferated faster on the chitosan-alginate scaffold than on the chitosan scaffold (Figure6- 2). Furthermore, the cell viability assay revealed more live cells on chitosan-alginate than on pure chitosan (Figure 6-3). These results are not surprising, as alginate is known to promote cell expansion; chitosan has excellent cell adhesive property due to cationic nature[19] and its degradation product is a GAG-like glucosamine residue that is known to induce chondrogenesis.[19,28]Thus chitosan-alginate hybrid material may combine favorable properties of chitosan and alginate in terms of cellular attachment and proliferation.

A scaffold for articular cartilage should maintain the normal phenotypic characteristics of chondrocytes. A round cellular morphology is known to be indicative of characteristics of non-dedifferentiated chondrocytes,[18] a normal chondrocytic phenotype that results from organization of sparse active actine filaments.[11,29,30] Conversely, a flat or spread morphology indicates the dedifferentiated state of the cell, which is believed to be mediated by the formation of actin stress fibers.[31,32] The ability of chitosan to maintain round cellular morphology has been previously demonstrated for short periods of cell

culture times (e.g., from 48 hours to a week).[21, 33]Here, we extended the cell culture time up to three weeks and found similar results for the first two weeks but not for prolonged cell culture time. (Figures 6-4 D and F). On the other hand, the cells maintained a round shape on chitosan-alginate for the same period (Figures 6-4C and E). Primary chondrocytes isolated from bovine articular cartilage showed a trend similar to immortalized chondrocytes (data not shown). Compared to chitosan, chitosan alginate showed better maintained phenotype of chondrocytes, presumably resulting from special characteristics of alginate material in promoting chondrocyte recovery.[34-36]

Both electrophoresis and Western Blot results showed that type II collagen was the dominant collagen produced by chondrocytes on both chitosan and chitosan-alginate scaffolds. Collagen type II is a biological marker for chondrocytic phenotype, while collagen type I is a marker for induction of fibrous or fibrocartilaginous tissue.[4, 33, 37] The chitosan-alginate scaffold showed prolonged support for collagen type II production as compared to the chitosan scaffold. This result shows a correlation between the biosynthesis of collagen type II and change in cell morphology, consistent with results reported in literature.[14, 19, 36, 38]

It is established that chondrocytes grown in monolayer culture for extended periods exhibit a more elongated morphological appearance, produce less matrix proteoglycans, and preferentially synthesize type I rather than type II collagen.[39, 40] Chitosan-alginate showed better productivity in biosynthesis of collagen type II than pure chitosan, which might be attributable to the ability of alginate to induce

redifferentiation of culture-expanded, dedifferentiated cells. It has been reported that after dedifferentiation to a fibroblastic morphological appearance in monolayer culture, cells seeded into alginate beads reestablished characteristics of differentiated chondrocytes.[41]

The cells on the chitosan tended to form a monolayer, a possible marker of chondrocyte dedifferentiation and fibroblastic phenotype.[42, 43] In contrast, the cells on chitosan-alginate materials formed much larger cell clusters (Figure 6-5). Large cell clusters of chondrocytes in alginate beads have been shown to have the dominant product of collagen type II, while small cell clusters of monolayer of chondrocytes are shown to have the dominant product of collagen type I.[33] Thus, this result also suggests that the chitosan-alginate hybrid material is superior to chitosan in retaining chondrocytic phenotype and inducing chondrogenesis.

In addition, chitosan-alginate hybrid scaffolds have other advantageous attributes as a tissue engineering material compared to chitosan, including high mechanical strength, minimal swelling in water, the ability to incorporate proteins in solutions of neutral pH, and excellent in vivo tissue compatibility.[25]

6.5 Conclusions

The ability of chitosan-alginate to promote proliferation of chondrocyte cells and production of collagen Type II as shown in this study raises the possibility of using chitosan-alginate as an improvement over the chitosan alone for cartilage repair and regeneration. As a scaffolding material, chitosan-alginate exhibits combined superior biological and mechanical properties over its chitosan

counterpart, and shows great potential to accelerate tissue growth and retain the phenotype of chondrocytes. Although the chitosan-alginate developed in this study targets tissue engineering for cartilage, its use can surely be expanded to other tissue engineering applications in view of its superior mechanical, microstructural and biological properties.

Notes to Chapter Six

1. Kim, B. S. & Mooney, D. J. Development of biocompatible synthetic extracellular matrices for tissue engineering. Trends Biotechnol 16, 224-30 (1998).

2. Minuth, W. W., Sittinger, M. & Kloth, S. Tissue engineering: generation of differentiated artificial tissues for biomedical applications. Cell Tissue Res 291, 1-11 (1998).

3. Niklason, L. E. & Langer, R. S. Advances in tissue engineering of blood vessels and other tissues. Transpl Immunol 5, 303-6 (1997).

4. Suh, J. K. & Matthew, H. W. Application of chitosan-based polysaccharide biomaterials in cartilage tissue engineering: a review. Biomaterials 21, 2589-98 (2000).

5. Kosher, R. A. & Church, R. L. Stimulation of in vitro somite chondrogenesis by procollagen and collagen. Nature 258, 327-30 (1975).

6. Kosher, R. A., Lash, J. W. & Minor, R. R. Environmental enhancement of in vitro chondrogenesis. IV. Stimulation of somite chondrogenesis by exogenous chondromucoprotein. Dev Biol 35, 210-20 (1973).

7. Lash, J. W., Rosene, K., Minor, R. R., Daniel, J. C. & Kosher, R. A. Environmental enhancement of in vitro chondrogenesis. 3. The influence of external potassium ions and chondrogenic differentiation. Dev Biol 35, 370-5 (1973).

8. Hunziker, E. B. Articular cartilage repair: basic science and clinical progress. A review of the current status and prospects. Osteoarthritis Cartilage 10, 432-63 (2002).

9. Glowacki, J. Engineered cartilage, bone, joints, and menisci. Potential for temporomandibular joint reconstruction. Cells Tissues Organs 169, 302-8 (2001).

10. van Susante, J. L. C. et al. Linkage of chondroitin-sulfate to type I collagen scaffolds stimulates the bioactivity of seeded chondrocytes in vitro. Biomaterials 22, 2359-69 (2001).

11. Nehrer, S. et al. Canine chondrocytes seeded in type I and type II collagen implants investigated in vitro. J Biomed Mater Res 38, 95-104 (1997).

12. Ushida, T., Furukawa, K., Toita, K. & Tateishi, T. Three-dimensional seeding of chondrocytes encapsulated in collagen gel into PLLA scaffolds. Cell Transplant 11, 489-94 (2002).

13. Perka, C., Arnold, U., Spitzer, R. S. & Lindenhayn, K. The use of fibrin beads for tissue engineering and subsequential transplantation. Tissue Eng 7, 359-61 (2001).

14. Aigner, J. et al. Cartilage tissue engineering with novel nonwoven structured biomaterial based on hyaluronic acid benzyl ester. J Biomed Mater Res 42, 172-81 (1998).

15. Freed, L. E. et al. Neocartilage formation in vitro and in vivo using cells cultured on synthetic biodegradable polymers. J Biomed Mater Res 27, 11-23 (1993).

16. Sittinger, M. et al. Resorbable polyesters in cartilage engineering: affinity and biocompatibility of polymer fiber structures to chondrocytes. J Biomed Mater Res 33, 57-63 (1996).

17. Kisiday, J. et al. Self-assembling peptide hydrogel fosters chondrocyte extracellular matrix production and cell division: implications for cartilage tissue repair. Proc Natl Acad Sci U S A 99, 9996-10001 (2002).

18. Mallein-Gerin, F., Garrone, R. & van der Rest, M. Proteoglycan and collagen synthesis are correlated with actin organization in dedifferentiating chondrocytes. Eur J Cell Biol 56, 364-73 (1991).

19. Sechriest, V. F. et al. GAG-augmented polysaccharide hydrogel: a novel biocompatible and biodegradable material to support chondrogenesis. J Biomed Mater Res 49, 534-41 (2000).

20. Schulze, M., Kuettner, K. E. & Cole, A. A. [Adult human chondrocytes in

alginate culture. Preservation of the phenotype for further use in transplantation models]. Orthopade 29, 100-6 (2000).

21. Lahiji, A., Sohrabi, A., Hungerford, D. S. & Frondoza, C. G. Chitosan supports the expression of extracellular matrix proteins in human osteoblasts and chondrocytes. J Biomed Mater Res 51, 586-95 (2000).

22. Miralles, G. et al. Sodium alginate sponges with or without sodium hyaluronate: in vitro engineering of cartilage. J Biomed Mater Res 57, 268-78 (2001).

23. Hauselmann, H. J. et al. Synthesis and turnover of proteoglycans by human and bovine adult articular chondrocytes cultured in alginate beads. Matrix 12, 116-29 (1992).

24. Wee, S. & Gombotz, W. R. Protein release from alginate matrices. Adv Drug Deliv Rev 31, 267-285 (1998).

25. Li, Z., Ramay, H. R., Hauch, K. D., Xiao, D. & Zhang, M. Chitosan-alginate hybrid scaffolds for bone tissue engineering. Biomaterials 26, 3919-28 (2005).

26. Yang, S., Leong, K. F., Du, Z. & Chua, C. K. The design of scaffolds for use in tissue engineering. Part I. Traditional factors. Tissue Eng 7, 679-89 (2001).

27. Prasitsilp, M., Jenwithisuk, R., Kongsuwan, K., Damrongchai, N. & Watts, P. Cellular responses to chitosan in vitro: the importance of deacetylation. J Mater Sci Mater Med 11, 773-8 (2000).

28. Kim, S. E. et al. Porous chitosan scaffold containing microspheres loaded with transforming growth factor-beta1: implications for cartilage tissue engineering. J Control Release 91, 365-74 (2003).

29. Gugala, Z. & Gogolewski, S. In vitro growth and activity of primary chondrocytes on a resorbable polylactide three-dimensional scaffold. J Biomed Mater Res 49, 183-91 (2000).

30. Nehrer, S. et al. Matrix collagen type and pore size influence behaviour of seeded canine chondrocytes. Biomaterials 18, 769-76 (1997).

31. Benya, P. D. Modulation and reexpression of the chondrocyte phenotype; mediation by cell shape and microfilament modification. Pathol Immunopathol Res 7, 51-4 (1988).

32. Mayne, R., Vail, M. S., Mayne, P. M. & Miller, E. J. Changes in type of collagen synthesized as clones of chick chondrocytes grow and eventually lose division capacity. Proc Natl Acad Sci U S A 73, 1674-8 (1976).

33. Lee, D. A., Reisler, T. & Bader, D. L. Expansion of chondrocytes for tissue engineering in alginate beads enhances chondrocytic phenotype compared to conventional monolayer techniques. Acta Orthop Scand 74, 6-15 (2003).

34. Caterson, E. J. et al. Polymer/alginate amalgam for cartilage-tissue engineering. Ann N Y Acad Sci 961, 134-8 (2002).

35. Marijnissen, W. J. et al. Alginate as a chondrocyte-delivery substance in combination with a non-woven scaffold for cartilage tissue engineering. Biomaterials 23, 1511-7 (2002).

36. Caterson, E. J. et al. Three-dimensional cartilage formation by bone marrow-derived cells seeded in polylactide/alginate amalgam. J Biomed Mater Res 57, 394-403 (2001).

37. Lee, C. R., Grodzinsky, A. J., Hsu, H. P. & Spector, M. Effects of a cultured autologous chondrocyte-seeded type II collagen scaffold on the healing of a chondral defect in a canine model. J Orthop Res 21, 272-81 (2003).

38. Li, W. J., Danielson, K. G., Alexander, P. G. & Tuan, R. S. Biological response of chondrocytes cultured in three-dimensional nanofibrous poly(epsilon-caprolactone) scaffolds. J Biomed Mater Res 67A, 1105-14 (2003).

39. Benya, P. D. & Shaffer, J. D. Dedifferentiated chondrocytes reexpress the differentiated collagen phenotype when cultured in agarose gels. Cell 30, 215-24 (1982).

40. von der Mark, K., Gauss, V., von der Mark, H. & Muller, P. Relationship between cell shape and type of collagen synthesised as chondrocytes lose their cartilage phenotype in culture. Nature 267, 531-2 (1977).

41. Homicz, M. R. et al. Human septal chondrocyte redifferentiation in alginate, polyglycolic acid scaffold, and monolayer culture. Laryngoscope 113, 25-32 (2003).

42. Nettles, D. L., Elder, S. H. & Gilbert, J. A. Potential Use of Chitosan as a Cell Scaffold Material for Cartilage Tissue Engineering. Tissue Eng 8, 1009-1016 (2002).

43. De Haart, M., Marijnissen, W. J., van Osch, G. J. & Verhaar, J. A. Optimization of chondrocyte expansion in culture. Effect of TGF beta-2, bFGF and L-ascorbic acid on bovine articular chondrocytes. Acta Orthop Scand 70, 55-61 (1999).

Chapter Seven

Hybrid chitosan-alginate scaffolds for bone tissue engineering

7.1 Introduction

A biodegradable scaffold in bone tissue engineering serves as a temporary skeleton inserted into the sites of defective or lost bone to support and stimulate bone tissue regeneration while it gradually degrades and is replaced by new bone tissue.[5-7]Both bioactive ceramics and polymers have been developed and analyzed for use as tissue engineering scaffolds. Bioactive ceramics have a chemical composition resembling that of natural bone, allow osteogenesis to occur, and can provide a bony contact or bonds with host bone. [8, 9]In spite of their favorable biological properties, bioceramics are inherently brittle and have low biodegradation rates, which severely limit their clinical usage. Biopolymers, on the other hand, have some distinct advantages over ceramic materials. Their biodegradation rates and mechanical properties can be tailored to a certain extent for specific applications. They are particularly amenable to implantation and can be easily manufactured into desired shapes.[10,11] The major concern associated with most natural polymer scaffolds is low mechanical strength and shape retention failure.

The development of biodegradable porous scaffolds made from naturally derived chitosan and alginate continues to progress. The new chitosan-alginate scaffold has significantly increased mechanical strength as compared with its chitosan counterpart and is structurally stable due to the strong ionic bonding

between the amine groups of chitosan and the carboxyl groups of alginate. It can promote both osteoblast and chondrocytes cell proliferation and helps the osteoblast to mineralize both *in vitro* and *in vivo*, while maintaining the function of osteoblast. A powerful advantage is that it can be prepared from solutions of physiological pH, providing safe conditions for incorporation of proteins. Just as importantly, it can also promote rapid vascularization and deposition of collagens.

7.2 Materials and Methods

7.21 Cell culture and imaging

Scaffolds were sectioned into circular discs of 13 mm diameter and 3 mm thickness. The scaffold discs were sterilized with ethylene oxide gas and placed in a 12-well cell culture plate. Approximately 5×10^5 osteoblast-like MG63 cells (American Type Culture Collection, ATCC) in 1 ml Dulbecco's Modified Eagle Medium (D-MEM)(Invitrogen life technologies) were seeded on the scaffold discs. The medium contained 10% fetal bovine serum (FBS), 50 IU. ml^{-1} penicillin and 50 $\mu g.ml^{-1}$ streptomycin. The samples were then placed in an incubator for 30 minutes and transferred to another cell culture plate. The medium was changed after 24 hours for the first time and every three days thereafter.

The morphology of the cells cultured on scaffolds was examined by scanning electron microscopy (SEM, JEOL, JSM-840A and 7000). For SEM observation, scaffolds were fixed with "Karnovsky's Fixative" overnight at room temperature and dehydrated in 50%, 75%, 95%, and 100% ethanol respectively for two hours.

The samples were then dried by critical point drying, coated with Au/Pd, and examined with SEM.

7.22 Histology

Scaffolds seeded with osteoblasts were washed twice with PBS and fixed with 4% paraformaldehyde for histological assay. The scaffolds were embedded in paraffin and cut into 5 μm thick sections using a microtome. The sections were stained with Masson's trichrome, mounted on glass slides, and examined with a Nikon 200 microscope.

7.23 Von Kossa stain

Samples were first stained in 5% $AgNO_3$ solution under light for 60 minutes, and developed in 1% Kodak film developer D-76 for two minutes, followed by fixation in 5% hypo solution (sodium thiosulfate) for 5 minutes and counterstaining with Nuclear Fast Red for 5 minutes.

7.24 Cell proliferation and viability

Cell proliferation was assessed using the colorimetric indicator Alamar Blue (Alamar BioSciences, Sacramento, CA). Alamar Blue changes color upon reduction by the membrane potential across a cell. Scaffolds cultured with an Alamar Blue indicator and cell medium were subject to absorbance measurement. A calibration curve was generated to quantify the number of cells present using this technique. Because Alamar Blue does not alter the viability of cells, it permits continuous monitoring of cells in culture. 1 ml 10% (V/V) Alamar

Blue indicator in cell culture media was introduced to 12-well tissue culture plates containing scaffolds and cells. The plates were incubated for several hours at 37 °C until the medium color visibly changed to pink. Three 300 μl of the Alamar Blue media was placed into a 96-well cell culture plate. Absorbance of the solution was measured with a Diode Array Spectrophotometer at wavelengths of 570 nm and 600 nm.

7.25 In vivo study

Skeletally mature, female adult Sprague–Dawley rats (approximately 2 months old, weighing 200 g each) were anesthetized with phenol barbiturate. A scaffold measuring 4 mm × 4 mm × 4 mm loaded with bone marrow was implanted into the lateral side of the thigh. All rats were monitored for signs of infection. All surgical incisions healed without evidence of infection or other complications. Rats were euthanized with overdose of anesthetic to harvest the implanted scaffold in groups of three at 1, 2, 4, 8, and 12 weeks after surgery. The histological assessment was the same as *in vitro* with the exception that the harvested samples were immersed in 10% formaldehyde.

7.3 Results

7.31 Osteoblast integration and function

Cell attachment to a material, proliferation, and differentiation over time are indications of cellular compatibility and determine the suitability of the material for tissue engineering applications. To study cell adhesion, proliferation and osteoconductivity, chitosan and chitosan-alginate scaffolds of discs 13 mm in

diameter and 3 mm in thickness were seeded with MG63 osteoblast cells and cultured in standard culture medium without osteogenic reagents. Osteoblast-like MG63 cell lines isolated from a human osteosarcoma were selected because they express a number of characteristic features of osteoblasts.[12]

Osteoblast proliferation on both chitosan and chitosan-alginate scaffolds was assessed using the Alamar Blue assay. The numbers of cells on pure chitosan and chitosan-alginate scaffolds were measured to be $3.54 \pm 0.012 \times 10^5$ and $3.91 \pm 0.017 \times 10^5$ respectively at day 3 and $4.53 \pm 0.011 \times 10^5$ and $5.02 \pm 0.039 \times 10^5$ respectively at day 7(Figure 7-1).

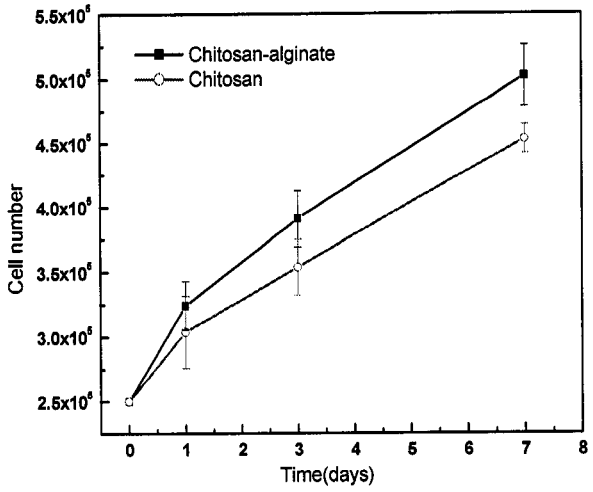

Figure 7- 1. Cell proliferation on chitosan-alginate and chitosan scaffolds.

Figure 2 shows SEM micrographs of osteoblasts on the chitosan scaffold after three (Figure 7-2A) and seven (Figure 7-4B) days of culture. At day three,

osteoblast cells on the chitosan scaffold showed an elongated shape and were anchored to the surface by discrete filopodia. The SEM micrographs in Figures 2C and 2D detail the morphology of individual osteoblast cells on the chitosan-alginate scaffold after 3 and 7 days of cell culture, respectively. Osteoblast cell clusters on chitosan-alginate scaffolds after 3 and 7 days of culture are shown in Figure 7-2E and Figure 7-4F, respectively. More cells were seen on the chitosan-alginate scaffold than on the chitosan scaffold throughout the period of study. A number of microvilli appeared on the dorsal surfaces of cells. The majority of cells on the both scaffolds gathered together and formed clusters, while the others randomly attached on the material surface. The surface of the cells on the chitosan appeared to be smoother than those on the chitosan-alginate scaffold. New cells appeared on the outer layers of the cell clusters. Most notably, cell morphology on the chitosan-alginate scaffold differed distinctly from the chitosan scaffold in that a layer of small particles covered the cells grown on the chitosan-alginate scaffold. These particles are bone minerals as identified by energy dispersive spectroscopy (EDS). Formation of calcium phosphate salts, or mineral deposition, is a primary function of osteoblast cells.[13]The chemical compositions of cell surfaces and extracellular matrices (ECM) were characterized by EDS (Figure 7-2). The EDS spectra in Figure 7-2 were taken from the cell surfaces as well as the scaffold matrices (marked with white square frames) shown on the

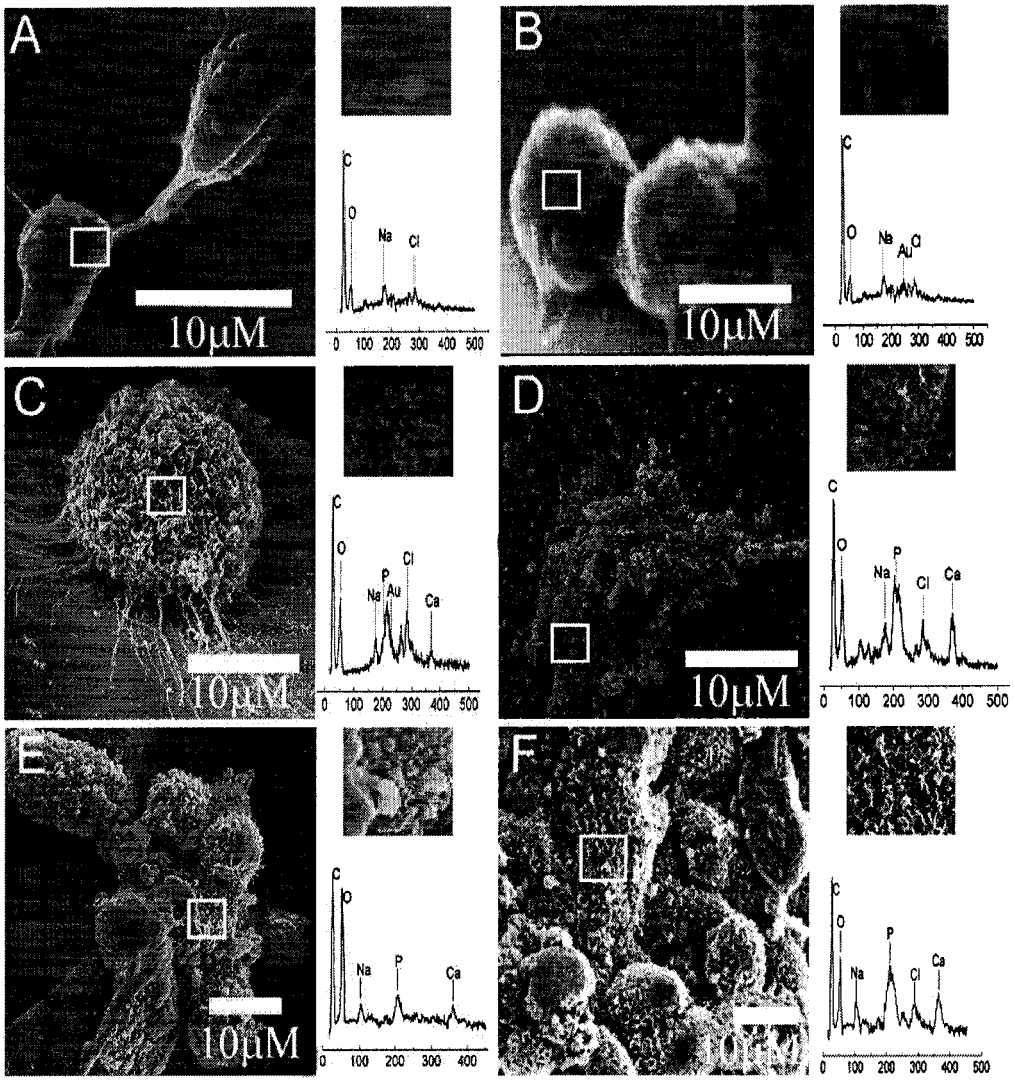

Figure 7- 2. SEM photographs of osteoblasts cultured on chitosan and chitosan-alginate scaffolds and EDS Osteoblast cells on chitosan after(A) 3 and (B) 7 days of culture; individual osteoblast cells on chitosan-alginate after (C) 3 and (D) 7 days of cell culture; Clusters of cells on chitosan-alginate after (E) 3 and (F) 7 days of cell culture. EDS spectra show the chemical compositions of cell surfaces and extracellular matrices. The spectra were taken from the areas marked with white square frames on the SEM micrographs.

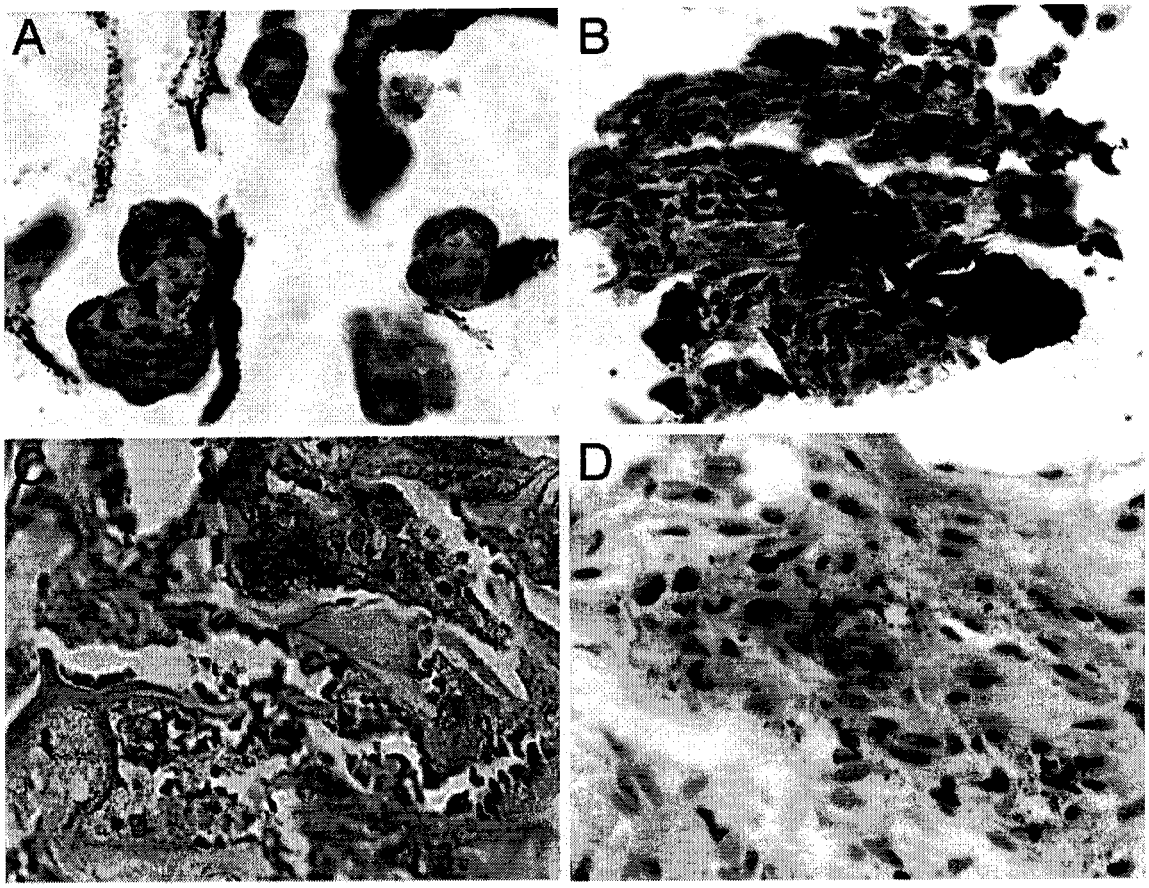

Figure 7- 3. Optical images of Von Kossa histological stain assay on chitosan-alginate scaffolds after (A) 10 days and (B) 28 days of culture in vitro; and (C) 4 weeks and (D) 8 weeks after implantation in vivo. (Original 20 × optical magnification)

accompanying SEM images. The EDS cell surface spectra of osteoblasts on the chitosan scaffold showed no sign of phosphate or calcium after 7 days of culture. In contrast, it showed both calcium and phosphate signals from the cells on the chitosan-alginate scaffold as well as the extracellular matrix, and their amounts increased from day 3 to day 7. These results suggest that both the individual

cells and cell clusters on the chitosan-alginate scaffold contributed to the production of calcium and phosphate.

Mineral deposition in large areas was confirmed by Von Kossa[14] assay on chitosan-alginate scaffolds after culture both *in vitro* (Figures 7-3A and 7-3B) and harvested *in vivo* at 4 and 8 weeks after implantation (Figures 7-3C and 7-3D respectively). Black, red, and pink correspond to calcified areas, nuclei, and cytoplasm, respectively. During *in vitro* studies, calcium appeared scattered around the cell clusters on the scaffold at day 10, and more calcium was seen on day 28 and some of it gathered to form chunks. The mineralization increased with cell culture time, in agreement with the results from the EDS analysis shown above. During *in vivo studies,* calcium was seen on the scaffold at week 4. The presence of calcium phosphate indicates the survival of osteoblasts and osteocytes within the scaffold matrix. The scaffold harvested at week 8 shows more calcium phosphate of different sizes. The presence and increase over time of calcium and phosphate indicates that the chitosan-alginate scaffold promoted bone cell growth and mineral deposition[15].

7.32 In vivo biocompatibility

Tissue compatibility of chitosan-alginate scaffolds infused with bone marrow was assessed *in vivo* by implanting them into muscles of rats and harvesting after 1, 2, 4, 8, and 12 weeks of implantation. The scaffolds were stained with H&E and Masson's trichrome (Figure. 4). Figures. 4A and 4B show the tissue response

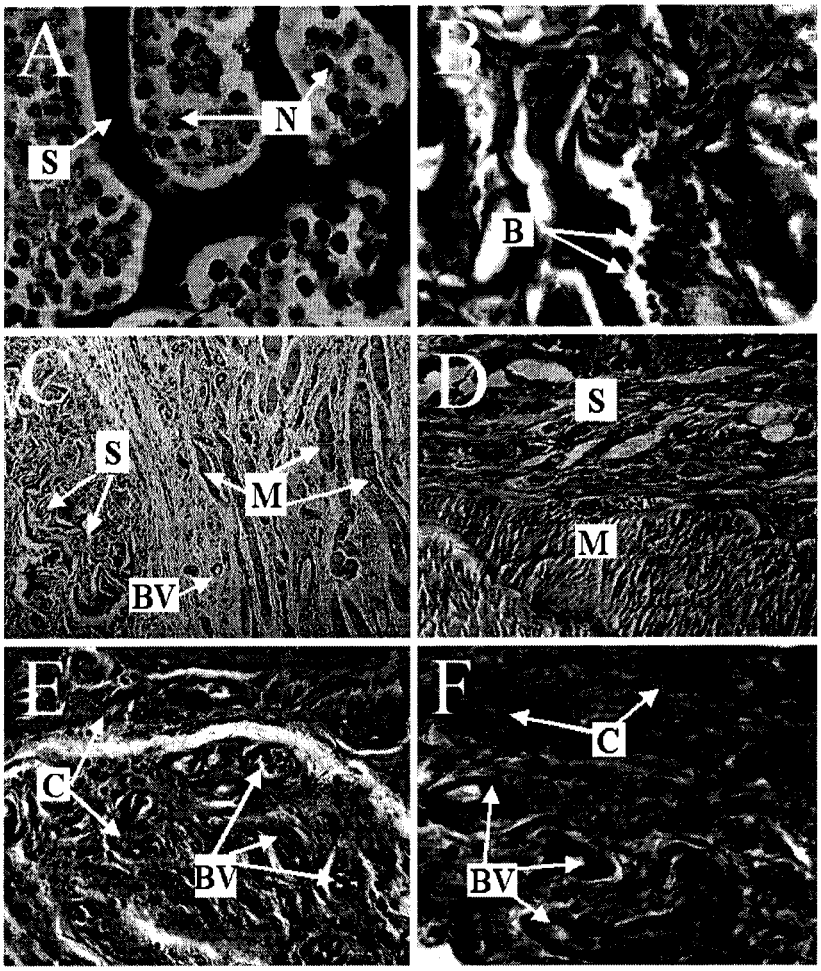

Figure 7- 4 Optical micrographs of scaffolds harvested at different times after implantation. Scaffolds stained with H&E at (A) week 1 and (B) week 2 at showing foreign body reactions. (C) and (D) scaffolds were stained with H&E at week 12 showing no evidence of fiberotic layers and good integration of scaffolds with tissue. (E) Scaffolds stained with Masson's Trichome at week 4 showing the formation of a large number of blood vessels (BV) in red and the initial appearance of collagen in blue surrounding the blood vessels. (F) scaffolds at week 12 showing that the blood vessels increased in size and collagen penetrated the entire scaffold (C,D optical magnification 10X and A, B, E, F optical magnification 20X).

to the scaffold implantation at week 1 and 2, respectively, after implantation. It is seen that marked neutrophiles migrated from blood into the scaffolds, but subsided quickly over time from week 1 to week 2, suggesting that the occurrence of an initial inflammation was caused by the tissue injury upon scaffold implantation rather than the material[16]. The formation of blood sinus

(marked with letter B) was clearly seen at week 4. The images taken at week 12 (Figures 7-4C and 7-4D) show no visible evidence of fibrosis between the muscles (M) and scaffold (S), which is not the case observed for most synthetic polymers where fibrotic layers are usually formed due to the adverse foreign body reaction caused by acidic degradation products [17].

Masson's trichrome was used to stain the harvested scaffolds to visualize the formation of collagen and vascularization. Collagen (marked with letter C) in blue appeared 4 weeks after implantation (Figure7-4E) and increased quickly over time; at week 12 (Figure7-4F), collagen was deposited throughout the entire scaffold indicating that the cells had fully penetrated the scaffold. A vascularized environment is necessary for the construction of a large volume of tissue. At week 4, a large number of small blood vessels were seen in the scaffold, and the size of the blood vessels increased over time from week 4 to week 12 (Figure7-4F). The highly angiogenic response of the host to the implanted construct ensured sufficient nutrients in the scaffold and allowed all types of cells to survive and proliferate after extended periods. At week 12, the scaffolds had been completely degraded and new tissue was well integrated with adjacent muscles cells.

7.4 Discussion

Studies have shown that natural polymers have better biological properties than synthetic polymers[10, 18]. Among natural polymers that have been researched up to date, chitosan has been identified to be one of the most promising

candidates as a tissue engineering scaffolding material due to its excellent biological properties[16, 18, 19]. The major concern with chitosan (and other natural polymers) for clinical use is its weak mechanical strength. Although we expected that the chitosan-alginate scaffold would have biological property equivalent to chitosan, our experiments showed that the chitosan-alginate scaffold is surprisingly superior to its chitosan counterpart in terms of tissue compatibility, formation of mineral matrices and vascularization. Previous studies found that chitosan elicited a neutrophil response 2 to 4 weeks after implantation[16,20,21]. Wooley et. al. have conducted a thorough *in vivo* study on chitosan implants.[16] They found that chitosan had a low level of cellular migration; fully cellular infiltration never occurred during the period of the study. Collagen was never deposited in the entire chitosan implant, and the vascularization was not noted until 8 to 12 weeks after implantation. In contrast, vascularization in the hybrid chitosan-alginate scaffolds occurred as early as 2 weeks after implantation and at week 4 a large number of well developed blood vessels were distributed throughout the scaffold. Collagen appeared at week 4 and was deposited throughout the entire scaffold at week 12. Calcium deposition occurred by week 4, increased with implantation time, and formed small patches by week 8. The scaffold was integrated with adjacent muscle cells well by week 12. These encouraging results support the potential applications of the chitosan-alginate scaffolds as a significantly improvement over other nature polymer-based

scaffolds and represent a notable advance in developing scaffolding materials for tissue engineering.

As far as degradation products are concerned, chitosan-alginate scaffolds are thought to be suitable for tissue engineering applications because both chitosan and alginate degradation products have been proven to be biocompatible and safe for *in vivo* applications by clinical practice where they served as scaffolds, drug carriers and cell encapsulaton. In addition to serving as tissue engineering scaffolds, the material can also be used in a broad range of biomedical applications, including serving as protein or peptide carriers for controlled and sustained release. In this bone tissue engineering study, we demonstrated that the hybrid chitosan-alginate scaffold can promote bone cell proliferation and mineralization both *in vitro* and *in vivo*; that it promotes rapid vascularization, and that it promotes deposition of connective tissue and calcified matrix within the entire scaffold architecture.

Notes to Chapter Seven

1. Niklason, L. E. & Langer, R. S. Advances in tissue engineering of blood vessels and other tissues. Transpl Immunol 5, 303-6 (1997).

2. Kim, B. S. & Mooney, D. J. Development of biocompatible synthetic extracellular matrices for tissue engineering. Trends Biotechnol 16, 224-30 (1998).

3. Minuth, W. W., Sittinger, M. & Kloth, S. Tissue engineering: generation of differentiated artificial tissues for biomedical applications. Cell Tissue Res 291, 1-11 (1998).

4. Suh, J. K. & Matthew, H. W. Application of chitosan-based polysaccharide biomaterials in cartilage tissue engineering: a review. Biomaterials 21, 2589-98 (2000).

5. Persidis, A. Tissue engineering. Nat Biotechnol 17, 508-10 (1999).

6. Service, R. F. Tissue Engineers Build New Bone. Science 289, 1498-1500 (2000).

7. Petite, H. et al. Tissue-engineered bone regeneration. Nat Biotechnol 18, 959-63 (2000).

8. Hench, L. L. & Wilson, J. Surface-active biomaterials. Science 226, 630-6 (1984).

9. Jarcho, M. Calcium phosphate ceramics as hard tissue prosthetics. Clin Orthop, 259-78 (1981).

10. Yang, S., Leong, K. F., Du, Z. & Chua, C. K. The design of scaffolds for use in tissue engineering. Part I. Traditional factors. Tissue Eng 7, 679-89 (2001).

11. Niklason, L. E. Engineering of bone grafts. Nat Biotechnol 18, 929-30 (2000).

12. Montanaro, L., Arciola, C. R., Campoccia, D. & Cervellati, M. In vitro effects on MG63 osteoblast-like cells following contact with two roughness-differing fluorohydroxyapatite-coated titanium alloys. Biomaterials 23, 3651-9 (2002)

13. Lu, H. H., El-Amin, S. F., Scott, K. D. & Laurencin, C. T. Three-dimensional, bioactive, biodegradable, polymer-bioactive glass composite scaffolds with improved mechanical properties support collagen synthesis and mineralization of human osteoblast-like cells in vitro. J Biomed Mater Res 64A, 465-74 (2003).

14. Sheehan D, H. B. Theory and practice of Histotechnology, 2nd Ed (Battelle Press, Ohio, 1980).

15. Boskey, A. L. Mineral-matrix interactions in bone and cartilage. Clin Orthop, 244-74 (1992).

16. VandeVord, P. J. et al. Evaluation of the biocompatibility of a chitosan scaffold in mice. J Biomed Mater Res 59, 585-90 (2002).

17. Lutolf, M. P. et al. Repair of bone defects using synthetic mimetics of collagenous extracellular matrices. Nat Biotechnol 21, 513-8 (2003).

18. Madihally, S. V. & Matthew, H. W. Porous chitosan scaffolds for tissue engineering. Biomaterials 20, 1133-42 (1999).

19. Lahiji, A., Sohrabi, A., Hungerford, D. S. & Frondoza, C. G. Chitosan supports the expression of extracellular matrix proteins in human osteoblasts and chondrocytes. J Biomed Mater Res 51, 586-95 (2000).

20. Hutmacher, D. W., Teoh, S. H., Zein, I., Ranawake, M. & Lau, S. Tissue engineering research: the engineer's role. Med Device Technol 11, 33-9 (2000).

21. Peluso, G. et al. Chitosan-mediated stimulation of macrophage function. Biomaterials 15, 1215-20 (1994).

22. Li, Z., Ramay, H. R., Hauch, K. D., Xiao, D. & Zhang, M. Chitosan-alginate hybrid scaffolds for bone tissue engineering. Biomaterials 26, 3919-28 (2005).

Chapter Eight

Improving Cell Seeding Capacity of Porous Scaffolds by On-site Gelation of Calcium Alginate

8.1 Introduction

Engineered cartilage tissue systems incorporating synthetic or natural biodegradable polymer scaffolds, growth factors, and seeded-chondrocytes comprise an ever improving class of materials for diseased and missing cartilage replacement that complements reconstructive and orthopedic surgery[1,2] Within this field, a common remedial approach is to harvest cells from a small tissue biopsy, expand them *in vitro*, and seed the population into scaffolds, producing an enhanced semi-artificial structure via the deposition of extracellular matrix (ECM) by integrated cells. In this process, seeded cells have been closely associated with enhancement of tissue formation in 3-dimensional constructs[3], including those for cartilage[4], bone[5], and cardiac tissue repair and regeneration.[6]

In producing high quality cell-assisted implantable materials, Almarza *et al* [7] has reported that cell seeding density significantly effects cartilage and bone formation. Specifically, it was concluded that the morphology, collagen and glycosaminoglycan content, and permeability of the engineered-cartilage were

closely related to cell seeding density. Production of uniform, dense cell layers is limited, though, by the complexity of the scaffold assembly, insufficient migratory abilities of cells into the structure, and cell movement to the periphery and out of the implantable materials.[6,8,9] Consequently, prolonged *in vitro* cell culture has been required to meet effective cell density and distribution profiles prior to implantation.[6-8,10] Unfortunately, this can induce de-differentiation of seeded cells, and can limit the utility of the procedure for patients requiring tissue therapy under expedited terms.

To circumvent elongated cell culture requirements, a number of methods for enhanced cell seeding in the scaffolds have been investigated.[6,8] A cell seeding device, utilizing the synergistic effects of the vacuum, centrifugal force and fluid flow, has been used with porous tubular scaffolds in work produced by Soletti *et al.*[11] Magnetic nanoparticles have been used to guide fibroblast cells evenly through commercially available scaffolds. Here, magnetite nanoparticles were directed with a magnetic field to induce "mag-seeding", subsequently increasing cell density and seeding efficiency.[3] Additionally, Zhao[12] and McFetridge[13] reported the use of a bioreactor for enhanced cell seeding. While all of these systems have been demonstrated as effective facilitators of even cell dispersion, most of them require large equipment, semi-invasive additives, or disruptive processes that can effect cellular characteristics and materials activity *in vivo*. To this end, a simplified lab bench-top method of cell seeding was

pursued to temporarily engage a well-distributed cell mixture with the scaffold body using a porous gel, prior to its structural decay.

Alginate is a family of polyanionic copolymers derived from brown sea algae with 1,4-linked a-D-mannuronic (M) and b-L-guluronic (G) residues in varying proportions. The copolymer is soluble in aqueous solutions and forms stable gels at room temperature in the presence of certain divalent cations (i.e. Ba^{2+}, Ca^{2+}). As these gels can be prompted to form on-site, they can secure cells inside scaffold pores, limiting their migration outwards, thereby promoting high cell seeding densities. Additionally, the gel has been shown to promote chondrocytes proliferation while conserving cellular functionality and phenotype.[14] It is important to note that these porous gels are able to facilitate nutrient and waste passage through the scaffolds upon implantation, but are prone to degradation *in vivo*, freeing encapsulated cells after they have been allowed to locally secure themselves to the scaffold.

A chitosan-alginate hybrid scaffold was used in combination with this gel assisted seeding technique. The chitosan-alginate hybrid scaffold is that which we have previously reported on regarding its efficacy for bone and cartilage tissue engineering.[14,15] These scaffolds possess over 90% porosity and interconnected pores with very good mechanical strength, favorable for cell seeding and growth. While these scaffolds foster cell attachment and development, their pore sizes permit cellular escape and uneven cell distribution,

which provides an excellent structure for on-site gel formation and could be evaluated as a cell-seeding stabilizer.

8.2 Materials and Methods

8.21 Preparation of chitosan–alginate scaffolds

Chitosan–alginate scaffolds were prepared following a method reported previously with some modifications.[3,12] Chitosan pellets (7.2gram) and sodium alginate powder (7.2 gram) were added to 300ml deionized water and blended to a produce a homogenous solution. To expedite homogeneity, the temperature of the solution was increased to 80°C and 3 ml of glacial acetic acid was added to dissolve the chitosan. Upon complete dissolution, a small electric blender (Oster Inc., Rye, NY) was used to blend the mixture to produce a uniform sol. The pH was adjusted to 7–7.4 using sodium hydroxide. The solution was then poured into 24-well cell culture plates, frozen at -20°C for 24 h, and lyophilized. The scaffolds were trimmed to 10x13mm (thickness x diameter) cylinders and crosslinked by immersion in a 1% w/v $CaCl_2$ solution for 10 min, washed with deionized water, and lyophilized again.

8.22 Cell seeding accompanied by on-site gelation

The scaffolds were sterilized with ethylene oxide (EO) gas and pretreated in a 12-well cell culture plate containing Dulbecco's Modified Eagle Medium (DMEM) for several days before cell seeding. Chondrocytes (HTB-94; American Type Culture Collection, Manassas, VA) were used as received, and cultured

with regular culture medium (DMEM with 10% fetal bovine serum and 1% penicillin/streptomycin antibiotics). Scaffolds were divided into two groups (n=12 for each group): (1) cells seeded on chitosan-alginate scaffold with a conventional, freely-diffusive seeding technique (NGA group) (2) cells seeded on scaffolds with the on-site gel assisted technique (GA group).

For the NGA group, cells were pelletized and resuspended with cell culture medium to obtain a final density of ~1× 10^7 cells/ml. Each scaffold was directly seeded with 1ml cell solution. After seeding, the scaffolds were incubated for 30 minutes, allowing for cell attachment, before more media was added. The scaffolds were moved to new culture plates and maintained in a humid, 5% CO_2 incubator.

For the GA group, chondrocytes were pelletized and resuspended in 1% sodium alginate solution (pH=7.4, ~1× 10^7 cells/ml). The scaffolds were seeded with 1 mL of the sodium alginate/chondrocyte solution, followed by drop-wise addition of 0.2 mmol calcium chloride (3 ml), serving to initiate alginate gelation, subsequently entrapping the chondrocytes in the scaffolds. The scaffolds were then placed in DMEM media and incubated before further evaluation. After seeding, the residual cell solutions of both groups were collected and analyzed to indicate the number of cells that were not seeded on to the scaffolds. The initial efficiency of cell seeding was then calculated as the following:

$$\text{Efficiency } (\%) \quad = 1 - \frac{\text{cells in residual solution}}{\text{cells in seeding solution}} \times 100$$

8.23 Morphological evaluation and DNA quantification

The morphology of scaffold-bound cells was observed by scanning electron microscopy (SEM; JEOL JSM-7000). In preparation for SEM evaluation, scaffolds were collected after thee days of culture and fixed with Karnovsky's fixative overnight at room temperature. Samples were dehydrated in 50, 75, 95 or 100% ethanol for 2 hours. Scaffolds were then dried using a critical point drying apparatus and then coated with Au/Pd.

DNA content was used to quantify cell distribution through the scaffold assemblies. Scaffolds were collected after chondrocyte culturing periods of 1 hour, 1 day, 3 days, and 7 days, and immersed in 4% paraformaldehyde fixative for 24 hours. Each sample was then sectioned into five layers (Figure 8-6B). To isolate the cells from the scaffold structures, two drops of sodium citrate was added to each layer, dissolving the scaffolds, followed by addition of 1 ml of DNAzol to extract the DNA. The solution was centrifuged at 5,000 G for 5 minutes and the supernatant was removed. DNA was then precipitated out of solution with the addition of 0.5 ml of 100% ethanol added to the supernatant (1 ml). Samples were mixed well and stored at room temperature for 1-3 minutes to allow the DNA to fully precipitate. DNA was then collected by centrifugation at 10,000 G for 10 minutes at 4°C and washed with 0.8 - 1.0 ml of 75% ethanol. The precipitate was then dissolved in 8 mM NaOH and UV absorbance was measured at 260 and 280nm. The DNA content was calculated such that one A260 unit equaled 50 μg of double-stranded DNA/ml. To calculate the cell

number, a standard curve based on DNA extracted from cell pellets with varying cell numbers ($5X10^5$, $1X10^6$, $1.5X10^6$, $2X10^6$, $3X10^6$, $4X10^6$) was produced. The cell number of the different scaffold layers was then calculated by the extracted DNA content measurements.

8.24 RT-PCR for collagen type I and type II gene activity

RNA was extracted using the Qiagen mini RNeasy kit from scaffolds incubated with chondrocytes for 2 or 3 weeks. The RNA concentration was measured by UV spectrometry at A260 and reverse transcription (RT) was performed with One Step RT kit from Qiagen Inc. The exon specific primer pairs, 5"GACTTTTCTCCCCTCTCTTTCTAAG3" (for upstream primer) and 5"AGAGGTGTTTGACACAGAATAGCAC3" (for downstream primer) were synthesized by Integrated DNA Technology. These primers work at the C-terminal propeptide domain of human collagen type II gene, proa1(II) (with tm of 60°C and products size of 250bp). We also designed the human collagen type I primers, 5"GGCAGCCAGTTTGAATATAATGTAG3" as upstream primers, and 5"AGTAGATGTGCAGAAGAAATGGAAG3" as downstream primers, with tm of 60°C and products of 515bp in size. As an internal standard, the upstream primer 5"TTCTAGGCGGACTATGACTTAGTTG3 and the downstream primer 5"GACTTCCTGTAACAATGCATCTCAT3" of ß-actin (CTAB) cDNA with product weight 288bp were synthesized. Total RNA (2µg) was used for first strand cDNA synthesis. The cDNA was amplified for 35 cycles at 94°C (1 min), 60°C (1 min), and 72°C (2 min). Analysis of all the PCR products was performed by agarose

gel (1.00%) electrophoresis with ethidium bromide staining.

8.3 Results and Discussion

It has been asserted that high quality cell seeding requires high spatial uniformity of attached cells, high scaffold cellularity to enhance the tissue development rate, and sufficient nutrient and oxygen supplies to maintain cell viability upon sequestration in the scaffold. In this work, it was demonstrated that a large number of cells could be seeded into a porous scaffold, using a transient, porous calcium-alginate gel. The viscous nature of the gel inhibits mobility of the cell population, limiting outward migration of the porous matrix, as illustrated in Figure 8-1.

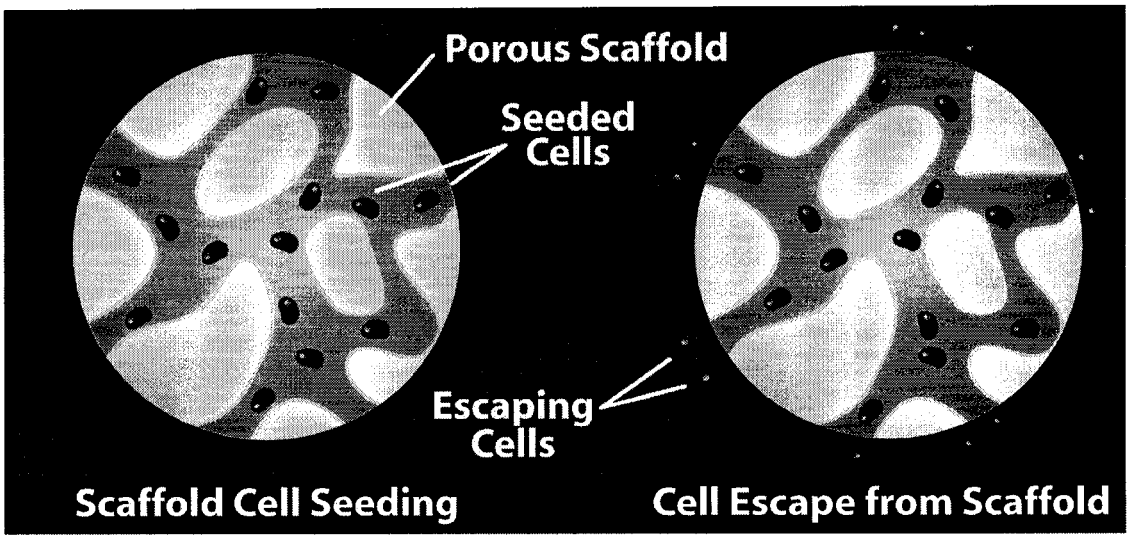

Figure 8 1 Illustration of cell seeding. After chondrocyte seeding of the chitosan-alginate scaffold, cells can escape the porous matrix unless their mobility is limited. The addition of a calcium-alginate gel can localize cells in the scaffold, and assist their attachment to the neighboring scaffold wall.

SEM micrographs revealed the differences in cell attachment behaviors between the gel assisted (GA) and conventional non-gel assisted (NGA) seeding methods throughout chitosan-alginate scaffolds (Figure 8-2). Higher cell density of the GA scaffolds was observed versus the intermittent cell attachment of the NGA scaffolds. Also, higher magnification SEM images show a thin gel coat covering the cells inhabiting the GA scaffolds. This was also believed to be the production of ECM in the local environment because of high activity levels of seeded cells by the alginate gel-chondrocytes combo reported high level of ECM production [16-18]. Images indicating live versus dead cells in Figure 3 reveal that in large, both the GA scaffolds and NGA scaffolds retained viable cells and very few cells were dead. However, the GA scaffolds demonstrate a more uniform cell distribution, covering larger expanses of the scaffold surface.

To illustrate the ability of the GA scaffold system in promoting increased cell density and minimizing cellular escape from the scaffold, the number of encased cells was determined using a DNA quantification assay (Figure 8-4). By this analysis, it was observed that through the restrictive properties of the aliginate gel, the GA scaffolds conserved ~95% of all seeded cells in the scaffold matrix from day 0 to day 1. The NGA scaffolds, though, demonstrated about 15% decrease in the cell population after day 1, indicating that the seeded cells were

escaping

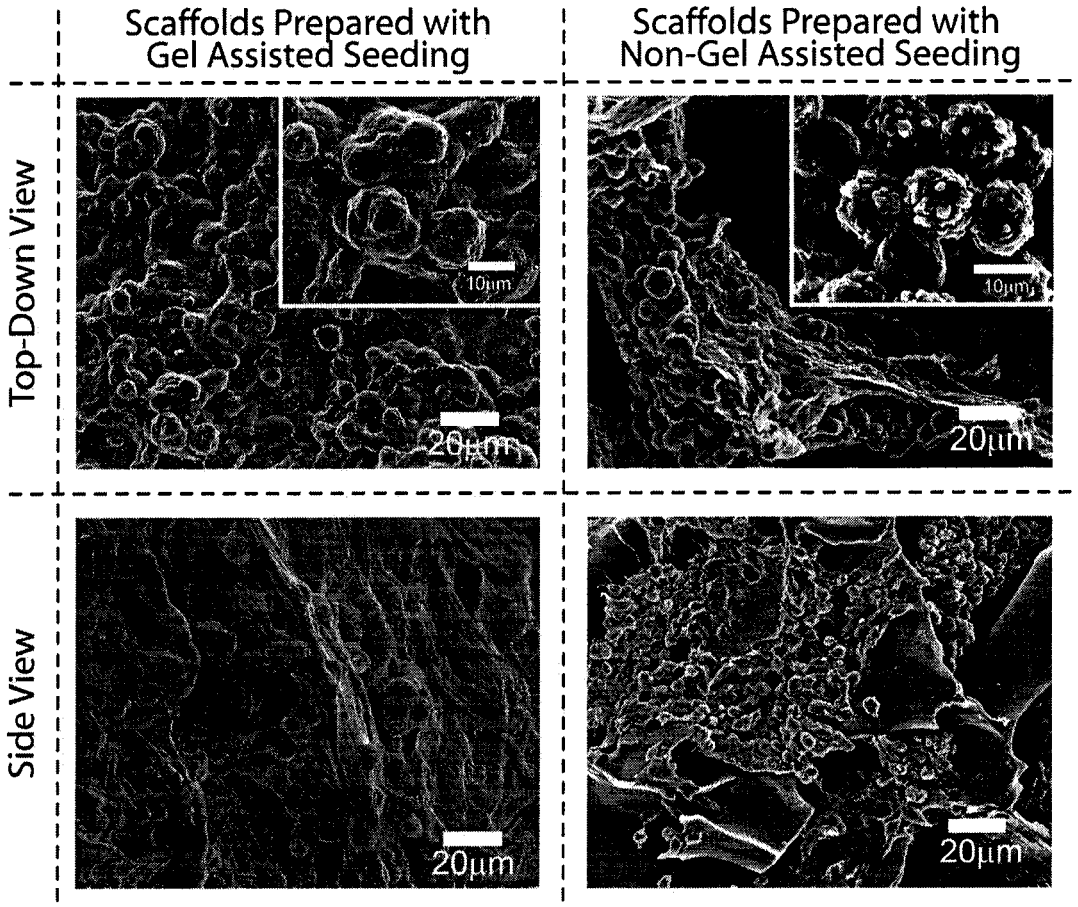

Figure 8-2 SEM micrographs of the top and side views of the chondrocyte-seeded scaffolds with and without calcium-alginate gel assistance.

and migrating outwards from the scaffold or otherwise leaking into the cell culture media. Accordingly, the total number of dividing cells in the NGA scaffolds was not as high as that of the GA scaffolds at 7 days post seeding due to a lower initial cell seeding number. At the end of the 7-day incubation period, the total cell population inhabiting the GA scaffold increased 80% versus an observed 33% increase for the NGA scaffold. In doing so, the GA method demonstrated a (1)

higher initial cell number, (2) faster growth rate, and (3) higher cell density and total cell number.

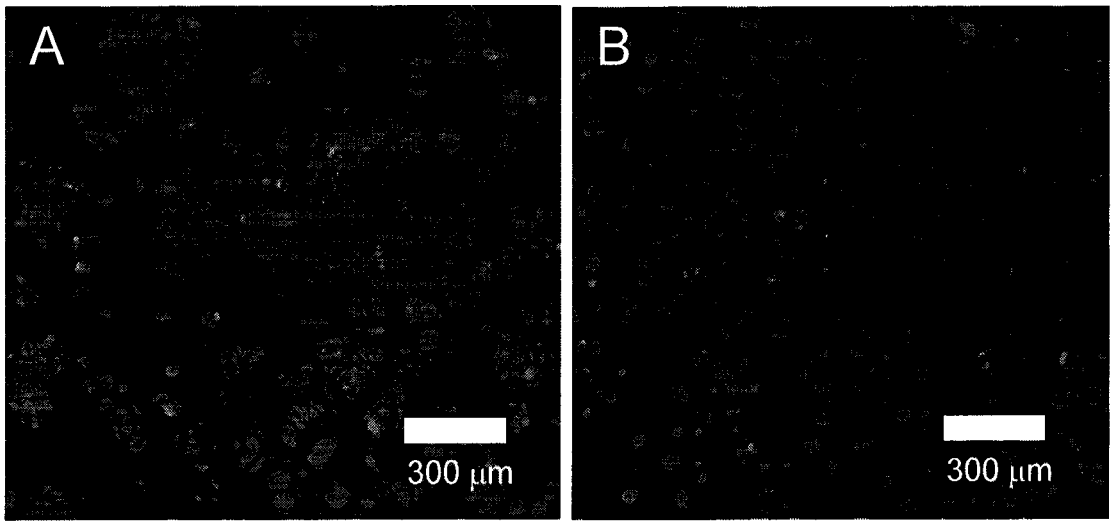

Figure 8-3 Live/dead fluorescence images of chitosan-alginate scaffolds after 7 days of cell culture. Cells on scaffolds were seeded by (A) gel assisted seeding and (B) conventional non-gel assisted seeding.

Cell distribution was evaluated after 7 days of incubation by DNA quantification of sequential scaffold layers, as illustrated in Figure 8-5. The larger cell population of the GA versus NGA scaffolds is corroborated by this data. The total cell number in GA scaffolds increased by 90% while the NGA scaffolds exhibited only 37% growth after 7 days of cell incubation. GA cell quantities for days 0 and 7 showed an even distribution of cells throughout the scaffold while there appeared to be an increase in cell number at the top and bottom layers on day 7. This indicates that the static cell culture environment may hinder nutrient and waste diffusion, and consequently cell growth as well. Conversely, the NGA

scaffolds did not exhibit an even cell distribution, with significantly higher cell numbers (24%) at the bottom of the scaffold versus upper layers at later time points (16%). This was believed to be due to the gravitational force on the cells, pulling the unsecured bodies through the large scaffold pores. At the same time, an increase in cell number through all scaffold slices was observed with time, indicating that chitosan-alginate hybrid scaffolds foster chondrocytic growth, in addition to exhibiting a preferable mechanical properties profile.

As the cells added to the scaffold by the NGA seeding method enter the scaffold by gravitational force, pore sizes of the scaffold influence cell seeding efficiency.[3] Specifically, scaffolds with pore sizes below 100μm inhibit the permeation of cells inward, limiting uniform seeding, while scaffolds with pores greater than 500μm allow cells to enter with ease, but suffer from large-scale cellular escape during *in vitro* culture. In this work, scaffold pore sizes were maintained between 100 and 300μm allowing uniform cellular infusion, but suffered from active cell movement, necessitating gel stabilization to sustain overall uniformity.

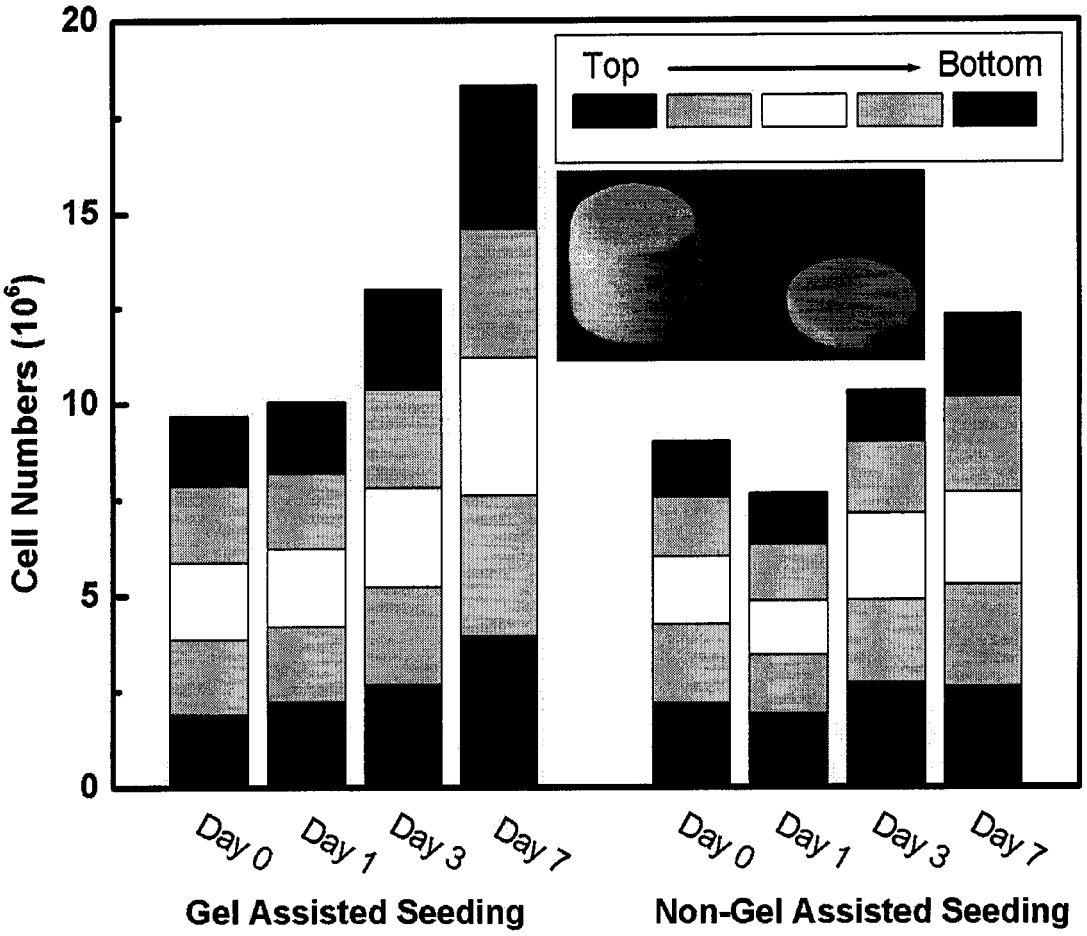

Figure 8 4 Porous chitosan-alginate scaffolds were infused with a gel-chondrocyte combination to limit cell mobility upon entry. The scaffold was then sectioned (top), dissolved, and DNA quantification was used to identify the number of cells in each sequential slice. This data was collected over seven days, demonstrating increased cell sequestration and overall density for scaffolds using the gel assisted seeding (bottom). Bottom inset shows uncompromised scaffold (left) and scaffold section (right).

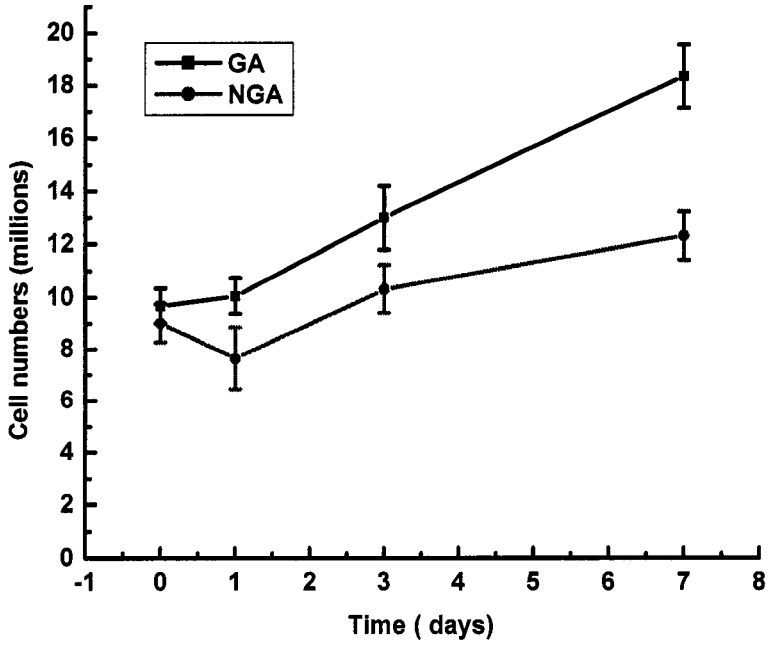

Figure 8-5 Total cell quantity inside the gel assisted (black squares) and non-gel assisted (red circles) chitosan-alginate scaffolds

To verify that the seeded cells were still expressive of chondrocytic cell function upon initiation into the scaffold/gel system, relative expression of collagen type I and II were examined by RT-PCR. Figure 8-6 illustrates this expression as well as that of the house-keeping gene, ß-actin (CTAB). Semi-quantitative analysis of the band areas and intensities were performed, and the ratio of collagen type I and II genes relative to CTAB expression was calculated. As shown in Figure 8-5, the collagen type I gene of the NGA scaffold-bound cells almost doubled between weeks two to three, while the collagen type II expression decreased during that time. The cells in the GA scaffolds, though, demonstrated only a slight increase in collage type I gene activity, accompanied

by an increase in collagen type II expression. This shift in gene activity could be associated with the phenotypic change of the cells as they moved to the scaffolds' outer surfaces, different than that of the round, chondrocytic morphology maintained through gel assisted attachment to the pore walls.

It has been observed that the calcium alginate gel is a porous matrix, with individual pores on the order of 5-200nm in diameter.[19,20] These pores allow for the diffusion of small molecules such as glucose and oxygen, while diffusion of the larger proteins from the gels have been shown to be dependent on their molecular weight.[21] The pores allow for nutrient-waste exchange during initial seeding of the cells, unlike other gels that limit small molecule diffusion. In addition, cells are caused to move at a slower pace through the viscous gel, allowing them to localize and bind to the scaffold wall prior to exposure of an escape path. In a sodium-rich environment, the calcium ions of the gel are supplanted and the alginate structure breaks down with time.[22,23] As such, the gel provides a temporary matrix supporting the encapsulated cells while they find neighboring scaffold surfaces with which to adhere, while simultaneously providing a semi-diffusive environment for nutrient and waste exchange. With time, the calcium-alginate gel breaks down or exits the scaffold, opening diffusive channels in which bound chondrocytes may expand and form ECM within the confines of the scaffold.

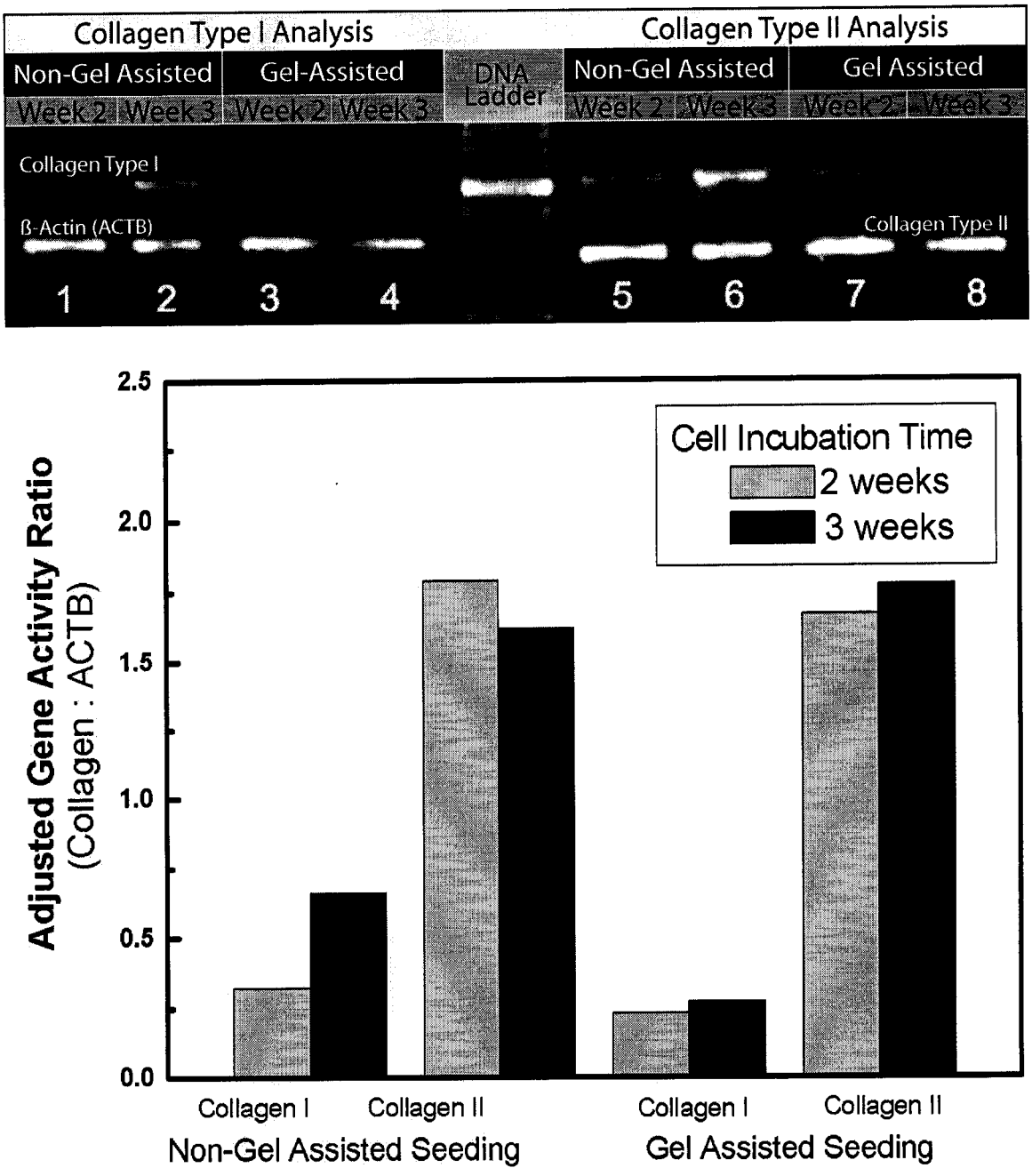

Figure 8-6 Agarose gel of cDNA of Callagen types I and II and the house keeping gene, β-actin (ACTB) expressed by chondrocytes encapsulated in a chitosan-alginate scaffold (top). Semi-quantitative analysis of the gene expression (bottom), showed that cells from scaffolds without gel-assisted seeding increased their collagen I expression indicating the possibility of de-differentiation. Cells immobilized by the calcium-agarose gel during seeding, showed no such increase and maintained collagen II expression after three weeks.

While artificial scaffolds bearing regions of highly-dense cellular clusters more closely mimic *in vivo* conditions for enhanced compatibility, they also induce the formation of larger quantities of ECM and assist chondrocytes in maintaining their functional status and morphology. Long *in vitro* incubation periods of chondrocytes with prepared scaffolds has led to the possibility of cellular de-differentitaion, contamination in vitro leading to infections *in vivo*.[24] These incubation times can be reduced with better, more efficient seeding practices. Calcium-alginate gels have been shown to stabilize seeded cells, promote proliferation of dense chordocyte clusters, and ultimately produce more robust ECM regions within implanted scaffolds, further enhancing the scaffold-body interface.

8.4 Conclusions

On-site calcium alginate gel formation has been shown to support uniform cell seeding on engineered tissue scaffolds, while also increasing overall cell density. Chondrocytes maintained in the gel demonstrated normal biological activity, as indicated by collagen type I and type II gene expression as well as SEM analysis. It has been noted that this form of transient stabilization can be applied to other scaffold systems, especially to those of other polymeric and ceramic porous scaffolds in combination with alternative cell lines to produce a new class of pre-seeded tissue systems.

Notes to Chapter Eight

1. Randolph, M.A., K. Anseth, and M.J. Yaremchuk, *Tissue engineering of cartilage.* Clin Plast Surg, 2003. **30**(4): p. 519-37.

2. Koch, R.J. and G.K. Gorti, *Tissue engineering with chondrocytes.* Facial Plast Surg, 2002. **18**(1): p. 59-68.

3. Shimizu, K., A. Ito, and H. Honda, *Enhanced cell-seeding into 3D porous scaffolds by use of magnetite nanoparticles.* J Biomed Mater Res B Appl Biomater, 2006. **77**(2): p. 265-72.

4. Freed, L.E., et al., *Tissue engineering of cartilage in space.* Proc Natl Acad Sci U S A, 1997. **94**(25): p. 13885-90.

5. Holy, C.E., M.S. Shoichet, and J.E. Davies, *Engineering three-dimensional bone tissue in vitro using biodegradable scaffolds: investigating initial cell-seeding density and culture period.* J Biomed Mater Res, 2000. **51**(3): p. 376-82.

6. Radisic, M., et al., *High-density seeding of myocyte cells for cardiac tissue engineering.* Biotechnol Bioeng, 2003. **82**(4): p. 403-14.

7. Almarza, A.J. and K.A. Athanasiou, *Effects of initial cell seeding density for the tissue engineering of the temporomandibular joint disc.* Ann Biomed Eng, 2005. **33**(7): p. 943-50.

8. Vunjak-Novakovic, G. and M. Radisic, *Cell seeding of polymer scaffolds.* Methods Mol Biol, 2004. **238**: p. 131-46.

9. Li, Y., et al., *Effects of filtration seeding on cell density, spatial distribution, and proliferation in nonwoven fibrous matrices.* Biotechnol Prog, 2001. **17**(5): p. 935-44.

10. Liu, X. and P.X. Ma, *Polymeric scaffolds for bone tissue engineering.* Ann Biomed Eng, 2004. **32**(3): p. 477-86.

11. Soletti, L., et al., *A seeding device for tissue engineered tubular structures.* Biomaterials, 2006. **27**(28): p. 4863-4870.

12. Zhao, F. and T. Ma, *Perfusion bioreactor system for human mesenchymal stem cell tissue engineering: dynamic cell seeding and construct development.* Biotechnol Bioeng, 2005. **91**(4): p. 482-93.

13. McFetridge, P.S., et al., *Endothelial and smooth muscle cell seeding onto processed ex vivo arterial scaffolds using 3D vascular bioreactors.* Asaio J, 2004. **50**(6): p. 591-600.

14. Li, Z. and M. Zhang, *Chitosan-alginate as scaffolding material for cartilage tissue engineering.* J Biomed Mater Res A, 2005. **75**(2): p. 485-93.

15. Li, Z., et al., *Chitosan-alginate hybrid scaffolds for bone tissue engineering.* Biomaterials, 2005. **26**(18): p. 3919-28.

16. Aydelotte, M.B., et al., *Culture of chondrocytes in alginate gel: variations in conditions of gelation influence the structure of the alginate gel, and the arrangement and morphology of proliferating chondrocytes.* In Vitro Cell Dev Biol Anim, 1998. **34**(2): p. 123-30.

17. Tamponnet, C., et al., *Rabbit articular chondrocytes in alginate gel: characterisation of immobilized preparations and potential applications.* Appl Microbiol Biotechnol, 1992. **37**(3): p. 311-5.

18. Grandolfo, M., et al., *Culture and differentiation of chondrocytes entrapped in alginate gels.* Calcif Tissue Int, 1993. **52**(1): p. 42-8.

19. Wee, S. and W.R. Gombotz, *Protein release from alginate matrices.* Adv Drug Deliv Rev, 1998. **31**(3): p. 267-285.

20. L. Klein, J.S.a.K.G.V., *Pore size and properties of spherical Ca-alginate biocatalysts.* Eur. J. Appl. Microbiol. Biotechnol., 1983. **18**(86-91).

21. Martinsen, A., et al., *Comparison of different methods for determination of molecular weight and molecular weight distribution of alginates.* Carbohydrate Polymers, 1991. **15**(2): p. 171.

22. Hauselmann, H.J., et al., *Synthesis and turnover of proteoglycans by human and bovine adult articular chondrocytes cultured in alginate beads.* Matrix, 1992. **12**(2): p. 116-29.

23. Wang, L., et al., *Evaluation of sodium alginate for bone marrow cell tissue engineering.* Biomaterials, 2003. **24**(20): p. 3475-81.

24. O'Brien, F.J., et al., *The effect of pore size on cell adhesion in collagen-GAG scaffolds.* Biomaterials, 2005. **26**(4): p. 433-41.

Bibliography

1. UNPD. World population ageing:1950-2050. 2002.

2. AAOS. Musculoskeletal Conditions in the U.S. (second edition). 1999

3. USBJD. US Bone and Joint decade. http://www.usbjd.org.

4. Bush GW. National Bone and Joint Decade proclamation. Office of the press secretary 2002.

5. Ilizarov GA, Ledyaev VI. The replacement of long tubular bone defects by lengthening distraction osteotomy of one of the fragments. 1969. Clin Orthop Relat Res 1992(280):7-10.

6. Cancedda R, Dozin B, Giannoni P, Quarto R. Tissue engineering and cell therapy of cartilage and bone. Matrix Biol 2003;22(1):81-91.

7. El-Ghannam A. Bone reconstruction: from bioceramics to tissue engineering. Expert Rev Med Devices 2005;2(1):87-101.

8. Sharma B, Elisseeff JH. Engineering structurally organized cartilage and bone tissues. Ann Biomed Eng 2004;32(1):148-59.

9. Meyer U, Joos U, Wiesmann HP. Biological and biophysical principles in extracorporal bone tissue engineering. Part III. Int J Oral Maxillofac Surg 2004;33(7):635-41.

10. Hammond JS, Beckingham IJ, Shakesheff KM. Scaffolds for liver tissue engineering. Expert Rev Med Devices 2006;3(1):21-7.

11. Arosarena O. Tissue engineering. Curr Opin Otolaryngol Head Neck Surg 2005;13(4):233-41.

12. Barry FP, Murphy JM. Mesenchymal stem cells: clinical applications and biological characterization. Int J Biochem Cell Biol 2004;36(4):568-84.

13. Barry FP. Biology and clinical applications of mesenchymal stem cells. Birth Defects Res C Embryo Today 2003;69(3):250-6.

14. Devine SM, Peter S, Martin BJ, Barry F, McIntosh KR. Mesenchymal stem cells: stealth and suppression. Cancer J 2001;7 Suppl 2:S76-82.

15. Salgado AJ, Coutinho OP, Reis RL. Bone tissue engineering: state of the art and future trends. Macromol Biosci 2004;4(8):743-65.

16. Muschler GF, Nakamoto C, Griffith LG. Engineering principles of clinical cell-based tissue engineering. J Bone Joint Surg Am 2004;86-A(7):1541-58.

17. Hayflick L. The Limited In Vitro Lifetime Of Human Diploid Cell Strains. Exp Cell Res 1965;37:614-36.

18. MacLeod RA, Dirks WG, Matsuo Y, Kaufmann M, Milch H, Drexler HG. Widespread intraspecies cross-contamination of human tumor cell lines arising at source. Int J Cancer 1999;83(4):555-63.

19. Masters JR. HeLa cells 50 years on: the good, the bad and the ugly. Nat Rev Cancer 2002;2(4):315-9.

20. Nelson-Rees WA, Daniels DW, Flandermeyer RR. Cross-contamination of cells in culture. Science 1981;212(4493):446-52.

21. Nelson-Rees WA. Responsibility for truth in research. Philos Trans R Soc Lond B Biol Sci 2001;356(1410):849-51.

22. Cenni E, Granchi D, Ciapetti G, Savarino L, Corradini A, Vancini M, Giunti A. Gene expression of bone-associated cytokines in MG63 osteoblast-like cells incubated with acrylic bone cement extracts in minimum essential medium. J Biomater Sci Polym Ed 2002;13(12):1283-94.

23. Hattar S, Berdal A, Asselin A, Loty S, Greenspan DC, Sautier JM. Behaviour of moderately differentiated osteoblast-like cells cultured in contact with bioactive glasses. Eur Cell Mater 2002;4:61-9.

24. Montanaro L, Arciola CR, Campoccia D, Cervellati M. In vitro effects on MG63 osteoblast-like cells following contact with two roughness-differing fluorohydroxyapatite-coated titanium alloys. Biomaterials 2002;23(17):3651-9.

25. Scaduto AA, Lieberman JR. Gene therapy for osteoinduction. Orthop Clin North Am 1999;30(4):625-33.

26. Lieberman JR, Daluiski A, Stevenson S, Wu L, McAllister P, Lee YP, Kabo JM, Finerman GA, Berk AJ, Witte ON. The effect of regional gene therapy with bone morphogenetic protein-2-producing bone-marrow cells on the

repair of segmental femoral defects in rats. J Bone Joint Surg Am 1999;81(7):905-17.

27. Woo BH, Fink BF, Page R, Schrier JA, Jo YW, Jiang G, DeLuca M, Vasconez HC, DeLuca PP. Enhancement of bone growth by sustained delivery of recombinant human bone morphogenetic protein-2 in a polymeric matrix. Pharm Res 2001;18(12):1747-53.

28. Vehof JW, Takita H, Kuboki Y, Spauwen PH, Jansen JA. Histological characterization of the early stages of bone morphogenetic protein-induced osteogenesis. J Biomed Mater Res 2002;61(3):440-9.

29. Vehof JW, Haus MT, de Ruijter AE, Spauwen PH, Jansen JA. Bone formation in transforming growth factor beta-I-loaded titanium fiber mesh implants. Clin Oral Implants Res 2002;13(1):94-102.

30. Vehof JW, Fisher JP, Dean D, van der Waerden JP, Spauwen PH, Mikos AG, Jansen JA. Bone formation in transforming growth factor beta-1-coated porous poly(propylene fumarate) scaffolds. J Biomed Mater Res 2002;60(2):241-51.

31. Vehof JW, de Ruijter AE, Spauwen PH, Jansen JA. Influence of rhBMP-2 on rat bone marrow stromal cells cultured on titanium fiber mesh. Tissue Eng 2001;7(4):373-83.

32. Guilak F, Awad HA, Fermor B, Leddy HA, Gimble JM. Adipose-derived adult stem cells for cartilage tissue engineering. Biorheology 2004;41(3-4):389-99.

33. Goessler UR, Hormann K, Riedel F. Tissue engineering with chondrocytes and function of the extracellular matrix (Review). Int J Mol Med 2004;13(4):505-13.

34. Goessler UR, Bugert P, Bieback K, Baisch A, Sadick H, Verse T, Kluter H, Hormann K, Riedel F. Expression of collagen and fiber-associated proteins in human septal cartilage during in vitro dedifferentiation. Int J Mol Med 2004;14(6):1015-22.

35. Sachlos E, Czernuszka JT. Making tissue engineering scaffolds work. Review: the application of solid freeform fabrication technology to the production of tissue engineering scaffolds. Eur Cell Mater 2003;5:29-39; discussion 39-40.

36. Kuboki Y, Takita H, Kobayashi D, Tsuruga E, Inoue M, Murata M, Nagai N, Dohi Y, Ohgushi H. BMP-induced osteogenesis on the surface of hydroxyapatite with geometrically feasible and nonfeasible structures: topology of osteogenesis. J Biomed Mater Res 1998;39(2):190-9.

37. Story BJ, Wagner WR, Gaisser DM, Cook SD, Rust-Dawicki AM. In vivo performance of a modified CSTi dental implant coating. Int J Oral Maxillofac Implants 1998;13(6):749-57.

38. Karageorgiou V, Kaplan D. Porosity of 3D biomaterial scaffolds and osteogenesis. Biomaterials 2005;26(27):5474-91.

39. Liu X, Ma PX. Polymeric scaffolds for bone tissue engineering. Ann Biomed Eng 2004;32(3):477-86.

40. Yuan H, Kurashina K, de Bruijn JD, Li Y, de Groot K, Zhang X. A preliminary study on osteoinduction of two kinds of calcium phosphate ceramics. Biomaterials 1999;20(19):1799-806.

41. Chvapil M. Collagen sponge: theory and practice of medical applications. J Biomed Mater Res 1977;11(5):721-41.

42. Chvapil M, Chvapil T, Jacobs S, Owen JA, Horton HL, Heine MW. Laboratory and clinical testing of an intravaginal contraceptive collagen sponge. Contraception 1977;15(6):693-703.

43. Tsuruga E, Takita H, Itoh H, Wakisaka Y, Kuboki Y. Pore size of porous hydroxyapatite as the cell-substratum controls BMP-induced osteogenesis. J Biochem (Tokyo) 1997;121(2):317-24.

44. Zeltinger J, Sherwood JK, Graham DA, Mueller R, Griffith LG. Effect of pore size and void fraction on cellular adhesion, proliferation, and matrix deposition. Tissue Eng 2001;7(5):557-72.

45. Simon JL, Roy TD, Parsons JR, Rekow ED, Thompson VP, Kemnitzer J, Ricci JL. Engineered cellular response to scaffold architecture in a rabbit trephine defect. J Biomed Mater Res A 2003;66(2):275-82.

46. Hulbert SF, Young FA, Mathews RS, Klawitter JJ, Talbert CD, Stelling FH. Potential of ceramic materials as permanently implantable skeletal prostheses. J Biomed Mater Res 1970;4(3):433-56.

47. Boyan BD, Hummert TW, Dean DD, Schwartz Z. Role of material surfaces in regulating bone and cartilage cell response. Biomaterials 1996;17(2):137-46.

48. Boyan BD, Lohmann CH, Romero J, Schwartz Z. Bone and cartilage tissue engineering. Clin Plast Surg 1999;26(4):629-45, ix.

49. Wiesmann HP, Joos U, Meyer U. Biological and biophysical principles in extracorporal bone tissue engineering. Part II. Int J Oral Maxillofac Surg 2004;33(6):523-30.

50. Meyer U, Joos U, Wiesmann HP. Biological and biophysical principles in extracorporal bone tissue engineering. Part I. Int J Oral Maxillofac Surg 2004;33(4):325-32.

51. Wiesmann HP, Nazer N, Klatt C, Szuwart T, Meyer U. Bone tissue engineering by primary osteoblast-like cells in a monolayer system and 3-dimensional collagen gel. J Oral Maxillofac Surg 2003;61(12):1455-62.

52. MacArthur BD, Please CP, Taylor M, Oreffo RO. Mathematical modelling of skeletal repair. Biochem Biophys Res Commun 2004;313(4):825-33.

53. Andersson H, van den Berg A. Microfabrication and microfluidics for tissue engineering: state of the art and future opportunities. Lab Chip 2004;4(2):98-103.

54. LeGeros RZ, Craig RG. Strategies to affect bone remodeling: osteointegration. J Bone Miner Res 1993;8 Suppl 2:S583-96.

55. Cullinane DM ET. Biomechanics of bone. In: Bilezikian JP, Raisz LG, Rodan GA, editors. Principles of bone biology.. 2002:17-32.

56. LeGeros RZ. Properties of osteoconductive biomaterials: calcium phosphates. Clin Orthop Relat Res 2002(395):81-98.

57. LeGeros RZ. Calcium phosphate materials in restorative dentistry: a review. Adv Dent Res 1988;2(1):164-80.

58. LeGeros RZ. Calcium phosphates in oral biology and medicine. Monogr Oral Sci 1991;15:1-201.

59. Parsons JR. Cartilage. In: Black, J., and Hastings, G., eds. Handbook of Biomaterials Properties . 1998:40-46.

60. Hench LL, Polak JM. Third-generation biomedical materials. Science 2002;295(5557):1014-7.

61. Hench LL. Biomaterials: a forecast for the future. Biomaterials 1998;19(16):1419-23.

62. Hench LL. Biomaterials. Science 1980;208(4446):826-31.

63. Hench LL. Bioactive ceramics. Ann N Y Acad Sci 1988;523:54-71.

64. Hench LL. Ceramics, glasses, and composites in medicine. Med Instrum 1973;7(2):136-44.

65. Hench LL, Xynos ID, Polak JM. Bioactive glasses for in situ tissue regeneration. J Biomater Sci Polym Ed 2004;15(4):543-62.

66. Thompson ID, Hench LL. Mechanical properties of bioactive glasses, glass-ceramics and composites. Proc Inst Mech Eng [H] 1998;212(2):127-36.

67. Hench LL, Wilson J. Surface-active biomaterials. Science 1984;226(4675):630-6.

68. Saravanapavan P, Jones JR, Verrier S, Beilby R, Shirtliff VJ, Hench LL, Polak JM. Binary CaO-SiO(2) gel-glasses for biomedical applications. Biomed Mater Eng 2004;14(4):467-86.

69. Polak J, Hench L. Gene therapy progress and prospects: in tissue engineering. Gene Ther 2005;12(24):1725-33.

70. Kim BS, Putnam AJ, Kulik TJ, Mooney DJ. Optimizing seeding and culture methods to engineer smooth muscle tissue on biodegradable polymer matrices. Biotechnol Bioeng 1998;57(1):46-54.

71. Kim BS, Mooney DJ. Development of biocompatible synthetic extracellular matrices for tissue engineering. Trends Biotechnol 1998;16(5):224-30.

72. Ratner BD. The engineering of biomaterials exhibiting recognition and specificity. J Mol Recognit 1996;9(5-6):617-25.

73. Ratner BD. Surface modification of polymers: chemical, biological and surface analytical challenges. Biosens Bioelectron 1995;10(9-10):797-804.

74. Robert Lanza RL, Joseph Vacanti. PRINCIPLES OF TISSUE ENGINEERING: ACADEMIC PRESS; 2000. 995 p.

75. LeGeros RZ, Lin S, Rohanizadeh R, Mijares D, LeGeros JP. Biphasic calcium phosphate bioceramics: preparation, properties and applications. J Mater Sci Mater Med 2003;14(3):201-9.

76. Ohgushi H, Caplan AI. Stem cell technology and bioceramics: from cell to gene engineering. J Biomed Mater Res 1999;48(6):913-27.

77. Reddi AH. Morphogenesis and tissue engineering of bone and cartilage: inductive signals, stem cells, and biomimetic biomaterials. Tissue Eng 2000;6(4):351-9.

78. Toquet J, Rohanizadeh R, Guicheux J, Couillaud S, Passuti N, Daculsi G, Heymann D. Osteogenic potential in vitro of human bone marrow cells cultured on macroporous biphasic calcium phosphate ceramic. J Biomed Mater Res 1999;44(1):98-108.

79. Ripamonti U, Ma S, Reddi AH. The critical role of geometry of porous hydroxyapatite delivery system in induction of bone by osteogenin, a bone morphogenetic protein. Matrix 1992;12(3):202-12.

80. Ohgushi H, Miyake J, Tateishi T. Mesenchymal stem cells and bioceramics: strategies to regenerate the skeleton. Novartis Found Symp 2003;249:118-27; discussion 127-32, 170-4, 239-41.

81. Koerten HK, van der Meulen J. Degradation of calcium phosphate ceramics. J Biomed Mater Res 1999;44(1):78-86.

82. LeGeros RZ. Biodegradation and bioresorption of calcium phosphate ceramics. Clin Mater 1993;14(1):65-88.

83. Athanasiou KA, Niederauer GG, Agrawal CM. Sterilization, toxicity, biocompatibility and clinical applications of polylactic acid/polyglycolic acid copolymers. Biomaterials 1996;17(2):93-102.

84. Yang S, Leong KF, Du Z, Chua CK. The design of scaffolds for use in tissue engineering. Part I. Traditional factors. Tissue Eng 2001;7(6):679-89.

85. Stock UA, Mayer JE, Jr. Tissue engineering of cardiac valves on the basis of PGA/PLA Co-polymers. J Long Term Eff Med Implants 2001;11(3-4):249-60.

86. Athanasiou KA, Agrawal CM, Barber FA, Burkhart SS. Orthopaedic applications for PLA-PGA biodegradable polymers. Arthroscopy 1998;14(7):726-37.

87. Reed AM, Gilding DK, Wilson J. Biodegradable elastomeric biomaterials--polyethylene oxide/polyethylene terephthalate copolymers. Trans Am Soc Artif Intern Organs 1977;23:109-15.

88. Vert M, Mauduit J, Li S. Biodegradation of PLA/GA polymers: increasing complexity. Biomaterials 1994;15(15):1209-13.

89. Vert M, Li SM, Garreau H. Attempts to map the structure and degradation characteristics of aliphatic polyesters derived from lactic and glycolic acids. J Biomater Sci Polym Ed 1994;6(7):639-49.

90. Kohn DH, Sarmadi M, Helman JI, Krebsbach PH. Effects of pH on human bone marrow stromal cells in vitro: implications for tissue engineering of bone. J Biomed Mater Res 2002;60(2):292-9.

91. Wake MC, Gerecht PD, Lu L, Mikos AG. Effects of biodegradable polymer particles on rat marrow-derived stromal osteoblasts in vitro. Biomaterials 1998;19(14):1255-68.

92. Bergsma JE, Rozema FR, Bos RR, Boering G, de Bruijn WC, Pennings AJ. In vivo degradation and biocompatibility study of in vitro pre-degraded as-polymerized polyactide particles. Biomaterials 1995;16(4):267-74.

93. Suganuma J, Pachence J, Traub JA, Alexander H, Ricci JL, Casar RS. In vivo evaluation of collagen-coated Dacron fiber in bone. Clin Mater 1994;15(1):43-50.

94. Zhang R, Ma PX. Poly(alpha-hydroxyl acids)/hydroxyapatite porous composites for bone-tissue engineering. I. Preparation and morphology. J Biomed Mater Res 1999;44(4):446-55.

95. Zhang Y, Zhang M. Synthesis and characterization of macroporous chitosan/calcium phosphate composite scaffolds for tissue engineering. J Biomed Mater Res 2001;55(3):304-12.

96. Lu HH, El-Amin SF, Scott KD, Laurencin CT. Three-dimensional, bioactive, biodegradable, polymer-bioactive glass composite scaffolds with improved mechanical properties support collagen synthesis and mineralization of human osteoblast-like cells in vitro. J Biomed Mater Res 2003;64A(3):465-74.

97. Zhang Y, Ni M, Zhang M, Ratner B. Calcium phosphate-chitosan composite scaffolds for bone tissue engineering. Tissue Eng 2003;9(2):337-45.

98. Khan YM, Katti DS, Laurencin CT. Novel polymer-synthesized ceramic composite-based system for bone repair: an in vitro evaluation. J Biomed Mater Res A 2004;69(4):728-37.

99. Zhao F, Yin Y, Lu WW, Leong JC, Zhang W, Zhang J, Zhang M, Yao K. Preparation and histological evaluation of biomimetic three-dimensional hydroxyapatite/chitosan-gelatin network composite scaffolds. Biomaterials 2002;23(15):3227-34.

100. Desbrieres J. Viscosity of semiflexible chitosan solutions: influence of concentration, temperature, and role of intermolecular interactions. Biomacromolecules 2002;3(2):342-9.

101. Delben F, Lapasin R, Pricl S. Flow properties of N-(carboxymethyl) chitosan aqueous systems in the sol and gel domains. Int J Biol Macromol 1990;12(1):9-13.

102. Mao JS, liu HF, Yin YJ, Yao KD. The properties of chitosan-gelatin membranes and scaffolds modified with hyaluronic acid by different methods. Biomaterials 2003;24(9):1621-9.

103. Lee JE, Kim KE, Kwon IC, Ahn HJ, Lee SH, Cho HC, Kim HJ, Seong SC, Lee MC. Effects of the controlled-released TGF-beta1 from chitosan microspheres on chondrocytes cultured in a collagen/chitosan/glycosaminoglycan scaffold. Biomaterials 2004;25(18):4163-73.

104. Liu WG, Zhang JR, Cao ZQ, Xu FY, Yao KD. A chitosan-arginine conjugate as a novel anticoagulation biomaterial. J Mater Sci Mater Med 2004;15(11):1199-203.

105. Ye P, Xu ZK, Wu J, Innocent C, Seta P. Nanofibrous poly(acrylonitrile-co-maleic acid) membranes functionalized with gelatin and chitosan for lipase immobilization. Biomaterials 2006.

106. Li Z, Ramay HR, Hauch KD, Xiao D, Zhang M. Chitosan-alginate hybrid scaffolds for bone tissue engineering. Biomaterials 2005;26(18):3919-28.

107. Matsumoto T, Kawai M, Masuda T. Rheological properties and fractal structure of concentrated polyion complexes of chitosan and alginate. Biorheology 1993;30(5-6):435-41.

108. Wang L, Khor E, Lim LY. Chitosan-alginate-CaCl(2) system for membrane coat application. J Pharm Sci 2001;90(8):1134-42.

109. Li X. The use of chitosan to increase the stability of calcium alginate beads with entrapped yeast cells. Biotechnol Appl Biochem 1996;23 (Pt 3):269-72.

110. Li Z, Zhang M. Chitosan-alginate as scaffolding material for cartilage tissue engineering. J Biomed Mater Res A 2005;75(2):485-93.

111. Madihally SV, Matthew HW. Porous chitosan scaffolds for tissue engineering. Biomaterials 1999;20(12):1133-42.

112. Zhang H, Neau SH. In vitro degradation of chitosan by a commercial enzyme preparation: effect of molecular weight and degree of deacetylation. Biomaterials 2001;22(12):1653-8.

113. Ren D, Yi H, Wang W, Ma X. The enzymatic degradation and swelling properties of chitosan matrices with different degrees of N-acetylation. Carbohydr Res 2005;340(15):2403-10.

114. Kim KW, Thomas RL, Lee C, Park HJ. Antimicrobial activity of native chitosan, degraded chitosan, and O-carboxymethylated chitosan. J Food Prot 2003;66(8):1495-8.

115. Kiang T, Wen J, Lim HW, Leong KW. The effect of the degree of chitosan deacetylation on the efficiency of gene transfection. Biomaterials 2004;25(22):5293-301.

116. Aye KN, Karuppuswamy R, Ahamed T, Stevens WF. Peripheral enzymatic deacetylation of chitin and reprecipitated chitin particles. Bioresour Technol 2006;97(4):577-82.

117. Kj, niksen A-L, Nystr, m B, Nakken T, Palmgren O, Tande T. Effect of surfactant concentration, pH, and shear rate on the rheological properties of aqueous systems of a hydrophobically modified chitosan and its unmodified analogue. Polymer Bulletin 1997;38(1):71.

118. Vasir JK, Tambwekar K, Garg S. Bioadhesive microspheres as a controlled drug delivery system. Int J Pharm 2003;255(1-2):13-32.

119. Colombo P, Bettini R, Massimo G, Catellani PL, Santi P, Peppas NA. Drug diffusion front movement is important in drug release control from swellable matrix tablets. J Pharm Sci 1995;84(8):991-7.

120. Khare AR, Peppas NA. Release behavior of bioactive agents from pH-sensitive hydrogels. J Biomater Sci Polym Ed 1993;4(3):275-89.

121. De Vos P, De Haan B, Pater J, Van Schilfgaarde R. Association between capsule diameter, adequacy of encapsulation, and survival of microencapsulated rat islet allografts. Transplantation 1996;62(7):893-9.

122. Spargo BJ, Rudolph AS, Rollwagen FM. Recruitment of tissue resident cells to hydrogel composites: in vivo response to implant materials. Biomaterials 1994;15(10):853-8.

123. Wee S, Gombotz WR. Protein release from alginate matrices. Adv Drug Deliv Rev 1998;31(3):267-285.

124. J. Schuh WF, W. Gombotz and S.F. Wee. Intranasal localization and antibody response to polycation-coated ova-encapsulated alginate microbeads. Vet. Pathol 1996;33(5).

125. Otterlei M, Ostgaard K, Skjak-Braek G, Smidsrod O, Soon-Shiong P, Espevik T. Induction of cytokine production from human monocytes stimulated with alginate. J Immunother 1991;10(4):286-91.

126. Zimmermann H, Zimmermann D, Reuss R, Feilen PJ, Manz B, Katsen A, Weber M, Ihmig FR, Ehrhart F, Gessner P and others. Towards a medically approved technology for alginate-based microcapsules allowing long-term immunoisolated transplantation. J Mater Sci Mater Med 2005;16(6):491-501.

127. Smidsrod O, Skjak-Braek G. Alginate as immobilization matrix for cells. Trends Biotechnol 1990;8(3):71-8.

128. Kwok KK, Groves MJ, Burgess DJ. Production of 5-15 microns diameter alginate-polylysine microcapsules by an air-atomization technique. Pharm Res 1991;8(3):341-4.

129. Grandolfo M, D'Andrea P, Paoletti S, Martina M, Silvestrini G, Bonucci E, Vittur F. Culture and differentiation of chondrocytes entrapped in alginate gels. Calcif Tissue Int 1993;52(1):42-8.

130. Paoletti S, Gamini A, Zanetti F. Conformational aspects of ionic polysaccharides: laser light scattering of aqueous solutions of hyaluronic acid and alginate. Biochem Soc Trans 1991;19(2):494-5.

131. Cesaro A, Delben F, Paoletti S. Thermodynamics of the proton dissociation of natural polyuronic acids. Int J Biol Macromol 1990;12(3):170-6.

132. Puolakkainen PA, Ranchalis JE, Gombotz WR, Hoffman AS, Mumper RJ, Twardzik DR. Novel delivery system for inducing quiescence in intestinal stem cells in rats by transforming growth factor beta 1. Gastroenterology 1994;107(5):1319-26.

133. Leinfelder U, Brunnenmeier F, Cramer H, Schiller J, Arnold K, Vasquez JA, Zimmermann U. A highly sensitive cell assay for validation of purification regimes of alginates. Biomaterials 2003;24(23):4161-72.

134. Zimmermann H, Hillgartner M, Manz B, Feilen P, Brunnenmeier F, Leinfelder U, Weber M, Cramer H, Schneider S, Hendrich C and others. Fabrication of homogeneously cross-linked, functional alginate microcapsules validated by NMR-, CLSM- and AFM-imaging. Biomaterials 2003;24(12):2083-96.

135. Tschimirov JI, Kislova TV, Braudo EE, Schierbaum FR, Straschnenko ES, Tolstoguzov VB, Augustat S. [Rheological properties of a calcium alginate-potato starch hydrolysate-water system]. Nahrung 1979;23(5):501-8.

136. Fuongfuchat A, Jamieson AM, Blackwell J, Gerken TA. Rheological studies of the interaction of mucins with alginate and polyacrylate. Carbohydr Res 1996;284(1):85-99.

137. Baldursdottir SG, Kjoniksen AL, Karlsen J, Nystrom B, Roots J, Tonnesen HH. Riboflavin-photosensitized changes in aqueous solutions of alginate. Rheological studies. Biomacromolecules 2003;4(2):429-36.

138. Duggirala S, Deluca PP. Rheological characterization of cellulosic and alginate polymers. PDA J Pharm Sci Technol 1996;50(5):290-6.

139. Daubert. VDTaC. Rheological and textural properties of alginate-starch mixed gels: effects of starch type and concentration. 2001 AACC Annual Meeting 2001.

140. Lai HL, Abu'Khalil A, Craig DQ. The preparation and characterisation of drug-loaded alginate and chitosan sponges. Int J Pharm 2003;251(1-2):175-81.

141. T Takahashi KT, Y Machida, T Nagai. Characteristics of Polyion-complex of chitosan with sodium alginate and sodium polyacrylate. Int. J. Phar 1990;61:35-41.

142. Bodmeier R, Chen HG, Paeratakul O. A novel approach to the oral delivery of micro- or nanoparticles. Pharm Res 1989;6(5):413-7.

143. Yan X, Khor E, Lim LY. PEC films prepared from Chitosan-Alginate coacervates. Chem Pharm Bull (Tokyo) 2000;48(7):941-6.

144. Zheng CH, Liang WQ, Li F, Zhang YP, Fang WJ. Optimization and characterization of chitosan-coated alginate microcapsules containing albumin. Pharmazie 2005;60(6):434-8.

145. Coppi G, Iannuccelli V, Leo E, Bernabei MT, Cameroni R. Chitosan-alginate microparticles as a protein carrier. Drug Dev Ind Pharm 2001;27(5):393-400.

146. Mikos AG, Lyman MD, Freed LE, Langer R. Wetting of poly(L-lactic acid) and poly(DL-lactic-co-glycolic acid) foams for tissue culture. Biomaterials 1994;15(1):55-8.

147. Gravel M, Vago R, Tabrizian M. Use of natural coralline biomaterials as reinforcing and gas-forming agent for developing novel hybrid biomatrices: microarchitectural and mechanical studies. Tissue Eng 2006;12(3):589-600.

148. Yang S, Leong KF, Du Z, Chua CK. The design of scaffolds for use in tissue engineering. Part II. Rapid prototyping techniques. Tissue Eng 2002;8(1):1-11.

149. Guan J, Fujimoto KL, Sacks MS, Wagner WR. Preparation and characterization of highly porous, biodegradable polyurethane scaffolds for soft tissue applications. Biomaterials 2005;26(18):3961-71.

150. Zhao L, Chang J. Preparation and characterization of macroporous chitosan/wollastonite composite scaffolds for tissue engineering. J Mater Sci Mater Med 2004;15(5):625-9.

151. Cao Y, Davidson MR, O'Connor AJ, Stevens GW, Cooper-White JJ. Architecture control of three-dimensional polymeric scaffolds for soft tissue engineering. I. Establishment and validation of numerical models. J Biomed Mater Res A 2004;71(1):81-9.

152. Zhang Y, Zhang M. Calcium phosphate/chitosan composite scaffolds for controlled in vitro antibiotic drug release. J Biomed Mater Res 2002;62(3):378-86.

153. Maspero FA, Ruffieux K, Muller B, Wintermantel E. Resorbable defect analog PLGA scaffolds using CO2 as solvent: structural characterization. J Biomed Mater Res 2002;62(1):89-98.

154. Zhang R, Ma PX. Porous poly(L-lactic acid)/apatite composites created by biomimetic process. J Biomed Mater Res 1999;45(4):285-93.

155. ED S. Late stage of decomposition in binary mixtures. Phys Rev A 1979;20:595.

156. Yuan Z, Favis BD. Macroporous poly(L-lactide) of controlled pore size derived from the annealing of co-continuous polystyrene/poly(L-lactide) blends. Biomaterials 2004;25(11):2161-70.

157. Yoo PJ, Suh KY, Kang H, Lee HH. Polymer elasticity-driven wrinkling and coarsening in high temperature buckling of metal-capped polymer thin films. Phys Rev Lett 2004;93(3):034301.

158. Xie XM, Kong XM, Xiao TJ, Yang Y, Gao N, Tanioka A. Interface-Induced Coarsening Process in Polymer Blends. J Colloid Interface Sci 2001;234(1):24-27.

159. Murata Y, Jinno D, Kofuji K, Kawashima S. Properties of calcium-induced gel beads prepared with alginate and hydrolysates. Chem Pharm Bull (Tokyo) 2004;52(5):605-7.

160. O'Brien FJ, Harley BA, Yannas IV, Gibson LJ. The effect of pore size on cell adhesion in collagen-GAG scaffolds. Biomaterials 2005;26(4):433-41.

161. Porter BD, Oldham JB, He SL, Zobitz ME, Payne RG, An KN, Currier BL, Mikos AG, Yaszemski MJ. Mechanical properties of a biodegradable bone regeneration scaffold. J Biomech Eng 2000;122(3):286-8.

162. Chu TM, Orton DG, Hollister SJ, Feinberg SE, Halloran JW. Mechanical and in vivo performance of hydroxyapatite implants with controlled architectures. Biomaterials 2002;23(5):1283-93.

163. Thomson RC, Yaszemski MJ, Powers JM, Mikos AG. Fabrication of biodegradable polymer scaffolds to engineer trabecular bone. J Biomater Sci Polym Ed 1995;7(1):23-38.

164. Shanmugasundaram N, Ravichandran P, Reddy PN, Ramamurty N, Pal S, Rao KP. Collagen-chitosan polymeric scaffolds for the in vitro culture of human epidermoid carcinoma cells. Biomaterials 2001;22(14):1943-51.

165. Khalid MN, Agnely F, Yagoubi N, Grossiord JL, Couarraze G. Water state characterization, swelling behavior, thermal and mechanical properties of chitosan based networks. Eur J Pharm Sci 2002;15(5):425-32.

166. Vachoud L, Zydowicz N, Domard A. Physicochemical behaviour of chitin gels. Carbohydr Res 2000;326(4):295-304.

167. Aiba S. Studies on chitosan: 3. Evidence for the presence of random and block copolymer structures in partially N-acetylated chitosans. Int J Biol Macromol 1991;13(1):40-4.

168. M Sugimoto MM, Hitoshi Sashiwa, H Saimoto, Y Shigemasa. Preparation and characterization of water soluble chitin and chitosan derivatives. Carbohydrate Polymers 1998;36:49-59.

169. C.J. Brine PAS, J.P. Zikakis. Advances in Chitin and Chitosan. Elsevier, London,; 1992. 506-515 p.

170. King GN, Cochran DL. Factors that modulate the effects of bone morphogenetic protein-induced periodontal regeneration: a critical review. J Periodontol 2002;73(8):925-36.

171. King GN. The importance of drug delivery to optimize the effects of bone morphogenetic proteins during periodontal regeneration. Curr Pharm Biotechnol 2001;2(2):131-42.

172. Hauschka PV, Chen TL, Mavrakos AE. Polypeptide growth factors in bone matrix. Ciba Found Symp 1988;136:207-25.

173. Berger J, Reist M, Mayer JM, Felt O, Gurny R. Structure and interactions in chitosan hydrogels formed by complexation or aggregation for biomedical applications. Eur J Pharm Biopharm 2004;57(1):35-52.

174. Gombotz WR, Pettit DK. Biodegradable polymers for protein and peptide drug delivery. Bioconjug Chem 1995;6(4):332-51.

175. Roorda WE, Bodde HE, De Boer AG, Bouwstra JA, Junginer HE. Synthetic hydrogels as drug delivery systems. Pharm Weekbl Sci 1986;8(3):165-89.

176. Chang Y, Tsai CC, Liang HC, Sung HW. In vivo evaluation of cellular and acellular bovine pericardia fixed with a naturally occurring crosslinking agent (genipin). Biomaterials 2002;23(12):2447-57.

177. Liang HC, Chang WH, Lin KJ, Sung HW. Genipin-crosslinked gelatin microspheres as a drug carrier for intramuscular administration: in vitro and in vivo studies. J Biomed Mater Res A 2003;65(2):271-82.

178. Mi FL, Tan YC, Liang HF, Sung HW. In vivo biocompatibility and degradability of a novel injectable-chitosan-based implant. Biomaterials 2002;23(1):181-91.

179. Sung HW, Huang DM, Chang WH, Huang RN, Hsu JC. Evaluation of gelatin hydrogel crosslinked with various crosslinking agents as bioadhesives: in vitro study. J Biomed Mater Res 1999;46(4):520-30.

180. Yang Z, Zhang Y, Markland P, Yang VC. Poly(glutamic acid) poly(ethylene glycol) hydrogels prepared by photoinduced polymerization: Synthesis, characterization, and preliminary release studies of protein drugs. J Biomed Mater Res 2002;62(1):14-21.

181. Peppas NA, Bures P, Leobandung W, Ichikawa H. Hydrogels in pharmaceutical formulations. Eur J Pharm Biopharm 2000;50(1):27-46.

182. Kim SW, Bae YH, Okano T. Hydrogels: swelling, drug loading, and release. Pharm Res 1992;9(3):283-90.

183. Yu X, Cheng M, Chen H. [Methods for the pre-treatment of biological tissues for vascular scaffold]. Sheng Wu Yi Xue Gong Cheng Xue Za Zhi 2004;21(3):476-81.

184. Minuth WW, Sittinger M, Kloth S. Tissue engineering: generation of differentiated artificial tissues for biomedical applications. Cell Tissue Res 1998;291(1):1-11.

185. Niklason LE, Langer RS. Advances in tissue engineering of blood vessels and other tissues. Transpl Immunol 1997;5(4):303-6.

186. Suh JK, Matthew HW. Application of chitosan-based polysaccharide biomaterials in cartilage tissue engineering: a review. Biomaterials 2000;21(24):2589-98.

187. Kosher RA, Church RL. Stimulation of in vitro somite chondrogenesis by procollagen and collagen. Nature 1975;258(5533):327-30.

188. Kosher RA, Lash JW, Minor RR. Environmental enhancement of in vitro chondrogenesis. IV. Stimulation of somite chondrogenesis by exogenous chondromucoprotein. Dev Biol 1973;35(2):210-20.

189. Lash JW, Rosene K, Minor RR, Daniel JC, Kosher RA. Environmental enhancement of in vitro chondrogenesis. 3. The influence of external potassium ions and chondrogenic differentiation. Dev Biol 1973;35(2):370-5.

190. Hunziker EB. Articular cartilage repair: basic science and clinical progress. A review of the current status and prospects. Osteoarthritis Cartilage 2002;10(6):432-63.

191. Glowacki J. Engineered cartilage, bone, joints, and menisci. Potential for temporomandibular joint reconstruction. Cells Tissues Organs 2001;169(3):302-8.

192. van Susante JLC, Pieper J, Buma P, van Kuppevelt TH, van Beuningen H, van Der Kraan PM, Veerkamp JH, van den Berg WB, Veth RPH. Linkage of chondroitin-sulfate to type I collagen scaffolds stimulates the bioactivity of seeded chondrocytes in vitro. Biomaterials 2001;22(17):2359-69.

193. Nehrer S, Breinan HA, Ramappa A, Shortkroff S, Young G, Minas T, Sledge CB, Yannas IV, Spector M. Canine chondrocytes seeded in type I and type II collagen implants investigated in vitro. J Biomed Mater Res 1997;38(2):95-104.

194. Ushida T, Furukawa K, Toita K, Tateishi T. Three-dimensional seeding of chondrocytes encapsulated in collagen gel into PLLA scaffolds. Cell Transplant 2002;11(5):489-94.

195. Perka C, Arnold U, Spitzer RS, Lindenhayn K. The use of fibrin beads for tissue engineering and subsequential transplantation. Tissue Eng 2001;7(3):359-61.

196. Aigner J, Tegeler J, Hutzler P, Campoccia D, Pavesio A, Hammer C, Kastenbauer E, Naumann A. Cartilage tissue engineering with novel

nonwoven structured biomaterial based on hyaluronic acid benzyl ester. J Biomed Mater Res 1998;42(2):172-81.

197. Freed LE, Marquis JC, Nohria A, Emmanual J, Mikos AG, Langer R. Neocartilage formation in vitro and in vivo using cells cultured on synthetic biodegradable polymers. J Biomed Mater Res 1993;27(1):11-23.

198. Sittinger M, Reitzel D, Dauner M, Hierlemann H, Hammer C, Kastenbauer E, Planck H, Burmester GR, Bujia J. Resorbable polyesters in cartilage engineering: affinity and biocompatibility of polymer fiber structures to chondrocytes. J Biomed Mater Res 1996;33(2):57-63.

199. Kisiday J, Jin M, Kurz B, Hung H, Semino C, Zhang S, Grodzinsky AJ. Self-assembling peptide hydrogel fosters chondrocyte extracellular matrix production and cell division: implications for cartilage tissue repair. Proc Natl Acad Sci U S A 2002;99(15):9996-10001.

200. Mallein-Gerin F, Garrone R, van der Rest M. Proteoglycan and collagen synthesis are correlated with actin organization in dedifferentiating chondrocytes. Eur J Cell Biol 1991;56(2):364-73.

201. Sechriest VF, Miao YJ, Niyibizi C, Westerhausen-Larson A, Matthew HW, Evans CH, Fu FH, Suh JK. GAG-augmented polysaccharide hydrogel: a novel biocompatible and biodegradable material to support chondrogenesis. J Biomed Mater Res 2000;49(4):534-41.

202. Schulze M, Kuettner KE, Cole AA. [Adult human chondrocytes in alginate culture. Preservation of the phenotype for further use in transplantation models]. Orthopade 2000;29(2):100-6.

203. Lahiji A, Sohrabi A, Hungerford DS, Frondoza CG. Chitosan supports the expression of extracellular matrix proteins in human osteoblasts and chondrocytes. J Biomed Mater Res 2000;51(4):586-95.

204. Miralles G, Baudoin R, Dumas D, Baptiste D, Hubert P, Stoltz JF, Dellacherie E, Mainard D, Netter P, Payan E. Sodium alginate sponges with or without sodium hyaluronate: in vitro engineering of cartilage. J Biomed Mater Res 2001;57(2):268-78.

205. Hauselmann HJ, Aydelotte MB, Schumacher BL, Kuettner KE, Gitelis SH, Thonar EJ. Synthesis and turnover of proteoglycans by human and bovine adult articular chondrocytes cultured in alginate beads. Matrix 1992;12(2):116-29.

206. Prasitsilp M, Jenwithisuk R, Kongsuwan K, Damrongchai N, Watts P. Cellular responses to chitosan in vitro: the importance of deacetylation. J Mater Sci Mater Med 2000;11(12):773-8.

207. Kim SE, Park JH, Cho YW, Chung H, Jeong SY, Lee EB, Kwon IC. Porous chitosan scaffold containing microspheres loaded with transforming growth factor-beta1: implications for cartilage tissue engineering. J Control Release 2003;91(3):365-74.

208. Gugala Z, Gogolewski S. In vitro growth and activity of primary chondrocytes on a resorbable polylactide three-dimensional scaffold. J Biomed Mater Res 2000;49(2):183-91.

209. Nehrer S, Breinan HA, Ramappa A, Young G, Shortkroff S, Louie LK, Sledge CB, Yannas IV, Spector M. Matrix collagen type and pore size influence behaviour of seeded canine chondrocytes. Biomaterials 1997;18(11):769-76.

210. Benya PD. Modulation and reexpression of the chondrocyte phenotype; mediation by cell shape and microfilament modification. Pathol Immunopathol Res 1988;7(1-2):51-4.

211. Mayne R, Vail MS, Mayne PM, Miller EJ. Changes in type of collagen synthesized as clones of chick chondrocytes grow and eventually lose division capacity. Proc Natl Acad Sci U S A 1976;73(5):1674-8.

212. Lee DA, Reisler T, Bader DL. Expansion of chondrocytes for tissue engineering in alginate beads enhances chondrocytic phenotype compared to conventional monolayer techniques. Acta Orthop Scand 2003;74(1):6-15.

213. Caterson EJ, Li WJ, Nesti LJ, Albert T, Danielson K, Tuan RS. Polymer/alginate amalgam for cartilage-tissue engineering. Ann N Y Acad Sci 2002;961:134-8.

214. Marijnissen WJ, van Osch GJ, Aigner J, van der Veen SW, Hollander AP, Verwoerd-Verhoef HL, Verhaar JA. Alginate as a chondrocyte-delivery substance in combination with a non-woven scaffold for cartilage tissue engineering. Biomaterials 2002;23(6):1511-7.

215. Caterson EJ, Nesti LJ, Li WJ, Danielson KG, Albert TJ, Vaccaro AR, Tuan RS. Three-dimensional cartilage formation by bone marrow-derived cells seeded in polylactide/alginate amalgam. J Biomed Mater Res 2001;57(3):394-403.

216. Lee CR, Grodzinsky AJ, Hsu HP, Spector M. Effects of a cultured autologous chondrocyte-seeded type II collagen scaffold on the healing of a chondral defect in a canine model. J Orthop Res 2003;21(2):272-81.

217. Li WJ, Danielson KG, Alexander PG, Tuan RS. Biological response of chondrocytes cultured in three-dimensional nanofibrous poly(epsilon-caprolactone) scaffolds. J Biomed Mater Res 2003;67A(4):1105-14.

218. Benya PD, Shaffer JD. Dedifferentiated chondrocytes reexpress the differentiated collagen phenotype when cultured in agarose gels. Cell 1982;30(1):215-24.

219. von der Mark K, Gauss V, von der Mark H, Muller P. Relationship between cell shape and type of collagen synthesised as chondrocytes lose their cartilage phenotype in culture. Nature 1977;267(5611):531-2.

220. Homicz MR, Chia SH, Schumacher BL, Masuda K, Thonar EJ, Sah RL, Watson D. Human septal chondrocyte redifferentiation in alginate, polyglycolic acid scaffold, and monolayer culture. Laryngoscope 2003;113(1):25-32.

221. Nettles DL, Elder SH, Gilbert JA. Potential Use of Chitosan as a Cell Scaffold Material for Cartilage Tissue Engineering. Tissue Eng 2002;8(6):1009-1016.

222. De Haart M, Marijnissen WJ, van Osch GJ, Verhaar JA. Optimization of chondrocyte expansion in culture. Effect of TGF beta-2, bFGF and L-ascorbic acid on bovine articular chondrocytes. Acta Orthop Scand 1999;70(1):55-61.

223. Persidis A. Tissue engineering. Nat Biotechnol 1999;17(5):508-10.

224. Service RF. Tissue Engineers Build New Bone. Science 2000;289(5484):1498-1500.

225. Petite H, Viateau V, Bensaid W, Meunier A, de Pollak C, Bourguignon M, Oudina K, Sedel L, Guillemin G. Tissue-engineered bone regeneration. Nat Biotechnol 2000;18(9):959-63.

226. Jarcho M. Calcium phosphate ceramics as hard tissue prosthetics. Clin Orthop 1981(157):259-78.

227. Niklason LE. Engineering of bone grafts. Nat Biotechnol 2000;18(9):929-30.

228. Sheehan D HB. Theory and practice of Histotechnology, 2nd Ed. Ohio: Battelle Press; 1980. 226-227 p.

229. Boskey AL. Mineral-matrix interactions in bone and cartilage. Clin Orthop 1992(281):244-74.

230. VandeVord PJ, Matthew HW, DeSilva SP, Mayton L, Wu B, Wooley PH. Evaluation of the biocompatibility of a chitosan scaffold in mice. J Biomed Mater Res 2002;59(3):585-90.

231. Lutolf MP, Weber FE, Schmoekel HG, Schense JC, Kohler T, Muller R, Hubbell JA. Repair of bone defects using synthetic mimetics of collagenous extracellular matrices. Nat Biotechnol 2003;21(5):513-8.

232. Hutmacher DW, Teoh SH, Zein I, Ranawake M, Lau S. Tissue engineering research: the engineer's role. Med Device Technol 2000;11(1):33-9.

233. Peluso G, Petillo O, Ranieri M, Santin M, Ambrosio L, Calabro D, Avallone B, Balsamo G. Chitosan-mediated stimulation of macrophage function. Biomaterials 1994;15(15):1215-20.

234. Itskovitz-Eldor J, Schuldiner M, Karsenti D, Eden A, Yanuka O, Amit M, Soreq H, Benvenisty N. Differentiation of human embryonic stem cells into embryoid bodies compromising the three embryonic germ layers. Mol Med 2000;6(2):88-95.

235. Liu H, Roy K. Biomimetic three-dimensional cultures significantly increase hematopoietic differentiation efficacy of embryonic stem cells. Tissue Eng 2005;11(1-2):319-30.

236. Liu H, Lin J, Roy K. Effect of 3D scaffold and dynamic culture condition on the global gene expression profile of mouse embryonic stem cells. Biomaterials 2006;27(36):5978-89.

237. Stacey GN, Cobo F, Nieto A, Talavera P, Healy L, Concha A. The development of 'feeder' cells for the preparation of clinical grade hES cell lines: challenges and solutions. J Biotechnol 2006;125(4):583-8.

238. Oh SK, Choo AB. Human embryonic stem cells: technological challenges towards therapy. Clin Exp Pharmacol Physiol 2006;33(5-6):489-95.

239. Mallon BS, Park KY, Chen KG, Hamilton RS, McKay RD. Toward xeno-free culture of human embryonic stem cells. Int J Biochem Cell Biol 2006;38(7):1063-75.

240. Stojkovic M, Lako M, Strachan T, Murdoch A. Derivation, growth and applications of human embryonic stem cells. Reproduction 2004;128(3):259-67.

241. Przyborski SA. Differentiation of human embryonic stem cells after transplantation in immune-deficient mice. Stem Cells 2005;23(9):1242-50.

242. Bagley J, Rosenzweig M, Marks DF, Pykett MJ. Extended culture of multipotent hematopoietic progenitors without cytokine augmentation in a novel three-dimensional device. Exp Hematol 1999;27(3):496-504.

243. Boudreau NJ, Jones PL. Extracellular matrix and integrin signalling: the shape of things to come. Biochem J 1999;339 (Pt 3):481-8.

244. Geiger B, Bershadsky A, Pankov R, Yamada KM. Transmembrane crosstalk between the extracellular matrix--cytoskeleton crosstalk. Nat Rev Mol Cell Biol 2001;2(11):793-805.

245. Tan W, Krishnaraj R, Desai TA. Evaluation of nanostructured composite collagen--chitosan matrices for tissue engineering. Tissue Eng 2001;7(2):203-10.

246. Desai TA. Micro- and nanoscale structures for tissue engineering constructs. Med Eng Phys 2000;22(9):595-606.

247. Baharvand H, Hashemi SM, Kazemi Ashtiani S, Farrokhi A. Differentiation of human embryonic stem cells into hepatocytes in 2D and 3D culture systems in vitro. Int J Dev Biol 2006;50(7):645-52.

248. Taqvi S, Roy K. Influence of scaffold physical properties and stromal cell coculture on hematopoietic differentiation of mouse embryonic stem cells. Biomaterials 2006;27(36):6024-31.

249. Zeng X, Miura T, Luo Y, Bhattacharya B, Condie B, Chen J, Ginis I, Lyons I, Mejido J, Puri RK and others. Properties of pluripotent human embryonic stem cells BG01 and BG02. Stem Cells 2004;22(3):292-312.

250. Zeng X, Chen J, Liu Y, Luo Y, Schulz TC, Robins AJ, Rao MS, Freed WJ. BG01V: a variant human embryonic stem cell line which exhibits rapid growth after passaging and reliable dopaminergic differentiation. Restor Neurol Neurosci 2004;22(6):421-8.

251. Thomson JA, Itskovitz-Eldor J, Shapiro SS, Waknitz MA, Swiergiel JJ, Marshall VS, Jones JM. Embryonic stem cell lines derived from human blastocysts. Science 1998;282(5391):1145-7.

252. Thomson JA, Odorico JS. Human embryonic stem cell and embryonic germ cell lines. Trends Biotechnol 2000;18(2):53-7.

253. Kaufman DS, Thomson JA. Human ES cells--haematopoiesis and transplantation strategies. J Anat 2002;200(Pt 3):243-8.

254. Choo A, Padmanabhan J, Chin A, Fong WJ, Oh SK. Immortalized feeders for the scale-up of human embryonic stem cells in feeder and feeder-free conditions. J Biotechnol 2006;122(1):130-41.

255. Oh SK, Fong WJ, Teo Y, Tan HL, Padmanabhan J, Chin AC, Choo AB. High density cultures of embryonic stem cells. Biotechnol Bioeng 2005;91(5):523-33.

256. Richards M, Fong CY, Tan S, Chan WK, Bongso A. An efficient and safe xeno-free cryopreservation method for the storage of human embryonic stem cells. Stem Cells 2004;22(5):779-89.

257. Shamblott MJ, Axelman J, Wang S, Bugg EM, Littlefield JW, Donovan PJ, Blumenthal PD, Huggins GR, Gearhart JD. Derivation of pluripotent stem cells from cultured human primordial germ cells. Proc Natl Acad Sci U S A 1998;95(23):13726-31.

258. Bishop AE, Buttery LD, Polak JM. Embryonic stem cells. J Pathol 2002;197(4):424-9.

259. Hoffman LM, Carpenter MK. Characterization and culture of human embryonic stem cells. Nat Biotechnol 2005;23:699-708.

260. Mitsui K, Tokuzawa Y, Itoh H, Segawa K, Murakami M, Takahashi K, Maruyama M, Maeda M, Yamanaka S. The Homeoprotein Nanog Is Required for Maintenance of Pluripotency in Mouse Epiblast and ES Cells. Cell 2003;113(5):631-642.

261. Nichols J, al. E. Formation of Pluripotent Stem Cells in the Mammalian Embryo Depends on the POU Transcription Factor Oct4 Cell 1998;95(3):379-391.

262. Friedman JR, Kaestner KH. The Foxa family of transcription factors in development and metabolism. Cell Mol Life Sci 2006;63(19-20):2317-28.

263. Keane RW, al. E. Neural Differentiation, NCAM-Mediated Adhesion, and Gap Junctional Communication in Neuroectoderm. A Study in Vitro. J cell biol 1988;106(4):1307-1319.

264. Randolph MA, Anseth K, Yaremchuk MJ. Tissue engineering of cartilage. Clin Plast Surg 2003;30(4):519-37.

265. Koch RJ, Gorti GK. Tissue engineering with chondrocytes. Facial Plast Surg 2002;18(1):59-68.

266. Shimizu K, Ito A, Honda H. Enhanced cell-seeding into 3D porous scaffolds by use of magnetite nanoparticles. J Biomed Mater Res B Appl Biomater 2006;77(2):265-72.

267. Freed LE, Langer R, Martin I, Pellis NR, Vunjak-Novakovic G. Tissue engineering of cartilage in space. Proc Natl Acad Sci U S A 1997;94(25):13885-90.

268. Holy CE, Shoichet MS, Davies JE. Engineering three-dimensional bone tissue in vitro using biodegradable scaffolds: investigating initial cell-seeding density and culture period. J Biomed Mater Res 2000;51(3):376-82.

269. Radisic M, Euloth M, Yang L, Langer R, Freed LE, Vunjak-Novakovic G. High-density seeding of myocyte cells for cardiac tissue engineering. Biotechnol Bioeng 2003;82(4):403-14.

270. Almarza AJ, Athanasiou KA. Effects of initial cell seeding density for the tissue engineering of the temporomandibular joint disc. Ann Biomed Eng 2005;33(7):943-50.

271. Vunjak-Novakovic G, Radisic M. Cell seeding of polymer scaffolds. Methods Mol Biol 2004;238:131-46.

272. Li Y, Ma T, Kniss DA, Lasky LC, Yang ST. Effects of filtration seeding on cell density, spatial distribution, and proliferation in nonwoven fibrous matrices. Biotechnol Prog 2001;17(5):935-44.

273. Soletti L, Nieponice A, Guan J, Stankus JJ, Wagner WR, Vorp DA. A seeding device for tissue engineered tubular structures. Biomaterials 2006;27(28):4863-4870.

274. Zhao F, Ma T. Perfusion bioreactor system for human mesenchymal stem cell tissue engineering: dynamic cell seeding and construct development. Biotechnol Bioeng 2005;91(4):482-93.

275. McFetridge PS, Bodamyali T, Horrocks M, Chaudhuri JB. Endothelial and smooth muscle cell seeding onto processed ex vivo arterial scaffolds using 3D vascular bioreactors. Asaio J 2004;50(6):591-600.

276. Aydelotte MB, Thonar EJ, Mollenhauer J, Flechtenmacher J. Culture of chondrocytes in alginate gel: variations in conditions of gelation influence the structure of the alginate gel, and the arrangement and morphology of proliferating chondrocytes. In Vitro Cell Dev Biol Anim 1998;34(2):123-30.

277. Tamponnet C, Ramdi H, Guyot JB, Lievremont M. Rabbit articular chondrocytes in alginate gel: characterisation of immobilized preparations and potential applications. Appl Microbiol Biotechnol 1992;37(3):311-5.

278. L. Klein JSaKGV. Pore size and properties of spherical Ca-alginate biocatalysts. Eur. J. Appl. Microbiol. Biotechnol. 1983;18(86-91).

279. Martinsen A, Skjak-Braek G, Smidsrod O, Zanetti F, Paoletti S. Comparison of different methods for determination of molecular weight and molecular weight distribution of alginates. Carbohydrate Polymers 1991;15(2):171.

280. Wang L, Shelton RM, Cooper PR, Lawson M, Triffitt JT, Barralet JE. Evaluation of sodium alginate for bone marrow cell tissue engineering. Biomaterials 2003;24(20):3475-81.

VITA

Zhensheng Li was born in a country village in Hunan, People's Republic of China in 1972. He earned his Bachelor Degree of Medicine (equivalent to M.D. degree in USA) and his Master Degree of Orthopedic Surgery from Hunan Medical University (Now calls Xiangya Medical School of Zhongnan University) in 1997. He moved to Shenzhen soon after his graduation and worked as Resident and then Attending Orthopedics Surgeon at the Shenzhen People's Hospital, focusing on hand surgery, microsurgery and peripheral vasculosurgery. In 2001, he was invited to be a visiting scholar at the University of Washington Medical School, Department of Orthopedics and Sports Medicine, and worked in Dr. Thomas E. Trumble's laboratory for peripheral nerve regeneration research. In 2002, he transferred to Dr. Miqin Zhang's biomaterials group in the Department of Materials Science and Engineering and the University Washington Engineered Biomaterials, University of Washington. He moved back to China in February 2003 and resumed his position at Shenzhen People's Hospital. In June 2003, he left his position in Shenzhen and returned to the University of Washington to pursue his Ph.D. Degree. In 2007, he was awarded a Doctor of Philosophy Degree at the University of Washington in Materials Science and Engineering.